

Republic of Iraq
Ministry of Higher Education
and Scientific Research
Al-Nahrain University
College of Science
Department of Chemistry



Amino Acids as Corrosion Inhibitors for Carbon Steel in Saline Solution

A Thesis

Submitted to the College of Science/Al-Nahrain University as a partial fulfillment of the requirements for the Degree of Master of Science in Chemistry

By

Ala'a Bader Mohammed

B.Sc. Chemistry/College of Science for Women/University of Baghdad

Supervised by

Dr. Taghried Ali Salman

(Asst. Prof.)

March 2017

Jum. II 1438

Supervisor Certification

I, certify that this thesis entitled “**Amino acids as corrosion inhibitors for carbon steel in saline solution**” was prepared by “**Al'aa Bader Mohammed**” under my supervision at the College of Science/Al-Nahrain University as a partial fulfillment of the requirements for the Degree of Master of Science in Chemistry (Physical Chemistry).

Signature:

Name: **Dr. Taghried A. Salman**

Scientific Degree: Assistant Professor

Date:

In view of the available recommendations, I forward this Thesis for debate by Examining Committee.

Signature:

Name: **Dr. Emad Al-sarraj**

Title: Head of the Department of Chemistry

Committee Certification

We, the examining committee certify that we have read this thesis entitled “**Amino acids as corrosion inhibitors for carbon steel in saline solution**” and examined the student “ **Ala'a Bader Mohammed** “ in its contents and that in our opinion, it is accepted for the Degree of Master of Science, in Physical Chemistry.

Signature:

Name: Dr. Yousif K. AL-Haidarie

Scientific Degree: Professor

Date:

(Chairman)

Signature:

Name: Dr. Elham Majeed AL-Rufaie

Scientific Degree: Assistant Professor

Date:

(Member)

Signature:

Name: Dr. Khalida A. Samawi

Scientific Degree: Lecturer

Date:

(Member)

Signature:

Name: Dr. Taghried A. Salman

Scientific Degree: Assistant Professor

Date:

(Member/Supervised)

I, hereby certify upon the decision of the examining committee.

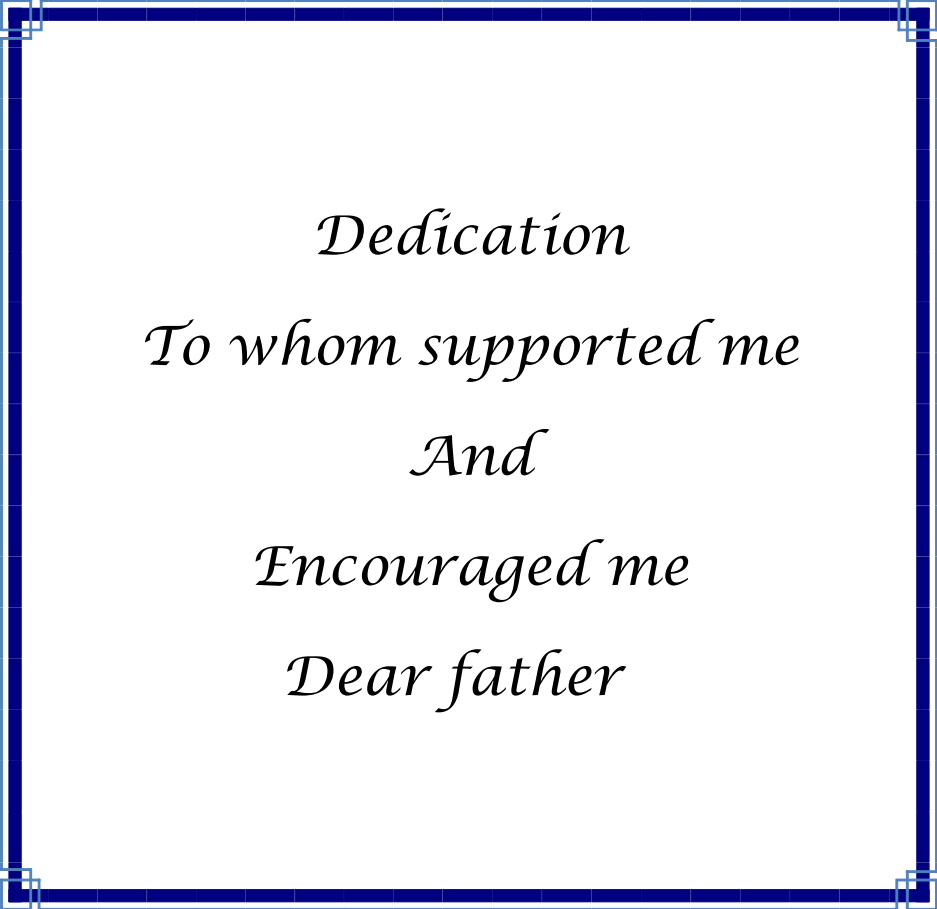
Signature:

Name: **Dr. Hadi M. A. Abood**

Scientific Degree: Professor

Title: Dean of College of Science

Date:



Dedication
To whom supported me
And
Encouraged me
Dear father



Acknowledgement

Thanks to almighty Allah for giving me strength and ability to perform and finish this work.

I would like to express my thanks and sincere gratitude to my supervisor Dr. Taghried Ali Salman for her support, guidance and advises in my M.Sc study.

I extend sincere thanks to Dr. Hassan N. Hashim for his help me in the experimental work.

I address my thanks to the Department of Chemistry in the Al-Nahrain University.

I am particularly thankful to my friends; Abeer Erfan, Ala' a Razzaq and Rana Gamall who helped me in my work.

Many thanks go to anyone who gave me help in my work.

Summary:

The present research involves potentiostatic investigation of the corrosion behavior of carbon steel alloy in saline (3.5% NaCl) solution. The general pattern and the experimental techniques used could be classified into three different aspects as follows:

1. The corrosion behavior of carbon steel specimen in saline solution (blank) and in the presence of inhibitors (Val, Ser, Trp and Lys) at pH (2 and 11) with various temperatures ranging between (293-313) K from the polarization curves over a range of potentials (-700 to -300) volt.
2. The inhibiting effect of amino acids (Val, Ser, Trp and Lys) as eco-friendly inhibitors at different concentrations on the corrosion of carbon steel alloy in the saline solution at pH (2 and 11) with five different temperatures.
3. Computational studies for inhibitors (Val, Ser, Trp and Lys) by using density functional theory (DFT) with 6-31G basis set in gas and aqueous phases.

The main results obtained from experimental studies may be presented as follows:

1. The corrosion current densities, corrosion rates and penetration rates for an uninhibited and inhibited saline solution are increasing with increasing temperature over a temperature range (293-313) K.
2. The inhibition efficiency values increase with increasing the concentration of inhibitors (Val, Ser, Trp and Lys) due to the adsorption of these compounds on the surface of the metal and decrease with increasing temperature in the range (293-313) K. the sequence of the IE values was for

Lys > Ser > Val > Trp at pH 2

Ser > Val > Trp > Lys at pH 11

L-lysine was shown to be more efficient for the protection of carbon steel in the acidic saline solution (pH 2). For basic saline solution, L-serine was the most efficient and suitable inhibitor particularly at a concentration of $1 \times 10^{-2} \text{ mol.L}^{-1}$.

3. The amino acids studied (Val, Ser, Trp and Lys) were act as anodic or cathodic or mixed type inhibitors, according to the values of corrosion potential.
4. The thermodynamic parameter of corrosion ΔG indicates that the process of corrosion spontaneous.
5. Kinetics of the corrosion was controlled by Arrhenius type equation and the data obtained showed that the activation energy (E_a) values are higher in the presence of the inhibitor molecules as compared with the values of blank solution. The positive sign of the activation enthalpies (ΔH^*) means the endothermic nature of the activated complex formation which means that required more energy to form its with increasing inhibitors concentrations. Large and negative change in the values of activation entropy (ΔS^*) means that the activated complex in the rate determining step represents association rather than the dissociation.
6. The adsorption process obeys Langmuir isotherm and the negative values of ΔG_{ads} and ΔH_{ads} indicate that the process were spontaneous and exothermic respectively. The values of ΔG_{ads} ranging between $(-40 \text{ kJ.mol}^{-1})$ to $(-20 \text{ kJ.mol}^{-1})$ meaning that the adsorption of these inhibitor molecules via chemisorptions and physisorption.

The results obtained from theoretical calculations of (Val, Ser, Trp and Lys) by using the density functional theory (DFT) (B3LYP) with 6–31G basis set. These results indicate that Trp is best inhibitor in aqueous phase and gas phase.

The Scanning Electron Microscopy (SEM) images of carbon steel in the presence (1×10^{-2} M) of amino acids showed that there were much less damage due to the formation of a protective film through adsorption process.

Contents

Item number	Subject	Page number
	List of Content	I
	List of Abbreviations and Symbols	III
	List of Figures	IV
	List of Tables	VII
Chapter One / Introduction		1
1.1	Corrosion	2
1.2	Electrochemical Method	3
1.3	Corrosion Kinetics	4
1.4	Carbon and Alloy Steel	7
1.5	Type of Corrosion	9
1.5.1	General Corrosion	9
1.5.2	Erosion-Corrosion	10
1.5.3	Pitting Corrosion	10
1.5.4	Crevice Corrosion	11
1.5.5	Intergranular Corrosion	11
1.5.6	Galvanic Corrosion	12
1.5.7	Stress Corrosion Cracking	12
1.5.8	Hydrogen Embrittlement	13
1.5.9	Filiform Corrosion	13
1.6	Corrosion Inhibitors	13
1.6.1	Mechanism of Inhibition	14
1.6.2	Inhibitors Classification	15
1.6.2.1	Inorganic Inhibitors	15
1.6.2.1.1	Anodic Inhibitor	16
1.6.2.1.2	Cathodic Inhibitor	16
1.6.2.2	Organic Inhibitors	16
1.7	Green Corrosion Inhibitors	17
1.7.1	Amino Acids as Green Corrosion Inhibitors	17
1.7.2	Classification of Amino Acids	19
1.8	Quantum Chemical and Corrosion Studies	20
1.9	Literature Survey	22
1.10	The Aim of the Research	29
Chapter Two / Experimental Part		30
2.1	Chemicals and Material	31
2.1.1	Carbon Steel Alloy	31

2.1.2	Chemicals	31
2.2	Inhibitors	31
2.3	Preparation of Solutions	33
2.4	Sample Preparation	34
2.5	Instruments	34
2.6	The Potentiostatic Set-Up	34
2.6.1	Potentiostat/Galvanostat device-M lab 200	34
2.6.2	Corrosion Cell	36
2.6.2.1	Three-Electrode System Set-up	36
2.6.3	Thermostat	38
2.7	Procedures of Corrosion Test	38
2.7.1	Open Circuit Potential Test	38
2.7.2	Tafel Extrapolation	39
2.8	Theoretical Test	40
Chapter Three / Results and discussion		41
3.1	The Polarization Curves	42
3.1.1	Corrosion Current Density and Corrosion Potential	58
3.1.2	The Tafel Slopes	62
3.2	Inhibition Efficiency and Surface Coverage	62
3.3	Transfer Coefficients	66
3.4	The Polarization Resistances	67
3.5	Effect of Temperature on the Corrosion of Carbon Steel	75
3.6	Thermodynamic Parameters of Corrosion	83
3.7	Thermodynamic Parameters of the Adsorption Isotherm	94
3.8	Theoretical Studies	102
3.9	Scanning electron microscopy (SEM)	107
Chapter Four / Conclusions and Recommendations		110
4.1	Conclusions	111
4.2	Recommendations	113
References		114

Abbreviations and Symbols

Abbreviations	Meaning
A	The pre-exponential factor
b_a	Anodic Tafel slope
b_c	Cathodic Tafel slope
C	Concentration
C_{inh}	The inhibitor concentration
CR	Corrosion rate
DFT	Density functional theory
E	Potential
E_a	The activation energy
E_{corr}	Corrosion potential
E_{HOMO}	Energy of the highest occupied molecular orbital
E_{LUMO}	Energy of the lowest unoccupied molecular orbital
E_{Total}	Total energy
F	The Faraday constant
h	The planks constant
i	Current density
i_0	The exchange current
i_{corr}	Corrosion current density
IE%	The inhibition efficiency
K_{ads}	The equilibrium constant
Lys	L-lysin
M	Molary
n	The number of electrons
N	The Avogadro's number
OCP	Open circuit potential
pH	Power of hydrogen
PR	Pentration rate
R	Gas constant
rds	The reductions reactions
R_p	Polarization resistance
SCE	Saturated calomel electrode
Ser	L-serine
T	Absolute temperature
t	time
Trp	L-tryptophan
Val	L-valine

Wt. %	Weight percentage
α_a	The transfer coefficients of the anodic
α_c	The transfer coefficients of the cathodic
γ	The global hardness
ΔE	Energy gap
ΔG	The Gibbs free-energy change
ΔH	Enthalpy change
ΔN	The fraction of electrons transferred from the inhibitor molecules to the metallic surface
ΔS	Entropy change
η	Over potential
θ	The surface coverage
μ	dipole moment
χ	The absolute electro negativity

List of figures

Figure number	Name of figures	Page number
1-1	Corrosion water pipes.	2
1-2	Mechanism of oxidation/reduction reactions for iron.	8
1-3	pH-Potential equilibrium diagram for the system iron-water at 25°C.	9
1-4	General corrosion type.	10
1-5	Erosion-corrosion type.	10
1-6	Pitting corrosion type.	11
1-7	Crevice corrosion type.	11
1-8	Intergranular corrosion type.	11
1-9	Galvanic corrosion type.	12
1-10	Stress corrosion cracking type.	12
1-11	Hydrogen embrittlement type.	13
1-12	Filiform corrosion type.	13
1-13	Adsorption of inhibitor on metal surface.	14
1-14	Classification of inhibitors.	15
1-15	General structure of amino acids.	18
2-1	Structures of amino acids.	32
2-2	Potentiostat/galvanostat device.	35
2-3	Schematic diagram of potentiostat.	35
2-4	Corrosion Cell.	36

2-5	Working electrode.	37
2-6	Reference electrode.	37
2-7	Complete system set up for polarization measurements.	38
2-8	Cathodic and anodic polarization digram.	39
3-1	Polarization curves for carbon steel corrosion in the blank (saline solution) and in presence of Val with different concentrations (a) 5×10^{-4} M, (b) 1×10^{-3} M, (c) 5×10^{-3} M and (d) 1×10^{-2} M at temperature range (293-313) K and pH 2.	43
3-2	Polarization curves for carbon steel corrosion in the blank (saline solution) and in presence of Ser with different concentrations (a) 5×10^{-4} M, (b) 1×10^{-3} M, (c) 5×10^{-3} M and (d) 1×10^{-2} M at temperature range (293-313) K and pH 2.	45
3-3	Polarization curves for carbon steel corrosion in the blank (saline solution) and in presence of Trp with different concentrations (a) 5×10^{-4} M, (b) 1×10^{-3} M, (c) 5×10^{-3} M and (d) 1×10^{-2} M at temperature range (293-313) K and pH 2.	47
3-4	Polarization curves for carbon steel corrosion in the blank (saline solution) and in presence of Lys with different concentrations (a) 5×10^{-4} M, (b) 1×10^{-3} M, (c) 5×10^{-3} M and (d) 1×10^{-2} M at temperature range (293-313) K and pH 2.	49
3-5	Polarization curves for carbon steel corrosion in the blank (saline solution) and in presence of Val with different concentrations (a) 5×10^{-4} M, (b) 1×10^{-3} M, (c) 5×10^{-3} M and (d) 1×10^{-2} M at temperature range (293-313) K and pH 11.	51
3-6	Polarization curves for carbon steel corrosion in the blank (saline solution) and in presence of Ser with different concentrations (a) 5×10^{-4} M, (b) 1×10^{-3} M, (c) 5×10^{-3} M and (d) 1×10^{-2} M at temperature range (293-313) K and pH 11.	53
3-7	Polarization curves for carbon steel corrosion in the blank (saline solution) and in presence of Trp with different concentrations (a) 5×10^{-4} M, (b) 1×10^{-3} M, (c) 5×10^{-3} M and (d) 1×10^{-2} M at temperature range (293-313) K and pH 11.	55

3-8	Polarization curves for carbon steel corrosion in the blank (saline solution) and in presence of Lys with different concentrations (a) 5×10^{-4} M, (b) 1×10^{-3} M, (c) 5×10^{-3} M and (d) 1×10^{-2} M at temperature range (293-313) K and pH 11.	57
3-9	Mechanism of inhibition of amino acids.	65
3-10	Arrhenius plots of $\log i_{\text{corr}}$ versus $1/T$ for the corrosion of carbon steel in saline solution (blank) and in the presence of inhibitors (Val, Ser, Trp and Lys) of various concentrations at pH 2.	78
3-11	Arrhenius plots of $\ln (i_{\text{corr}}/T)$ versus $1/T$ for the corrosion of carbon steel in saline solution (blank) and in the presence of inhibitors (Val, Ser, Trp and Lys) of various concentrations at pH 2.	79
3-12	Arrhenius plots of $\log i_{\text{corr}}$ versus $1/T$ for the corrosion of carbon steel in saline solution (blank) and in the presence of inhibitors (Val, Ser, Trp and Lys) of various concentrations at pH 11.	81
3-13	Arrhenius plots of $\ln (i_{\text{corr}}/T)$ versus $1/T$ for the corrosion of carbon steel in saline solution (blank) and in the presence of inhibitors (Val, Ser, Trp and Lys) of various concentrations at pH 11.	82
3-14	The variation of Gibbs free energies (ΔG) with temperature for the corrosion of carbon steel in saline solution (blank) and in the presence of inhibitors (Val, Ser, Trp and Lys) at pH 2.	85
3-15	The variation of Gibbs free energies (ΔG) with temperature for the corrosion of carbon steel in saline solution (blank) and in the presence of inhibitors (Val, Ser, Trp and Lys) at pH 11.	90
3-16	Langmuir isotherm plots for the adsorption of (Val, Ser, Trp and Lys) on carbon steel in saline solution at pH 2.	97
3-17	The variation of Gibbs free energies (ΔG_{ads}) with temperature for the adsorption of (Val, Ser, Trp and Lys) on carbon steel in saline solution at pH 2.	98
3-18	Langmuir isotherm plots for the adsorption of (Val, Ser, Trp and Lys) on carbon steel in saline solution at pH 11.	100

3-19	The variation of Gibbs free energies (ΔG_{ads}) with temperature for the adsorption of (Val, Ser, Trp and Lys) on carbon steel in saline solution at PH 11.	101
3-20	The energy of lowest unoccupied molecular orbital (E_{LUMO}) and the energy of highest occupied molecular orbital (E_{HOMO}) of amino acids.	103
3-21	Optimized structure of amino acids.	104
3-22	Scanning electron micrographs of (a) Polished carbon steel alloy, (b) carbon steel alloy immersed in saline solution.	107
3-23	Scanning electron micrographs of carbon steel immersed in (a) saline solution at pH 2 (b) saline solution at pH 2 in presence of 1×10^{-2} M Trp (c) saline solution at pH 2 in presence of 1×10^{-2} M Val (d) saline solution at pH 2 in presence of 1×10^{-2} M Ser and (e) saline solution at pH 2 in presence of 1×10^{-2} M Lys respectively.	108
3-24	Scanning electron micrographs of carbon steel immersed in (a) saline solution at pH 11 (b) saline solution at pH 11 in presence of 1×10^{-2} M Lys (c) saline solution at pH 11 in presence of 1×10^{-2} M Trp (d) saline solution at pH 11 in presence of 1×10^{-2} M Val and (e) saline solution at pH 11 in presence of 1×10^{-2} M Ser respectively.	109

List of tables

Table number		Page number
1-1	Classification of amino acids based on their group.	19
2-1	Chemical composition of carbon steel.	31
2-2	List of chemicals used.	31
2-3	Properties of amino acids.	33
2-4	The Instruments were use in this study.	34
3-1	Corrosion parameters of carbon steel in the blank (saline solution) and in presence of Val with different concentrations (5×10^{-4} , 1×10^{-3} , 5×10^{-3} and 1×10^{-2}) M at temperature range (293-313) K and pH 2.	44
3-2	Corrosion parameters of carbon steel in the blank (saline solution) and in presence of ser with different concentrations (5×10^{-4} , 1×10^{-3} , 5×10^{-3} and 1×10^{-2}) M at	46

	temperature range (293-313) K and pH 2.	
3-3	Corrosion parameters of carbon steel in the blank (saline solution) and in presence of Trp with different concentrations (5×10^{-4} , 1×10^{-3} , 5×10^{-3} and 1×10^{-2}) M at temperature range (293-313) K and pH 2.	48
3-4	Corrosion parameters of carbon steel in the blank (saline solution) and in presence of Lys with different concentrations (5×10^{-4} , 1×10^{-3} , 5×10^{-3} and 1×10^{-2}) M at temperature range (293-313) K and pH 2.	50
3-5	Corrosion parameters of carbon steel in the blank (saline solution) and in presence of Val with different concentrations (5×10^{-4} , 1×10^{-3} , 5×10^{-3} and 1×10^{-2}) M at temperature range (293-313) K and pH 11.	52
3-6	Corrosion parameters of carbon steel in the blank (saline solution) and in presence of Ser with different concentrations (5×10^{-4} , 1×10^{-3} , 5×10^{-3} and 1×10^{-2}) M at temperature range (293-313) K and pH 11.	54
3-7	Corrosion parameters of carbon steel in the blank (saline solution) and in presence of Trp with different concentrations (5×10^{-4} , 1×10^{-3} , 5×10^{-3} and 1×10^{-2}) M at temperature range (293-313) K and pH 11.	56
3-8	Corrosion parameters of carbon steel in the blank (saline solution) and in presence of Lys with different concentrations (5×10^{-4} , 1×10^{-3} , 5×10^{-3} and 1×10^{-2}) M at temperature range (293-313) K and pH 11.	58
3-9	Inhibition efficiencies and surface coverages of (Val, Ser, Trp and Lys) at various concentration with temperature range (293-313)K in saline solution at PH 2.	63
3-10	Inhibition efficiencies and surface coverages of (Val, Ser, Trp and Lys) at various concentration with temperature range (293-313)K in saline solution at PH 11.	64
3-11	Values of transfer coefficient (α_c , α_a), the polarization resistance (R_p) and equilibrium exchange current density (i_o) for corrosion of carbon steel in saline solution (blank) and in the presence of Val at pH 2 with various temperature range (293-313) K.	68
3-12	Values of transfer coefficient (α_c , α_a), the polarization resistance (R_p) and equilibrium exchange current density (i_o) for corrosion of carbon steel in saline solution (blank) and in the presence of Ser at pH 2 with	69

	various temperature range (293-313) K.	
3-13	Values of transfer coefficient (α_c , α_a), the polarization resistance (R_p) and equilibrium exchange current density (i_o) for corrosion of carbon steel in saline solution (blank) and in the presence of Trp at pH 2 with various temperature range (293-313) K.	70
3-14	Values of transfer coefficient (α_c , α_a), the polarization resistance (R_p) and equilibrium exchange current density (i_o) for corrosion of carbon steel in saline solution (blank) and in the presence of Lys at pH 2 with various temperature range (293-313) K.	71
3-15	Values of transfer coefficient (α_c , α_a), the polarization resistance (R_p) and equilibrium exchange current density (i_o) for corrosion of carbon steel in saline solution (blank) and in the presence of Val at pH 11 with various temperature range (293-313) K.	72
3-16	Values of transfer coefficient (α_c , α_a), the polarization resistance (R_p) and equilibrium exchange current density (i_o) for corrosion of carbon steel in saline solution (blank) and in the presence of Ser at pH 11 with various temperature range (293-313) K.	73
3-17	Values of transfer coefficient (α_c , α_a), the polarization resistance (R_p) and equilibrium exchange current density (i_o) for corrosion of carbon steel in saline solution (blank) and in the presence of Trp at pH 11 with various temperature range (293-313) K.	74
3-18	Values of transfer coefficient (α_c , α_a), the polarization resistance (R_p) and equilibrium exchange current density (i_o) for corrosion of carbon steel in saline solution (blank) and in the presence of Lys at pH 11 with various temperature range (293-313) K.	75
3-19	Activation energy (E_a), activation enthalpy (ΔH^*), and the entropy of activation (ΔS^*) for the corrosion of carbon steel in saline solution (blank) and in the presence of inhibitors (Val, Ser, Trp and Lys) of various concentrations at pH 2.	80
3-20	Activation energy (E_a), activation enthalpy (ΔH^*), and the entropy of activation (ΔS^*) for the corrosion of carbon steel in saline solution (blank) and in the presence of inhibitors (Val, Ser, Trp and Lys) of various concentrations at pH 11.	83
3-21	The thermodynamic parameters for the corrosion of	86

	carbon steel in saline solution (blank) and in the presence of Val over the temperature range (293-313) K at pH 2.	
3-22	The thermodynamic parameters for the corrosion of carbon steel in saline solution (blank) and in the presence of Ser over the temperature range (293-313) K at pH 2.	87
3-23	The thermodynamic parameters for the corrosion of carbon steel in saline solution (blank) and in the presence of Trp over the temperature range (293-313) K at pH 2.	88
3-24	The thermodynamic parameters for the corrosion of carbon steel in saline solution (blank) and in the presence of Lys over the temperature range (293-313) K at pH 2.	89
3-25	The thermodynamic parameters for the corrosion of carbon steel in saline solution (blank) and in the presence of Val over the temperature range (293-313) K at pH 11.	91
3-26	The thermodynamic parameters for the corrosion of carbon steel in saline solution (blank) and in the presence of Ser over the temperature range (293-313) K at pH 11.	92
3-27	The thermodynamic parameters for the corrosion of carbon steel in saline solution (blank) and in the presence of Trp over the temperature range (293-313) K at pH 11.	93
3-28	The thermodynamic parameters for the corrosion of carbon steel in saline solution (blank) and in the presence of Lys over the temperature range (293-313) K at pH 11.	94
3-29	Thermodynamic parameters for adsorption of the inhibitors on the surface of carbon steel in saline solution at PH 2.	99
3-30	Thermodynamic parameters for adsorption of the inhibitors on the surface of carbon steel in saline solution at PH 11.	102
3-31	Quantum parameters of amino acids.	106

Chapter One

Introduction

1.1 Corrosion

Most people are familiar with corrosion in some form or another, especially the rusting of an iron fence and the degradation of steel pilings or boat. Piping is another mean type of equipment undergo to corrosion such as water pipes in the home. Figure (1-1) represent the most common type for pipes corrosion. In some types of corrosion, there is no visible weight change or degradation, yet properties change and the material may fail unexpectedly because of some changes within the material ⁽¹⁾.



Figure (1-1): Corrosion water pipes.

In nature, most metals are found as an ore. All of these metals (except noble metals: gold, platinum, and silver) found in nature in the form of their oxides, hydroxides, carbonates, silicates, sulfides, sulfates, etc., which are thermodynamically more stable. The metals are extracted from these ores after preparation a large amount of energy, obtaining pure metals in their elemental forms. As a result, metals arrived to higher energy levels, their entropies are reduced, and they become more unstable. It is a natural tendency to go back to their oxidized forms of lower energies, by recombining with the elements present in the environment, in order to decrease the free energy ⁽²⁾. Corrosion is defined as the degradation of a metal by reaction with its environment. In addition to selecting the kind of metal, any major approach of the corrosion must involve steps about the nature of the environment and the

metal/environment interphase, such as the concentration of corrosive species in solution, fluid motion, the kinetic of metal oxidation and the reduction of the species at the metallic surface ⁽³⁾. Metal surfaces are widely used in a variety of industrial applications such as petroleum, textile and marine industries as a component of pumps or valves that carry various types of substances. However some of these substances are highly corrosive and containing such solutions as hydrochloric acid. Corrosion is a process playing an important role in economics and safety, especially for metals ⁽⁴⁾. Corrosion is a natural, spontaneous, and thermodynamically process. There are many processes which can control the corrosion rate. One such process is use of corrosion inhibitors. They are chemical substances which when added in small amount control the corrosion rates or retarding the corrosion process ⁽⁵⁾.

1.2 Electrochemical Method

Mixed potential theory derived by Wagner and Traud is one of the most important concepts in corrosion theory which explains the reactions mechanism of cathodic and anodic corrosion by a simple way. They assume that can be explain the corrosion reactions by assuming that cathodic and anodic partial reactions occur at the inter phase boundary metal/electrolyte at constant change with random distribution of location and time of the individual reaction ^(6,7).

The mixed potential theory takes into account two main postulates ⁽⁸⁾:

- ❖ Any electrochemical reaction can be classified into two or more fractional reduction and oxidation reactions.
- ❖ There is no net collection of electric charge during an electrochemical reaction.

Oxidation of the metal (corrosion) and reduction of species in solution are occur at the same rate and the net current is equal zero

$$i_{\text{net}} = i_{\text{red}} - i_{\text{ox}} = 0 \dots\dots\dots (1-1)$$

where i_{net} , i_{red} and i_{ox} are net current, reduction current and oxidation current respectively.

When a metal contacted with a solution, it will suppose a potential, that is dependent upon the metal and the nature of the solution. This potential is open circuit potential, when external potential is applied to the cell, is referred to as the corrosion potential E_{corr} . Electrochemically, corrosion rate can be measured from determination of the oxidation current at the corrosion potential. So the oxidation current is called the corrosion current i_{corr} . Equation (1-1) can be rewritten as ⁽⁹⁾:

$$i_{\text{net}} = i_{\text{corr}} - i_{\text{red}} = 0 \text{ at } E_{\text{corr}} \dots\dots\dots (1-2)$$

1.3 Corrosion Kinetics

The equilibrium potential (E_{eq}) is related with oxidation and reduction reactions. The electrode is polarized because of the electrode potential charges, when a current is applied to the electrode surface. The difference between this resultant potential (E) and equilibrium potential (E_{eq}) is called overpotential (η) ⁽¹⁰⁾:

$$\eta = E - E_{\text{eq}} \dots\dots\dots (1-3)$$

The polarization may be anodic or cathodic that depending on the processes on the electrode by moving the potential in the positive or negative site respectively. There are three important types of polarization ⁽¹⁰⁾:

$$\eta_{\text{total}} = \eta_{\text{act}} + \eta_{\text{conc}} + iR \dots\dots\dots (1-4)$$

where, η_{act} : is the activation overpotential, always present and it is the major polarization component at small polarization currents or voltages describing the charge transfer kinetics of an electrochemical reaction. Activation polarization refers to an electrochemical reaction that is controlled by the sequence of reaction at the metal-electrolyte interface. It is the controlling factor during corrosion in media containing a high concentration of active species.

η_{conc} : is the concentration overpotential, describing the mass transport limitation associated with electrochemical process. It is controlling at larger polarization currents or voltages. Concentration polarization generally controls when the concentration of the reducible species is low. The reduction rate is predominated by processes occurring within the bulk solution rather than at the metal surface.

iR : is an ohmic potential drop always occurs between the working electrode and the capillary tip of the reference electrode. This function takes into account the electrolytic resistivity of an environment when the anodic and cathodic elements are separated by this environment while still electrically coupled ^(1,11).

The rate for a reaction is limited by activation overvoltage, the relationship between the rate of reaction (can be expressed by a current density i) and the driving force for the reaction (potential E) is given by the Butler-Volmer equation:

$$i = i_0 \exp \left[\frac{\alpha n F (E - E_{rev})}{RT} \right] - i_0 \exp \left[\frac{-(1-\alpha) n F (E - E_{rev})}{RT} \right]$$

$$i = i_0 \exp \left[\frac{\alpha n F \eta}{RT} \right] - i_0 \exp \left[\frac{-(1-\alpha) n F \eta}{RT} \right] \dots \dots \dots (1-5)$$

Where, i_0 : exchange current density is a kinetic parameter representing the electrochemical reaction rate at equilibrium (the rate of oxidation and reduction must be equal), E_{rev} : is the reversible potential, F : is the Faraday constant, n : is the charge of ion in equivalents/mol, R : is the gas constant and α : is the charge transfer coefficient. The value of α is usually close to 0.5, but must be between 0 and 1.

For a sufficiently high value of anodic polarization from the reversible potential (overpotential $\eta_a > \sim 50$ mV). Therefore, the Butler-Volmer equation simplifies to:

$$i_{net} = i_0 \exp \left[\frac{\alpha n F \eta_a}{RT} \right] \dots\dots\dots (1-6)$$

Rearranging and gets the Tafel equation:

$$\eta_a = b_a \log \left[\frac{i}{i_0} \right] \dots\dots\dots (1-7)$$

b_a : is the anodic Tafel slope ($2.3 RT/\alpha nF$), for b_a equal to (0.12 V) and α : is equal 0.5 and n : is equal 1

A similar equation can be used for cathodic activation polarization:

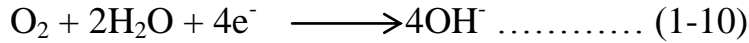
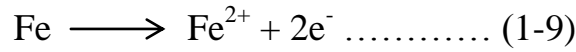
$$\eta_c = -b_c \log \left[\frac{|i|}{i_0} \right] \dots\dots\dots (1-8)$$

Corrosion conditions are far removed from the reversible potentials for any of the reactions ^(12,13).

1.4 Carbon and Alloy Steel

In commercial practice, carbon and alloy steels have some similar properties. Both contain some elements in varying percentages. Steel considered as a carbon steel when its manganese content is limited to 1.65 % max, silicon to 0.60% max, and copper to 0.60% max, except of deoxidizers and boron when specified, no other alloying element is intentionally added. Alloy steels have not only those grades which exceed the above limits, but also any grade to which any element other than those mentioned above is added in order to arrive to a specific alloying effect ⁽¹⁴⁾. It is important to explained the meaning of carbon steel that used in this research. The expression steel is usually taken to mean an iron-based alloy containing carbon in amounts less than about 2%. Carbon steels can be defined as steels that contain only residual amounts of elements other than carbon, except those such as silicon and aluminum added for deoxidation and those such as manganese and cerium added to get rid of certain deleterious effects of residual sulfur ⁽¹⁵⁾. Carbon steel has properties made up mostly of the element, and which depend upon carbon content for its structure. The most perfect form of carbon in the world is a diamond, which is 100% carbon. Carbon is present in all types of steel and is the principal hardening element ,determining the level of hardness or strength attainable by quenching. It raises tensile strength, hardness, resistance to wear and abrasion as the carbon content of steel is increased. It can be lowers ductility, toughness and machinability ⁽¹⁶⁾. Carbon steel is applied on a large scale in most industries due to its low cost and availability in ease for the fabrication of various reaction vessels such as cooling tower tanks, pipelines ...etc. ⁽¹⁷⁾. Corrosion process of carbon steel consists of a set of oxidation/ reduction reactions (figure (1-2)). Thus, the iron will be oxidized to form Fe^{2+} ions at the anodic sites and

the reduction reaction for iron in aerated solutions is the reduction of oxygen ⁽¹⁸⁾.



The dissolution of iron in concentrated saline solutions into ferrous cations we can be explained by these equations ⁽¹⁹⁾:

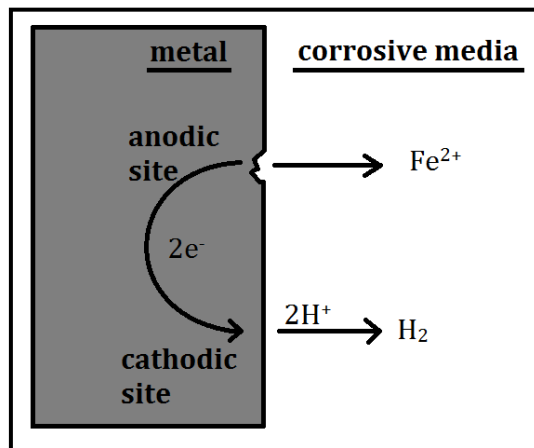
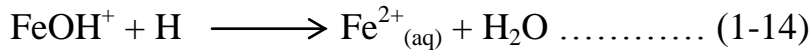
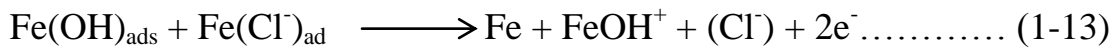


Figure (1-2): mechanism of oxidation/reduction reactions for iron.

Pourbaix diagrams for iron-water system at 25C^o (figure (1-3)) show the equilibrium phases at a given potential and pH. Pourbaix diagrams are based on thermodynamic calculations and do therefore not account for kinetics. For example of Fe, the Pourbaix diagram shows that Fe metal is stable at particular pH and potential conditions. At potentials more positive than -0.6 and at pH values less than 9, ferrous ion (Fe²⁺) is the stable substance. This indicates that iron will corrode under these

conditions. In other regions, it can be seen that the corrosion of iron produces ferric ions (Fe^{3+}), ferrous hydroxide [$\text{Fe}(\text{OH})_2$], ferric oxide (Fe_2O_3) and magnetite (Fe_3O_4). The presence of a relatively large immunity region, corrosion products are solid and possibly protective, indicates that iron may corrode much less under these potential/ pH conditions ⁽¹⁾.

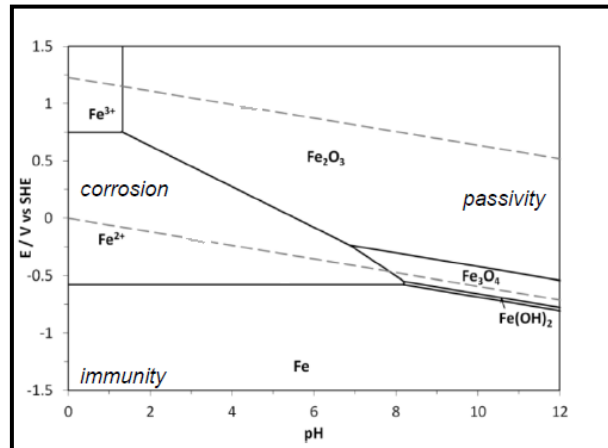


Figure (1-3): pH-Potential equilibrium diagram for the system iron-water at 25°C.

1.5 Type of Corrosion

Corrosion does not mean only in terms of rusting and tarnishing. However, corrosion damage occurs in many ways as well, resulting, for example, in failure by cracking or in absence of strength or ductility. In general, most types of corrosion, with exceptions of some type, occur by mechanisms of electrochemical, but corrosion products are not observable and metal weight loss not be necessarily appreciable to result in major damage. The main types of corrosion of carbon steel classified with physical properties and outward appearance are as follows ⁽²⁰⁾:

1.5.1 General Corrosion

General corrosion is a uniform attack and is the most commonly type of corrosion. It is characterized by electrochemical or chemical

reaction which transports uniformly over the entire exposed surface area. The metal becomes thinner and then corroded ⁽²¹⁾. The mechanism of uniform corrosion is summarized by rust formation of iron as shown in figure (1-4).

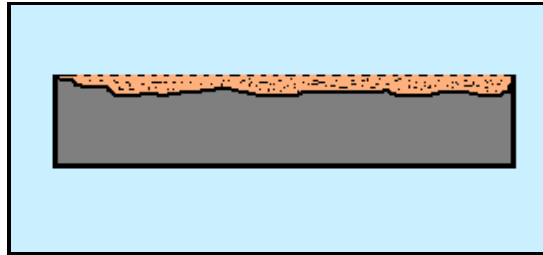


Figure (1-4): General corrosion type.

1.5.2 Erosion-Corrosion

Erosion corrosion is the acceleration in rate of deterioration on a metal because of relative movement between a corrosive media and the metal surface. Generally this movement is rapid and the effects of abrasion are involved. Metal is removed from this surface as dissolved ions or corrosion products are mechanically washed away from the surface of metal (figure (1-5)) ⁽²¹⁾.

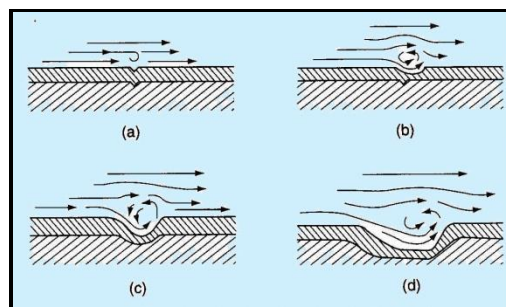


Figure (1-5): Erosion-corrosion type.

1.5.3 Pitting Corrosion

Local corrosion occurs in holes, that is, in gaps expanding from the surface to the inside of the metal as indicated in figure (1-6) ⁽²²⁾.

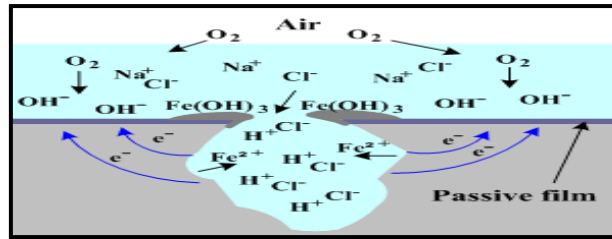


Figure (1-6): Pitting corrosion type.

1.5.4 Crevice Corrosion

Local corrosion usually is done in a very tight gap between two surfaces (metal or nonmetal). As is the case with pitting, the micro-environment within the crevice can greatly differ from the general medium (figure (1-7)). Concentration cells can cause this type of corrosion to occur at a very rapid rate ⁽²²⁾.

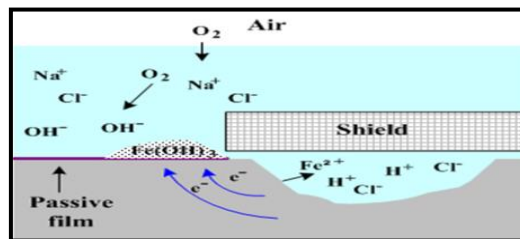


Figure (1-7): Crevice corrosion type.

1.5.5 Intergranular Corrosion

The microstructure of metals and alloys is made from grains, separated by boundaries of grain. Intergranular corrosion is localized deterioration along the grain boundaries, or immediately adjacent to grain boundaries, while the bulk of the grains remain largely unaffected by this attack as shown in figure (1-8). This type of corrosion was associated with chemical segregation effects or specific phases precipitated on the grain boundaries ⁽²³⁾.

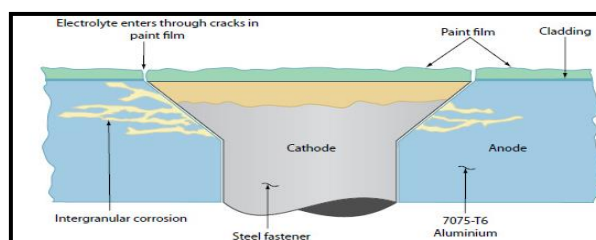


Figure (1-8): Intergranular corrosion type.

1.5.6 Galvanic Corrosion

Because various elements have different chemical activities, various alloys with different chemical compositions will have different chemical and electrochemical properties in the environment. Joining of different metals in a way such that an electrical circuit is completed through the joint and the environment will result in increasing the rate of corrosion of the active metal and reducing the rate of corrosion of the noble metal. The range of the change depends on a types of factors including the ratio of the areas of each alloy exposed to the environment, the potential difference between the alloys, the electrical resistivity of the joint, and the conductivity of these suppressants is usually extremely low and this should minimize the damage that galvanic coupling of dissimilar alloys can cause ⁽²⁴⁾. The most common examples of galvanic corrosion of aluminum alloys are when they are joined to steel or copper and exposed to a wet saline environment as shown in Figure (1-9).

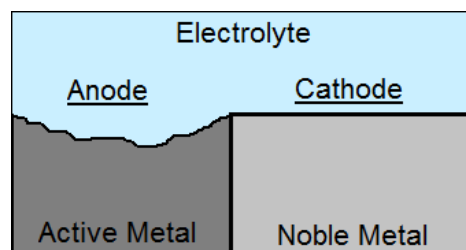


Figure (1-9): Galvanic corrosion type.

1.5.7 Stress Corrosion Cracking

Stress corrosion cracking stimulates formation of a fracture in the metal structure due to mechanical stress and a chemically aggressive medium as represented in figure (1-10) ⁽²⁵⁾.

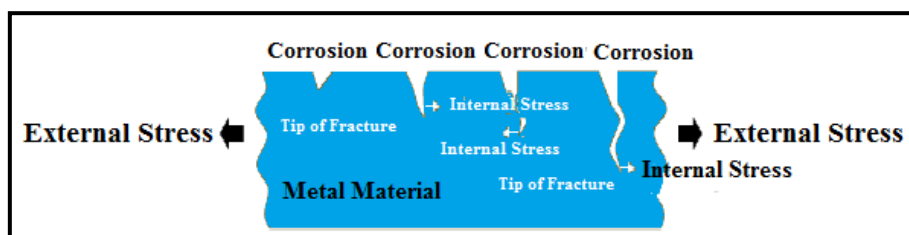


Figure (1-10): Stress corrosion cracking type.

1.5.8 Hydrogen Embrittlement

In this type of corrosion process, some of hydrogen atoms diffuse through steel and retained, where they recombine with each other, forming a very strong internal pressure that exceeds the strength of steel and forming gaps (figure (1-11)) ⁽²⁵⁾.

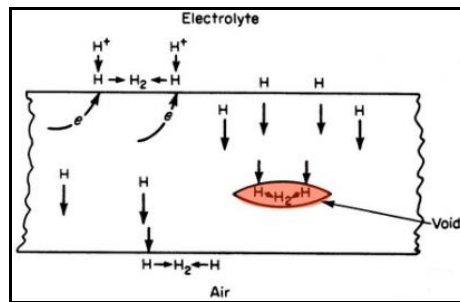


Figure (1-11): Hydrogen embrittlement type.

1.5.9 Filiform Corrosion

Filiform corrosion is a localized form of corrosion, (figure (1-12)), that is done under a kind of coatings. Steel, aluminum, and other alloys can be specially affected by this form of corrosion, which has been of particular concern in the food packaging industry ⁽²³⁾.

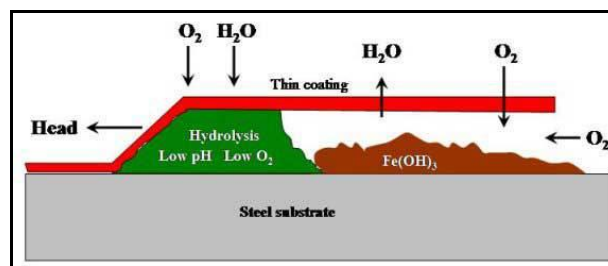


Figure (1-12): Filiform corrosion type.

1.6 Corrosion Inhibitors

Inhibitors are substances which when added in a small amount to a corrosive media, lower the corrosion rate. They reduce the corrosion rate by either acting as a barrier, by forming an adsorbed layer or lower the cathodic or anodic process ⁽²⁶⁾. The use of inhibitors is one of the most

operation methods for prevent against corrosion in aqueous media. The inhibitor become an effective must also transfer water from the metal surface, interact with anodic or cathodic reaction sites to retard the oxidation and reduction corrosion reaction, and prevent transportation of water and corrosion-active species on the surface of metal. In aqueous solution the action of inhibitors molecules may be due to the physical (electrostatic) adsorption or chemisorptions onto the metallic surface (figure (1-13))⁽²⁷⁾.

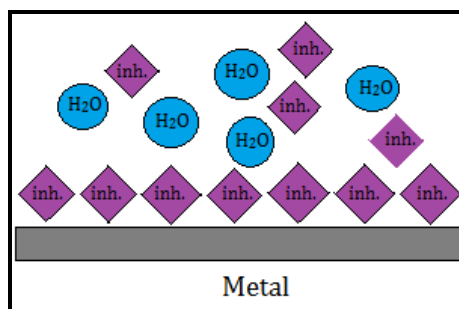


Figure (1-13): Adsorption of inhibitor on metal surface.

1.6.1 Mechanism of Inhibition

The mechanism of an ion acts as inhibitor for the corrosion of iron in neutral solution involves the following important steps:

- ❖ Lower the dissolution rate of the oxide film.
- ❖ Correction of the oxide film by promotion of the reformation of oxide.
- ❖ Correction of the oxide film by closing the pores and cover the surface by insoluble compounds.
- ❖ Block of the adsorption of aggressive anions⁽²⁸⁾.

1.6.2 Inhibitors Classification

The corrosion inhibitors are chemicals either natural or synthetic and could be classified by:

- ❖ The chemical type as organic or inorganic.
- ❖ The process of mechanism such as anodic, cathodic or both and by adsorption process.

In general, the inorganic inhibitors have cathodic or anodic actions. The organics inhibitors have cathodic and anodic or both actions and the protective by a film adsorption. Inhibitors can be subdivided according to their classification as shown in the figure (1-14) ⁽²⁹⁾:

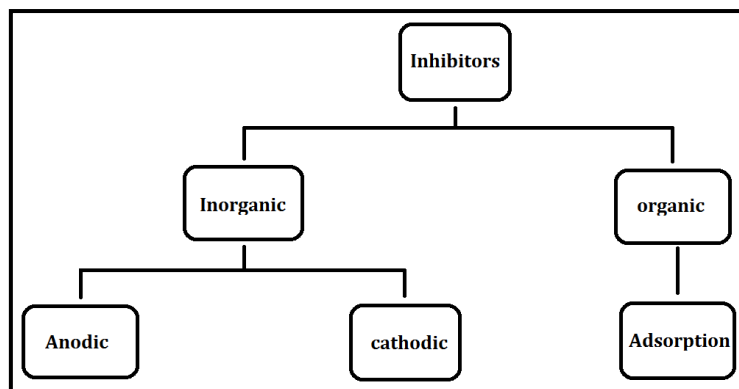


Figure (1-14): Classification of inhibitors.

1.6.2.1 Inorganic Inhibitors

Inorganic elements or metals have an important role in living organisms, when they are at trace amounts. The higher concentrations (abnormal) of all metals and their derivatives cause toxicity to all forms of lives. For example, chromium compounds, such as chromates were widely used as potential corrosion inhibitors in aqueous solution due to their high efficiency. In addition to the high inhibition efficiency, chromates exhibit high toxicity and so prohibited to use for industrial applications ⁽³⁰⁾.

1.6.2.1.1 Anodic Inhibitor

A chemical substance that prevents or lower the rate of the anodic or oxidation reaction via formation of a protective oxide film on the surface of the metal, leads to prevent corrosion ⁽³¹⁾. Some of examples of anodic inhibitors are chromates (salts containing CrO_4^{2-}), soluble hydroxides, phosphates, molybdate, nitrite and orthophosphate and imidazole ⁽³²⁾.

1.6.2.1.2 Cathodic Inhibitors

Cathodic inhibitors control corrosion by either lower the reduction rate (cathodic poisons) or by precipitating spontaneous on the cathodic areas (cathodic precipitator). Cathodic poisons, such as sulfides and selenides, are adsorbed on the surface of metal; while compounds of arsenic, bismuth, and antimony are reduced at the cathode and form a metallic layer. In neutral and alkaline solutions, inorganic anions, such as phosphates, silicates, and borates, form protective films that lower the cathodic reaction rate by limiting the diffusion of oxygen to the metal surface ⁽³³⁾.

1.6.2.2 Organic Inhibitors

Organic compounds containing hetro atoms such as nitrogen, sulphur and oxygen as polar functional groups in a conjugated system have been acted as corrosion inhibitors for steel. The complexes when formed are adsorbed on the metal surface to form a barrier film which separated the metal surface from the corrosive media present in the aggressive solution ⁽³⁴⁾. Organic inhibitors can be adsorbed on the metal surface by instead of water molecules and form a compact barrier film. The existence of lone pairs and π electrons in the inhibitor molecules accelerates the electron transfer from the inhibitor to the metal, forming a

coordinate covalent bond. The strength of the adsorption bond depends on the electron density, on the donor atom of the functional group of molecules and also on the polarisability of the functional group ⁽³⁵⁾.

1.7 Green Corrosion Inhibitors

Green corrosion inhibitors are biodegradable and do not have heavy metals or any toxic compounds. Some research groups are investigated the successful use of naturally substances to inhibit the corrosion of metals in acidic and alkaline environments ⁽³⁶⁾. It is worth mentioning that the effect of corrosion inhibitors is always caused by change in the state of the surface being protected due to adsorption or formation of hardly soluble compounds with metal cations. The use of inhibitor is type of the most practical ways to protect metal from corrosion ⁽³⁷⁾.

The majority of common inhibitors are organic compounds containing heteroatom, such as O, N, S and multiple bonds. Most of these compounds are not only expensive but also toxic for human and environments and therefore it is better to look for environmentally safe inhibitors ⁽³⁸⁾.

1.7.1 Amino Acids as Green Corrosion Inhibitors

Amino acids are a simple monomeric subunits joined with others by covalent bond to form the structure of the thousands of different proteins. There are twenty standard α -amino acids all of them are L-amino acids. The first amino acid to be discovered was asparagine in 1806, and the last amino acid of the twenty to be discovered, threonine, was not identified until 1938 ⁽³⁹⁾. The amino acids are the unity structural of proteins. All amino acids have α -carbon, to which are bonded four groups; (hydrogen, amino and carboxyl) group, and a unique side chain,

known as R-group as shown in figure (1-15). These molecules differ in their R-group, from which can be classify its into functional types ⁽⁴⁰⁾.

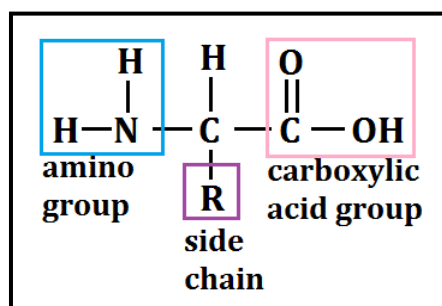
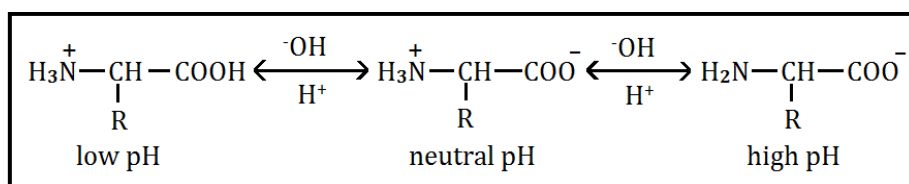


Figure (1-15): General structure of amino acids.

We commonly write amino acids with an carboxyl ($-\text{COOH}$) group and amino ($-\text{NH}_2$) group, but their actual structure is ionic and depends on the pH. The carboxyl group loses a proton, giving a carboxylate ion, and the amino group is protonated to form ammonium ion. This structure is called a dipolar ion or a zwitterion. An amino acid in acidic medium (low pH) have positive charge but in basic medium (high pH) it is have negative charge as shown below ⁽⁴¹⁾:



At neutral pH the carboxyl group of an amino acid is in its base form ($-\text{COO}^-$), and the amino group is in its acid form ($-\text{NH}_3^+$). Thus each amino acid can be behave as an acid and a base. The amphoteric form is used to describe this property. Molecules that have both positive and negative charges are called zwitterions ⁽⁴²⁾. Many researchers investigated the effect of inhibition of environment friendly inhibitors such as amino acids on metal corrosion. This is due to the amino acids are non-toxic, biodegradable, relatively cheap, and quickly soluble in

aqueous media and produced with high purity ⁽⁴³⁾. In general, the amino acids contain two ionisable functional groups have opposite chemical nature, the amine group which have basic property and the carboxyl group which have acidic property. These groups can coordinate with metal surface through the nitrogen atom of the amino group, oxygen atom of the carboxyl group and other hetro atoms such as sulphur. A combination of inhibitors with metal surface is likely to provide multiple effects required for effective corrosion inhibition ⁽⁴⁴⁾. Several researches have confirmed that amino acids can be used as corrosion inhibitors for many metals because of their functional groups they form complexes with metal ions which precursor from and on metal surfaces. These complexes coverage a large surface area and protecting the metals surfaces from corrosive agents that present in the environment ⁽⁴⁵⁾.

1.7.2 Classification of Amino Acids

There are several ways to classify amino acids based on several properties. Here, these molecules can be classified into six major groups, depending on their chemical composition and the general chemical characteristics of their R groups ⁽⁴⁶⁾. Table (1-1) illustrates this category.

Table (1-1): Classification of amino acids based on their group ⁽⁴⁶⁾.

Class	Class Name of the amino acids
Aliphatic	Glycine, Alanine, Valine, Leucine, Isoleucine.
Hydroxyl or Sulfur containing	Serine, Cysteine, Threonine, Methionine.
Cyclic	Proline
Aromatic	Phenylalanine, Tyrosine, Tryptophan.
Basic	Histidine, Lysine, Arginine.
Acidic and their Amide	Aspartate, Glutamate, Asparagine, Glutamine.

1.8 Quantum Chemical and Corrosion Studies

Quantum mechanics explains molecules interactions among nuclei and electrons, and molecular geometry in terms of minimum energy arrangements of nuclei. All quantum mechanical methods go back to the Schrödinger equation, which for the special case of hydrogen atom (a single particle in three dimensions) may be solved exactly. It is easy to generalize the Schrödinger equation to a multinuclear and multielectron system ⁽⁴⁷⁾.

$$\hat{H} \Psi = E \Psi \dots\dots\dots (1-15)$$

Where, Ψ : is a many-electron wavefunction, and \mathbf{H} : is the Hamiltonian operator.

Calculations of quantum-chemistry have been widely used to study the reaction mechanisms and to investigation the experimental results as well as to solve chemical ambiguities. This is an useful path to investigate the mechanisms of reaction in the molecule and its electronic structure levels 6. The structure and electronic parameters can be knowable through theoretical calculations using the computational methodologies of quantum chemistry. Density functional theory (DFT) methods become very common in the last years. This is because they can be exactitude similar to other methods in less time and with a smaller investment from the computational point of view ⁽⁴⁸⁾. Quantum chemical principles have been applied in widely field of corrosion studies. The use of border molecular energies to predict the ability of electron donating of an inhibitor (i.e energy of the highest occupied molecular orbital, E_{HOMO}), the tendency to accept electron (i.e energy of the lowest unoccupied molecular orbital, E_{LUMO}) and as a measure of the ease of reactivity (i.e energy gap), have been widely investigated by many researchers ⁽⁴⁹⁾.

The ionization potential (I) and the electron affinity (A) can be calculated by application of Koopman's theorem. This theorem states a relationship between the energies of the HOMO and the LUMO and the ionization potential and electron affinity, respectively ⁽⁵⁰⁾.

$$I = -E_{HOMO} \dots\dots\dots (1-16)$$

$$A = -E_{LUMO} \dots\dots\dots (1-17)$$

The absolute electronegativity (χ) and global hardness (γ) of the inhibitor molecule can be approximated as follows ⁽⁵¹⁾:

$$\chi = \frac{(E_{LUMO} + E_{HOMO})}{2} \dots\dots\dots (1-18)$$

$$\gamma = \frac{(E_{LUMO} - E_{HOMO})}{2} \dots\dots\dots (1-19)$$

This reactivity index measures the stabilization in energy when the system accepts an additional electronic charge from the environment. Thus the fraction of electrons transferred from the inhibitor molecules to the metallic surface, ΔN , is given by

$$\Delta N = \frac{\chi_{Fe} - \chi_{inh}}{2(\eta_{Fe} - \eta_{inh})} \dots\dots\dots (1-20)$$

Where, χ_{Fe} and χ_{inh} are the absolute electronegativity of iron and inhibitor molecule, respectively. η_{Fe} and η_{inh} are the absolute hardness of iron and the inhibitor molecule, respectively. A theoretical value of $\chi_{Fe} = +7.0$ eV and $\eta_{Fe} = 0$ eV⁻¹ ⁽⁵²⁾.

1.9 Literature Survey

S. Gowri, J. Sathiyabama, and S. Rajendran, (2014), studied the corrosion inhibition effect of carbon steel in sea water by L-Arginine-Zn²⁺ system. The inhibition efficiency of L-Arginine-Zn²⁺ system in controlling corrosion of carbon steel in sea water has been evaluated by the weight-loss method. The formulation consisting of 250 ppm of L-Arginine and 25 ppm of Zn²⁺ has 91% IE. A synergistic effect exists between L-Arginine and Zn²⁺. Polarization study reveals that the L-Arginine-Zn²⁺ system functions as an anodic inhibitor and the formulation control the anodic reaction predominantly. AC impedance spectra reveal that protective film is formed on the metal surface. Cyclic voltammetry study reveals that the protective film is more compact and stable even in a 3.5% NaCl environment. The nature of the protective film on a metal surface has been analyzed by FTIR, SEM, and AFM analysis ⁽⁵³⁾.

Hany M. Abd El-Lateef, Mohamed Ismael and Ibrahim M.A. Mohamed, (2015), studied the novel schiff base amino acid as corrosion inhibitors for carbon steel in CO₂-saturated 3.5% NaCl solution: experimental and computational study. Corrosion inhibition and adsorption behavior of some novel Schiff bases based on amino acids on carbon steel in CO₂-saturated 3.5% NaCl solution at 50°C was investigated using gravimetric, potentiodynamic polarization, linear polarization resistance corrosion rate, and scanning electron microscope (SEM)/energy-dispersive X-ray spectroscopy analysis (EDAX) techniques. Results show that the inhibition efficiency increases when the inhibitor concentration increases. Potentiodynamic polarization curves reveal that the used Schiff bases are mixed type inhibitors. Experimental data indicate that these Schiff base inhibitors adsorb at the carbon steel/solution interface according the Langmuir adsorption isotherm. SEM/EDAX was used to examine the

surface morphology of carbon steel samples in the absence and presence of the inhibitors. Quantum chemical calculations were further applied to explain the experimental results ⁽⁵⁴⁾.

A. Sahaya Raja, S. Rajendran, R. Nagalakshmi, J. AngelinThangakani and M. Pandiarajan, (2012), studied the environmental friendly inhibitor system glycine-Zn²⁺, has been investigated by weight loss method. A synergistic effect exists between glycine and Zn²⁺ system. The formulation consisting of 250 ppm of glycine and 50 ppm of Zn²⁺ offers good inhibition efficiency of 82%. Polarization study reveals that this formulation functions as an anodic inhibitor. The FTIR spectra study leads to the conclusion that the Fe²⁺-Gly complex formed on anodic sites of the metal surface controlled the anodic reaction and Zn(OH)₂ formed on the cathodic sites of the metal surface controlling the cathodic reaction. The surface morphology and the roughness of the metal surface have been analyzed with atomic force microscopy. A suitable mechanism of corrosion inhibition is proposed based on the results obtained from weight loss study and surface analysis technique. The eco-friendly inhibitor glycine-Zn²⁺ system may find application in cooling water system ⁽⁵⁵⁾.

Anthony Samy Sahaya Raja and Susai Rajendran, (2012), studied the inhibition of corrosion of carbon steel in well water by arginine-Zn²⁺ system. Environmental friendly inhibitor system arginine-Zn²⁺, has been investigated by weight-loss method. A synergistic effect exists between arginine and Zn²⁺ system. The formulation consisting of 250 ppm of arginine and 5 ppm of Zn²⁺ offers good inhibition efficiency of 98 %. Polarization study reveals that this formulation functions as an anodic inhibitor. AC impedance spectra reveal that a protective film is formed on

the metal surface. The FTIR spectral study leads to the conclusion that the Fe^{2+} - DL-arginine complex, formed on anodic sites of the metal surface, controls the anodic reaction. $\text{Zn}(\text{OH})_2$ formed on the cathodic sites of the metal surface controls the cathodic reaction. The surface morphology and the roughness of the metal surface were analyzed with Atomic Force Microscope. A suitable mechanism of corrosion inhibition is proposed based on the results obtained from weight loss study and surface analysis technique ⁽⁵⁶⁾.

A.Sahaya Raja, S.Rajendran, J.Sathiyabama, V.Prathipa, I.N. Karthika and A Krishnaveni, (2015), studied the use of L-Alanine as nature – friendly corrosion inhibitor for carbon steel in aqueous medium. The corrosion and inhibition behaviors of carbon steel in the presence of L-Alanine and ZnSO_4 have been studied using gravimetric method and electrochemical techniques. Results obtained by various techniques are close to each other and maximum Inhibition efficiency 83% is acknowledged at the inhibitor concentration of 250 ppm of L-Alanine and 5ppm Zn^{2+} . Synergistic parameters suggest that a synergistic effect exists between L –Alanine and Zn^{2+} . Statistical study of “F” test revealed that the synergistic effect existing between L-Alanine and Zn^{2+} . The effective synergistic formulation with 150 ppm of SDS has 98% corrosion inhibition efficiency and 100% biocidal efficiency. UV-visible absorption spectra indicates that a complex in solution is formed between L-Alanine - Fe^{2+} . Fluorescence spectral analysis was used in detecting the presence of an iron – inhibitor complex and the coordination sites of the metal inhibitor with iron were determined by the FT-IR spectra. Scanning electron microscopy (SEM) study confirmed that the inhibition of corrosion of carbon steel is through adsorption of the Inhibitors molecule on the surface of the metal. Energy dispersive analysis of X-rays (EDAX)

shows that in the presence of Inhibitors the suppression of Fe peaks , additional line of „N,, and „Zn“ signal and enhancement in „C“ and „O“ signal are observed. These data show that metal surface is covered by adsorbed layer of inhibitors molecule that protects carbon steel against corrosion. The surface morphology of the protective film on the metal surface was characterized by using atomic force microscopy (AFM). A suitable mechanism of corrosion inhibition is proposed based on the results obtained from weight loss study, electrochemical study and surface analysis technique. The eco-friendly inhibitor L - Alanine -Zn²⁺ system may find application in cooling water system ⁽⁵⁷⁾.

M.A. Migahed, E.M.S. Azzam and S.M.I. Morsy, (2009), studied the electrochemical behavior of carbon steel in acid chloride solution in the presence of dodecyl cysteine hydrochloride self-assembled on gold nanoparticles. In this work, the dodecyl cysteine hydrochloride surfactant was synthesized. The surface properties of this surfactant were studied using surface tension technique. The nanostructure of this surfactant with the prepared gold nanoparticles was investigated using TEM technique. The synthesized surfactant and its nanostructure with the prepared gold nanoparticles were examined as non-toxic corrosion inhibitors for carbon steel in 2 M HCl solution using potentiodynamic polarization and electrochemical impedance spectroscopy techniques. The results show that the percentage inhibition efficiency ($\eta\%$) for each inhibitor increases with increasing concentration until critical micelle concentration (CMC) is reached. The maximum inhibition efficiency approached 76.6% in the presence of 175 ppm of dodecyl cysteine and 90.8% in the presence of the same concentration of dodecyl cysteine hydrochloride self-assembled on gold nanoparticles. Polarization data indicate that the selected additives act as mixed type inhibitors.

The slopes of the cathodic and anodic Tafel lines (b_c and b_a) are approximately constant and independent of the inhibitor concentration. Analysis of the impedance spectra indicates that the charge transfer process mainly controls the corrosion process of carbon steel in 2 M HCl solution both in the absence and presence of the inhibitors. Adsorption of these inhibitors on carbon steel surface is found to obey the Langmuir adsorption isotherm. From the adsorption isotherms the values of adsorption equilibrium constants (K_{ads}) were calculated. The relatively high value of (K_{ads}) in case of dodecyl cysteine hydrochloride self-assembled on gold nanoparticles reveals a strong interaction between the inhibitor molecules and the metal surface ⁽⁵⁸⁾.

Khadim F. Al-Sultani and Shaymaa Abbas Abdulsada, (2013), studied the improvement corrosion resistance of low carbon steel by using natural corrosion inhibitor. The main objective of the present work involved the study of the inhibiting properties of natural product as Spearmint plant extract as a safety and an environmentally friendly corrosion inhibitor for low carbon steel in (3.5% NaCl) solution. Results showed when the immersion model in (3.5% NaCl) solution that contains the inhibitor with concentration of (15% in volume), it's getting a decrease in lost weight, indicating a layer of adequate oxide on the surface of the steel, indicating that the amount of loss weight decrease with increasing concentration of inhibitor and this shows the damper on his ability to form a protective layer ⁽⁵⁹⁾.

H. Zarrok, A. Zarrouk, R. Salghi, B. Hammouti, M. Elbakri, M. Ebn Touhami, F. Bentiss and H. Oudda, (2014), studied a cysteine derivative as a corrosion inhibitor for carbon steel in phosphoric acid solution. Inhibition of corrosion of carbon steel in phosphoric acid solution by use

of L-cysteine methyl ester hydrochloride has been investigated by measurement of weight loss and use of electrochemical methods. The efficiency of inhibition was increased by increasing the concentration of the inhibitor and reduced by increasing the temperature. Polarization studies revealed that this compound behaves as mixed type inhibitor. Electrochemical impedance spectroscopy showed that dissolution of the steel occurs as a result of charge-transfer. Adsorption of the inhibitor obeyed the Langmuir adsorption isotherm. Kinetic and thermodynamic data were calculated and are discussed ⁽⁶⁰⁾.

Ameena Mohsen Al-Bonayan, (2015), studied the corrosion inhibition of carbon steel in hydrochloric acid solution by senna-italica extract. The potential of Senna-Italica extract as a corrosion inhibitor for carbon steel in 1 M HCl was determined using electrochemical frequency modulation (EFM), electrochemical impedance spectroscopy (EIS), potentiodynamic polarization and weight loss methods. Surface examination was tested using scanning electron microscope with energy dispersive X-ray spectroscopy (SEM–EDX). The adsorption process obeyed Freundlich adsorption isotherm. Maximum inhibition was attained 92.6% at the concentration of 600 ppm for senna-italica extract. Potentiodynamic polarization measurement studies revealed that senna-italica extract behave as a mixed-type inhibitor in 1 M HCl. The inhibition efficiencies of senna-italica extract obtained from the all various measurements were in good agreement ⁽⁶¹⁾.

Jia-jun Fu, Su-ning Li, Ying Wang, Lin-hua Cao and Lu-de Lu, (2010), studied the corrosion inhibition behaviour of four selected amino acid compounds, namely L-cysteine, L-histidine, L-tryptophan and L-serine on mild steel surface in deaerated 1 M HCl solution were studied

electrochemically by Tafel polarization and electrochemical impedance spectroscopy methods and computationally by the quantum chemical calculation and molecular dynamics simulation. Electrochemical results show that these amino acid compounds inhibit the corrosion of mild steel in 1 M HCl solution significantly. The order of inhibition efficiency of these inhibitors follows the sequence: L-tryptophan > L-histidine > L-cysteine > L-serine. The quantum chemical calculations were performed to characterize the electronic parameters which are associated with inhibition efficiency. The molecular dynamics simulations were applied to find the equilibrium adsorption configurations and calculate the interaction energy between inhibitors and iron surface. Results obtained from Tafel and impedance methods are in good agreement. The electrochemical experimental results are supported by the theoretical data

(62)

1.10 The Aim of the Research

- ❖ Potentiostatic polarization measurement of corrosion behavior of carbon steel alloys in saline solution (3.5% NaCl) with different temperatures in the range of (293-313) K.
- ❖ Studying the inhibition effect of amino acids (L-lysine, L-serine, L-tryptophan and L-valine) for the corrosion of carbon steel at different concentrations (5×10^{-4} , 1×10^{-3} , 5×10^{-3} and 1×10^{-2}) M in the temperatures range (293 - 313) K at pH 2 and pH 11.
- ❖ Quantum mechanical completion using DFT method with B3LYP/6-31G basis set was applied to achieve correlation between the inhibitive effect and molecular structure of amino acids.
- ❖ Studying the surface morphologies of carbon steel in 3.5% NaCl solution in presence of 1×10^{-2} M of (L-lysine, L-serine, L-tryptophan and L-valine) in pH 2 and pH 11 by using scanning electron microscope (SEM) to show the effect of inhibitors on carbon steel surface.

Chapter Two

Experimental

2.1 Chemicals and Material

2.1.1 Carbon Steel Alloy

The chemical composition of carbon steel is listed in table (2-1).

Table (2-1): Chemical composition of carbon steel.

Element	Al	C	Cr	Cu	Mo	Ni	P	Si	Fe
Wt.%	0.06	0.19	0.04	0.02	0.03	0.017	0.018	0.35	rest

2.1.2 Chemicals

The chemicals used in this research are listed in table (2-2).

Table (2-2): List of chemicals used.

material	supplier	% purity
Acetone	ROMIL-SA	99.7
Diamond product spray	Struers	High quality diamond product
Ethanol	Sigma-aldrich	99.8
L-lysine	Fluka	99
L-serine	Fluka	99
L-tryptophan	Fluka	99
L-valine	Fluka	99
Sodium chloride	EDUTEK	99
Sodium hydroxide	BDH	99.9
Sulphuric acid	HIMEDIA	98

2.2 Inhibitors

As in the case with all experiments, the metal oxidation obtained during corrosion can be inhibited by adding organic substances to the electrolyte solution. An attempt was made in this research to use amino acids such as:

❖ **L-lysine (Lys)**

L-lysine or 2,6-Diaminohexanoic acid is an aliphatic and polar amino acid.

❖ **L-serine (Ser)**

L-serine or 2-Amino-3-hydroxypropanoic acid is a linear molecule and polar in nature. This amino acid is water-loving because of this polar characteristic.

❖ **L-tryptophan (Trp)**

L-tryptophan or 2-Amino-3-(1H-indol-3-yl) propanoic acid is a non-polar aromatic amino acid.

❖ **L-valine (Val)**

L-valine or 2-amino-3-methylbutanoic acid is a non-polar aliphatic amino acid.

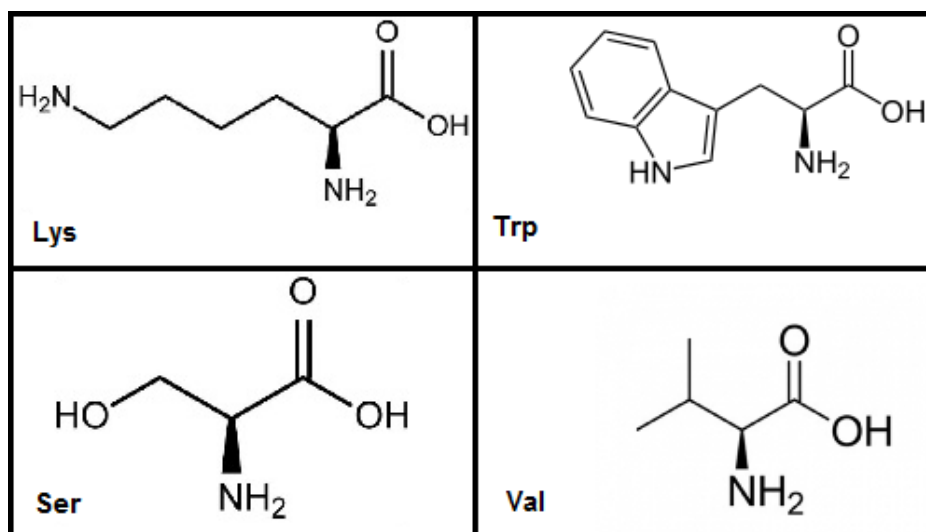


Figure (2-1): Structures of amino acids.

Table (2-3): Properties of amino acids.

Abbreviation	Val	Trp	Ser	Lys
Appearance	White powder	White powder	White Crystals	Reddish-brown Crystals
Chemical formula	$C_5H_{11}NO_2$	$C_{11}H_{12}N_2O_2$	$C_3H_7NO_3$	$C_6H_{14}N_2O_2$
Molar mass	117.15 $g \cdot mol^{-1}$	204.23 $g \cdot mol^{-1}$	105.09 $g \cdot mol^{-1}$	146.19 $g \cdot mol^{-1}$
Solubility in water	soluble	11.4 g/L at 25 °C	soluble	1.5 kg/L at 25 °C

2.3 Preparation of Solutions

1. Saline solution (3.5% NaCl) was prepared by dissolving 35g of NaCl in 1000 mL at pH (2 and 11) values.
2. L-Lysine was prepared with four different concentration (5×10^{-4} , 1×10^{-3} , 5×10^{-3} , and 1×10^{-2}) M by dissolving (0.073, 0.146, 0.73 and 1.46) g respectively in 1000 mL of 3.5% NaCl solution with pH (2 and 11).
3. L-serine was prepared with four different concentration (5×10^{-4} , 1×10^{-3} , 5×10^{-3} , and 1×10^{-2}) M by dissolving (0.0525, 0.105, 0.525 and 1.05) g respectively in 1000 mL of 3.5% NaCl solution with pH (2 and 11).
4. L-tryptophan was prepared with four different concentration (5×10^{-4} , 1×10^{-3} , 5×10^{-3} , and 1×10^{-2}) M by dissolving (0.102, 0.204, 1.02 and 2.04) g respectively in 1000 mL of 3.5% NaCl solution with pH (2 and 11).
5. L-valine was prepared with four different concentration (5×10^{-4} , 1×10^{-3} , 5×10^{-3} , and 1×10^{-2}) M by dissolving (0.0585, 0.117, 0.585 and 1.17) g respectively in 1000 mL of 3.5% NaCl solution with pH (2 and 11).
6. 1M H_2SO_4 solution was prepared to adjust pH 2.

7. 1M NaOH solution was prepared to adjust pH 11.

2.4 Sample Preparation

Circular carbon steel samples with 2cm in diameter and 1mm thickness were polished to mirror finish with emery paper in different grades (320, 500, 1000, 2400, 4000) with diamond product spray that contain ethanol with different size of diamond particles (1, 3, 6, 9) μm and then washed with ethanol, acetone and finally rinsed with distilled water.

2.5 Instruments

The instruments used in this study are tabulated in table (2-3).

Table (2-4): The Instruments were use in this study.

Instrument	Source	Model	Function
Potentiostat/ Galvanostat	Germany	M lab 200 with software	Corrosion test
Thermostat device	Danmark	HETOFRIG DT	Adjust the temperature of cell corrosion
pH meter	Singapore	BP3001	Adjust the pH of solution
Magnetic stirrer	France	Tacussel AGIMAX	Mix the component of solution
Scanning electron microscopy	Japan	FEI Inspect- S50	Morphoioy of surface

2.6 The Potentiostatic Set-Up

2.6.1 Potentiostat/Galvanostat Device-M lab 200

Potentiostatic polarization measurements were carried out by using Potentiostat. M Lab (WENKING MLab multichannel and SCI-MLab corrosion measuring system from Bank Electronics- Intelligent controls GmbH, Germany 2007) as shown in figure (2-2) and the schematic

diagram of potentiostat as shown in figure (2-3). It is a significant advance instrument for electrochemical measurements such as potential (E), current density (i) and develop E vs. $\log(i_{\text{corr}})$ plots (polarization curve). It is provided with electrochemical calculations such as Tafel line evaluation (cathodic and anodic regions). M Lab is adjusted by computer desktop running Windows XP.



Figure (2-2): Potentiostat/Galvanostat device.

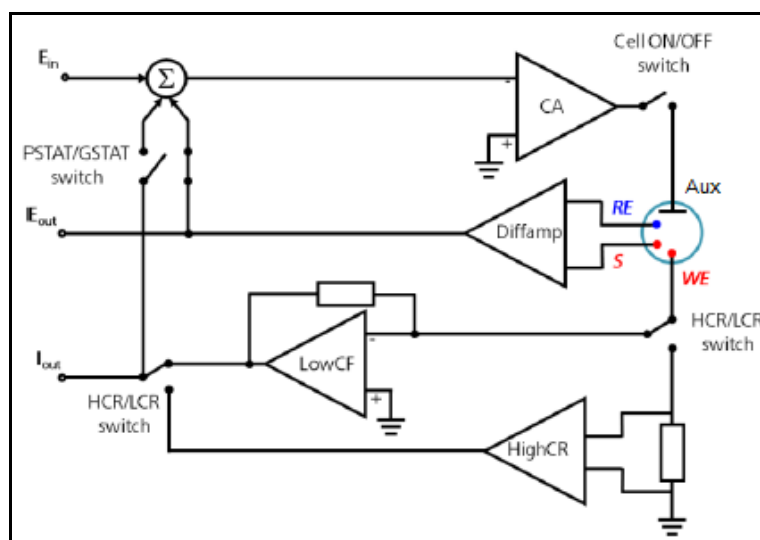


Figure (2-3): Schematic diagram of potentiostat.

2.6.2 Corrosion Cell

A container cell made of Pyrex with (1L) capacity consists of two vessels, internal, that contain working solution and external, that connecting with a thermostat device in order to adjust the temperature of the working solution. In addition to cover with openings to insert the three electrodes and thermometer to find out the temperature of the working solution inside the cell as shown in figure (2-4).



Figure (2-4): Corrosion cell set-up.

2.6.2.1 Three-Electrode System Set-up:

The potential of the working electrode was measured against the reference electrode, as long as an ohmic resistance sequence is reduced and the current is flow only between the platinum electrode and the working electrode. Detailed description of the electrodes were given below:

❖ Working Electrode

Circular carbon steel specimen placed on a holder in order to make specific surface area that only is being exposed to the examine solution. The conductive surface area is equal to 1cm^2 as shown in figure (2-5).



Figure (2-5): Working electrode.

❖ Reference Electrode

The reference electrode used in this search was saturated calomel electrode (SCE), having a potential of 0.2444 V at 25 °C. The electrode is made contact with the examined solution through a Luggin capillary. The bridge probe tip was fixed about (2mm) far from the surface of the working electrode as shown in figure (2-6).

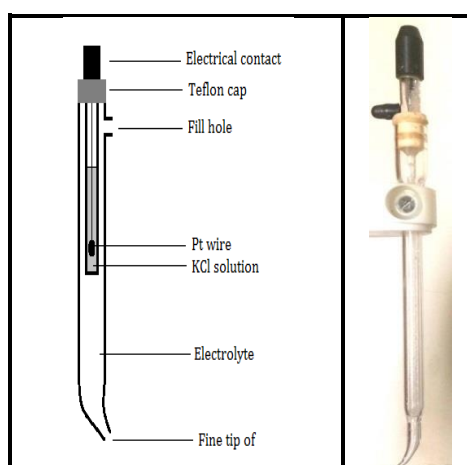
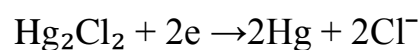


Figure (2-6): Reference electrode.

❖ Auxiliary Electrode

The auxiliary electrode used in the electrochemical cell was platinum electrode seated opposite to the working electrode.

2.6.3 Thermostat

Thermostat is a device that used in order to maintain the water temperature that flows through an external vessel of corrosion cell and equals to the required temperature. Figure (2-7) represent the system set-up for corrosion measurements.

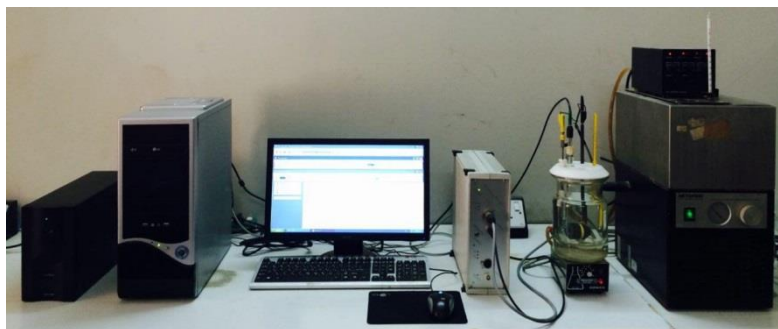


Figure (2-7): Complete system set-up for polarization measurements.

2.7 Procedures of Corrosion Test

The corrosion behavior of the carbon steel alloy in absence and presence of various concentrations Lys, Ser, Trp and Val inhibitors in 3.5% NaCl solution at different temperatures were studied by using Tafel extrapolation method to determine the corrosion potential and corrosion current density.

2.7.1 Open Circuit Potential Test

Open circuit potential (OCP), is the potential of the working electrode that measured against a reference electrode by a high impedance potentiometer so there is no current flows between the working electrode and the reference electrode. To evaluate the open circuit potential value of carbon steel alloy, the alloy was immersed in the saline solution (3.5% NaCl) in the absence and presence of inhibitors for 900 second. After reaching equilibrium between the working electrode

and testing solution, the obtained potential is known as open circuit potential.

2.7.2 Tafel Extrapolation

Mixed potential theory was based on the fundamentals of the Tafel extrapolation to obtain the corrosion rate. Potentiostat device software was used to carry out the polarization test. The segments for linear Tafel of cathodic and anodic curves were extrapolated to corrosion potential in order to obtain corrosion parameters. The potentiostatic experiments were carried out using WINKING M Lab potentiostat/galvanostat. Polarization curves measurements have been carried out by changing the electrode potential automatically from -200 mV to +200 mV versus the open circuit potential with an interval of 10 mV and scan rate of 2 mV/s. This wide range of potential allows the determination of corrosion potential (E_{corr}), corrosion current density (i_{corr}), anodic (b_a) and cathodic (b_c) Tafel slopes from the polarization diagram as shown in figure (2-8).

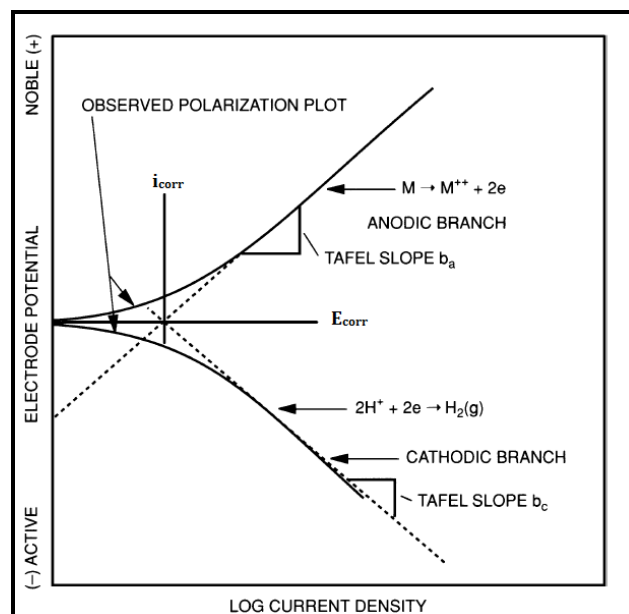


Figure (2-8): Cathodic and anodic polarization diagram ⁽³¹⁾.

2.8 Theoretical Test

Gaussian 09W program was used to make a correlation between the results of quantum chemical calculations and the experimental efficiencies of Lys, Ser, Trp and Val being corrosion inhibitors. The quantum chemical calculations have been performed by using the method of density functional theory (DFT) with Beck's three parameter exchange functional along with Lee-Yang-Parr non-local correlation functional (B3LYP) with and 6-31G basis set. The energy of the highest occupied molecular orbital (E_{HOMO}), the lowest unoccupied molecular orbital (E_{LUMO}), energy gap (ΔE), dipole moment (μ), total energy (E_{Total}), absolute electronegativity (χ), global hardness (γ) and the fraction of electrons transferred (ΔN) of the inhibitors were calculated by using the above given computer code package.

Chapter Three

Results and Discussion

3.1 The Polarization Curves

Figures (3-1) to (3-8) show the potentiostatic polarization curves of the carbon steel in 3.5% of sodium chloride solution (blank) and in the presence of various concentrations (5×10^{-4} , 1×10^{-3} , 5×10^{-3} and 1×10^{-2}) M of inhibitor molecules (Val, Ser, Trp and Lys) in acidic (pH 2) and basic (pH 11) media at five different temperatures ranging between 293K-313K.

The corrosion current densities (i_{corr}) and corrosion potentials (E_{corr}) have been obtained by extrapolation of the linear segments of cathodic and anodic Tafel lines to the point of intersection ⁽⁶³⁾. Tables (3-1) to (3-8) show the resulting data (the corrosion potential (E_{corr}), corrosion current densities (i_{corr}), anodic (b_a) and cathodic (b_c) Tafel slopes, corrosion rates (CR), and penetration rates (PR)) which have been obtained from polarization curves.

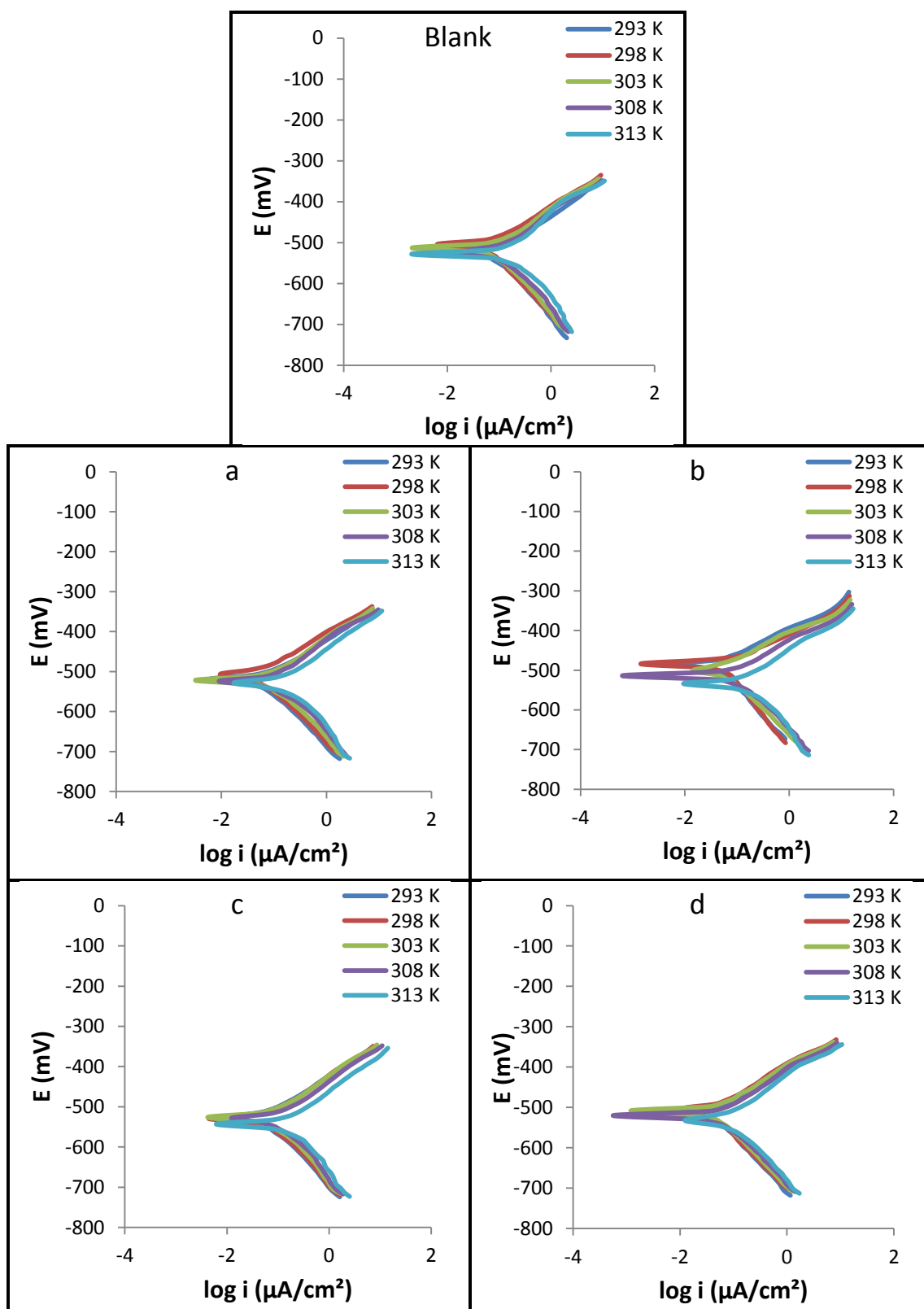


Figure (3-1): Polarization curves for carbon steel corrosion in the blank (saline solution) and in presence of Val with different concentrations (a) 5×10^{-4} M, (b) 1×10^{-3} M, (c) 5×10^{-3} M and (d) 1×10^{-2} M at temperature range (293-313) K and pH 2.

Table (3-1): Corrosion parameters of carbon steel in the blank (saline solution) and in presence of Val with different concentrations (5×10^{-4} , 1×10^{-3} , 5×10^{-3} and 1×10^{-2}) M at temperature range (293-313) K and pH 2.

Inh. [M]	T (K)	$-E_{\text{corr}}$ (mV)	i_{corr} ($\mu\text{A}/\text{cm}^2$)	Tafel slope (mV/dec)		CR ($\text{g}/\text{m}^2\text{d}$)	PR (mm/Y)
				$-b_c$	$+b_a$		
0	293	507.1	51.09	92.50	62.6	12.8	0.593
	298	513.9	55.67	136.7	73.2	13.9	0.646
	303	516.8	66.99	120.9	81.3	16.7	0.778
	308	525.8	87.14	107.0	95.1	21.8	1.010
	313	530.3	92.28	103.5	91.9	22.1	1.700
5×10^{-4}	293	510.3	36.42	90.60	65.8	9.10	0.423
	298	515.6	41.11	105.9	74.8	10.3	0.470
	303	517.9	50.04	94.10	66.2	12.5	0.581
	308	524.6	66.31	86.20	65.8	16.6	0.770
	313	529.1	71.60	92.20	70.4	17.9	0.807
1×10^{-3}	293	483.6	31.75	89.50	63.2	8.12	0.369
	298	489.6	35.83	91.50	65.1	8.91	0.416
	303	500.2	44.42	108.3	74.5	11.1	0.516
	308	512.1	58.42	91.20	68.0	14.6	0.678
	313	528.8	63.15	78.90	61.3	15.6	0.728
5×10^{-3}	293	524.8	28.81	72.00	53.2	7.26	0.338
	298	526.4	32.09	71.70	54.1	8.03	0.373
	303	529.1	38.79	78.10	59.9	9.87	0.459
	308	532.9	52.35	85.00	63.9	13.1	0.608
	313	535.5	59.15	97.00	70.9	14.7	0.686
1×10^{-2}	293	512.9	23.87	70.60	51.0	5.89	0.276
	298	517.1	26.99	104.2	67.7	6.81	0.324
	303	520.5	32.72	108.8	72.7	8.18	0.380
	308	525.2	43.94	100.2	74.5	11.0	0.510
	313	532.2	51.68	92.30	71.2	13.1	0.684

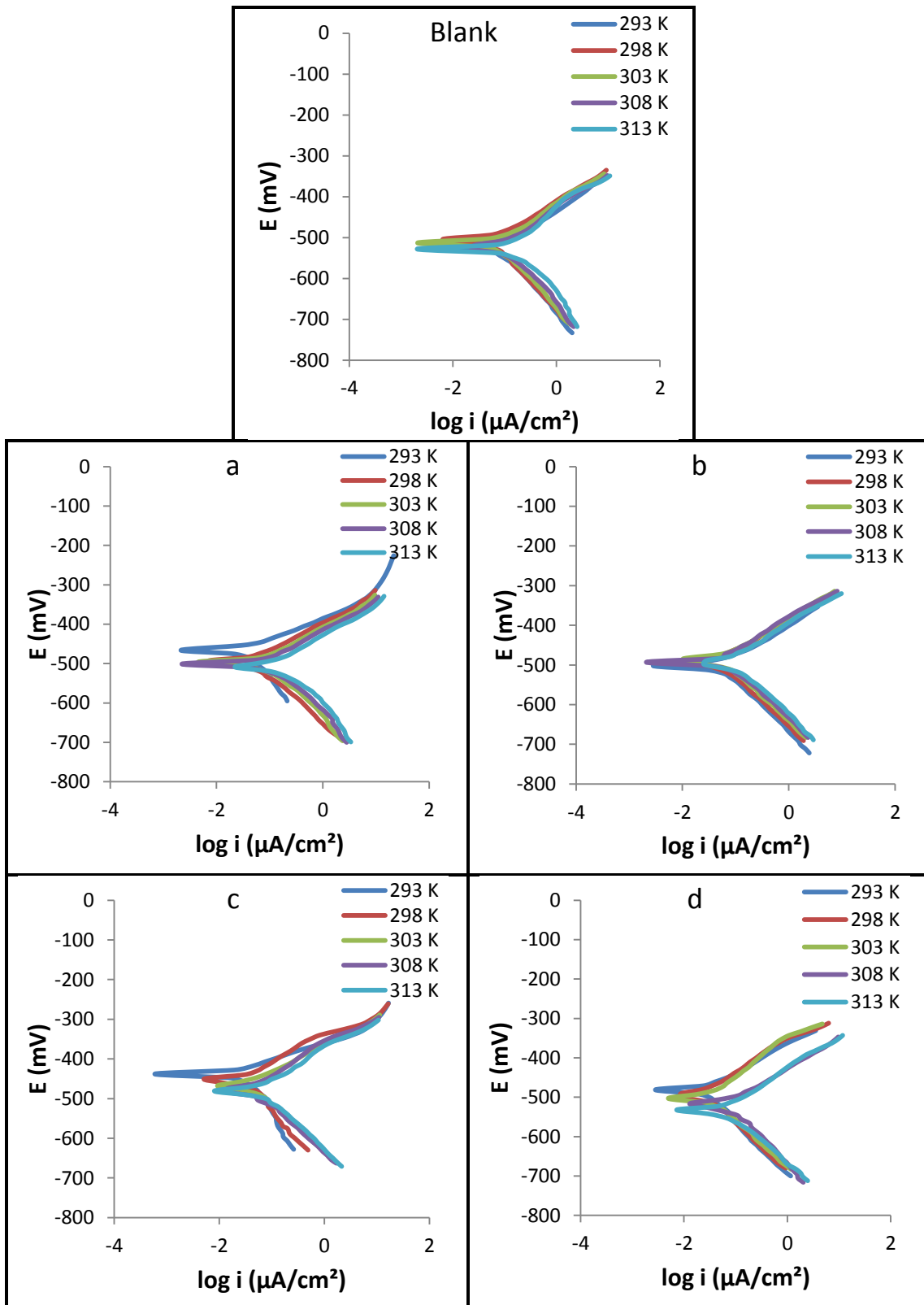


Figure (3-2): Polarization curves for carbon steel corrosion in the blank (saline solution) and in presence of Ser with different concentrations (a) 5×10^{-4} M, (b) 1×10^{-3} M, (c) 5×10^{-3} M and (d) 1×10^{-2} M at temperature range (293-313)K and pH 2.

Table (3-2): Corrosion parameters of carbon steel in the blank (saline solution) and in presence of Ser with different concentrations (5×10^{-4} , 1×10^{-3} , 5×10^{-3} and 1×10^{-2}) M at temperature range (293-313) K and pH 2.

Inh. [M]	T (K)	$-E_{\text{corr}}$ (mV)	i_{corr} ($\mu\text{A}/\text{cm}^2$)	Tafel slope (mV/dec)		CR ($\text{g}/\text{m}^2\text{d}$)	PR (mm/Y)
				$-b_c$	$+b_a$		
0	293	507.1	51.09	92.50	62.6	12.8	0.593
	298	513.9	55.67	136.7	73.2	13.9	0.646
	303	516.8	66.99	120.9	81.3	16.7	0.778
	308	525.8	87.14	107.0	95.1	21.8	1.010
	313	530.3	92.28	103.5	91.9	22.1	1.700
5×10^{-4}	293	485.2	33.76	121.9	68.7	8.44	0.392
	298	490.9	37.71	93.10	60.0	9.43	0.438
	303	499.1	46.67	97.90	62.4	11.7	0.542
	308	503.6	60.42	88.60	63.0	15.0	0.701
	313	509.7	67.31	98.30	66.7	17.0	0.798
1×10^{-3}	293	490.3	25.50	83.90	51.8	6.39	0.295
	298	492.7	30.48	98.70	58.6	7.63	0.355
	303	494.9	37.43	105.5	60.7	9.29	0.428
	308	496.4	49.64	99.60	65.1	12.4	0.576
	313	497.1	53.15	109.0	67.9	13.2	0.613
5×10^{-3}	293	437.7	23.10	108.0	59.4	5.78	0.269
	298	453.7	27.17	129.1	70.4	6.97	0.327
	303	463.9	32.85	131.3	64.8	8.18	0.381
	308	475.8	43.08	154.3	78.4	10.8	0.500
	313	479.4	50.18	126.6	71.7	13.0	0.589
1×10^{-2}	293	480.2	19.30	99.70	58.2	4.84	0.226
	298	491.3	25.41	127.7	68.0	6.35	0.295
	303	502.5	30.70	118.4	59.9	7.68	0.356
	308	520.8	40.73	104.7	61.7	10.2	0.473
	313	533.8	47.41	139.4	73.4	11.9	0.550

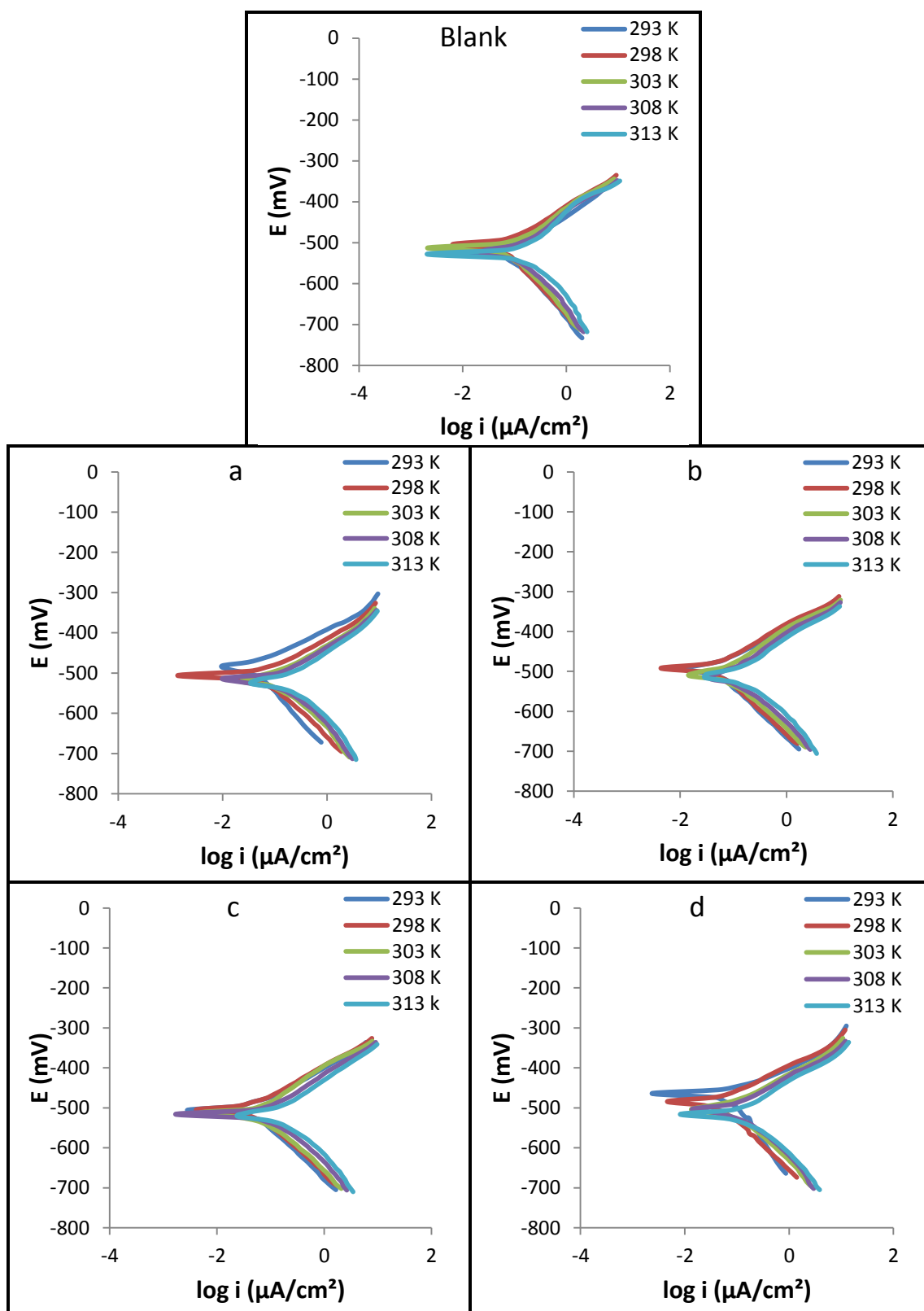


Figure (3-3): Polarization curves for carbon steel corrosion in the blank (saline solution) and in presence of Trp with different concentrations (a) 5×10^{-4} M, (b) 1×10^{-3} M, (c) 5×10^{-3} M and (d) 1×10^{-2} M at temperature range (293-313)K and pH 2.

Table (3-3): Corrosion parameters of carbon steel in the blank (saline solution) and in presence of Trp with different concentrations (5×10^{-4} , 1×10^{-3} , 5×10^{-3} and 1×10^{-2}) M at temperature range (293-313) K and pH 2.

Inh. [M]	T (K)	$-E_{\text{corr}}$ (mV)	i_{corr} ($\mu\text{A}/\text{cm}^2$)	Tafel slope (mV/dec)		CR ($\text{g}/\text{m}^2\text{d}$)	PR (mm/Y)
				$-b_c$	$+b_a$		
0	293	507.1	51.09	92.5	62.6	12.8	0.593
	298	513.9	55.67	136.7	73.2	13.9	0.646
	303	516.8	66.99	120.9	81.3	16.7	0.778
	308	525.8	87.14	107.0	95.1	21.8	1.010
	313	530.3	92.28	103.5	91.9	22.1	1.700
5×10^{-4}	293	497.9	44.29	150.9	98.9	10.6	0.511
	298	506.2	49.22	108.7	81.0	12.3	0.571
	303	513.1	59.66	85.30	67.2	14.9	0.693
	308	519.4	78.28	86.50	70.1	19.6	0.909
	313	521.3	86.57	90.60	61.4	21.6	1.000
1×10^{-3}	293	491.3	38.70	120.1	87.4	9.67	0.449
	298	498.2	43.17	117.9	88.2	10.8	0.501
	303	506.2	53.37	126.8	87.8	13.3	0.619
	308	516.6	72.35	113.9	85.6	17.8	0.837
	313	518.5	77.12	130.5	80.5	19.2	0.883
5×10^{-3}	293	507.1	34.55	89.40	68.2	8.12	0.409
	298	510.5	38.35	88.20	68.8	9.59	0.445
	303	514.8	48.81	95.70	70.1	12.2	0.567
	308	517.6	63.87	102.1	77.1	16.0	0.743
	313	519.1	69.71	108.5	70.4	17.4	0.811
1×10^{-2}	293	470.2	31.69	112.9	79.6	8.07	0.367
	298	486.3	35.93	98.10	73.6	8.98	0.417
	303	500.2	45.26	84.30	62.7	11.3	0.524
	308	504.0	60.50	94.30	72.0	15.1	0.702
	313	515.4	65.38	107.2	73.3	16.2	0.756

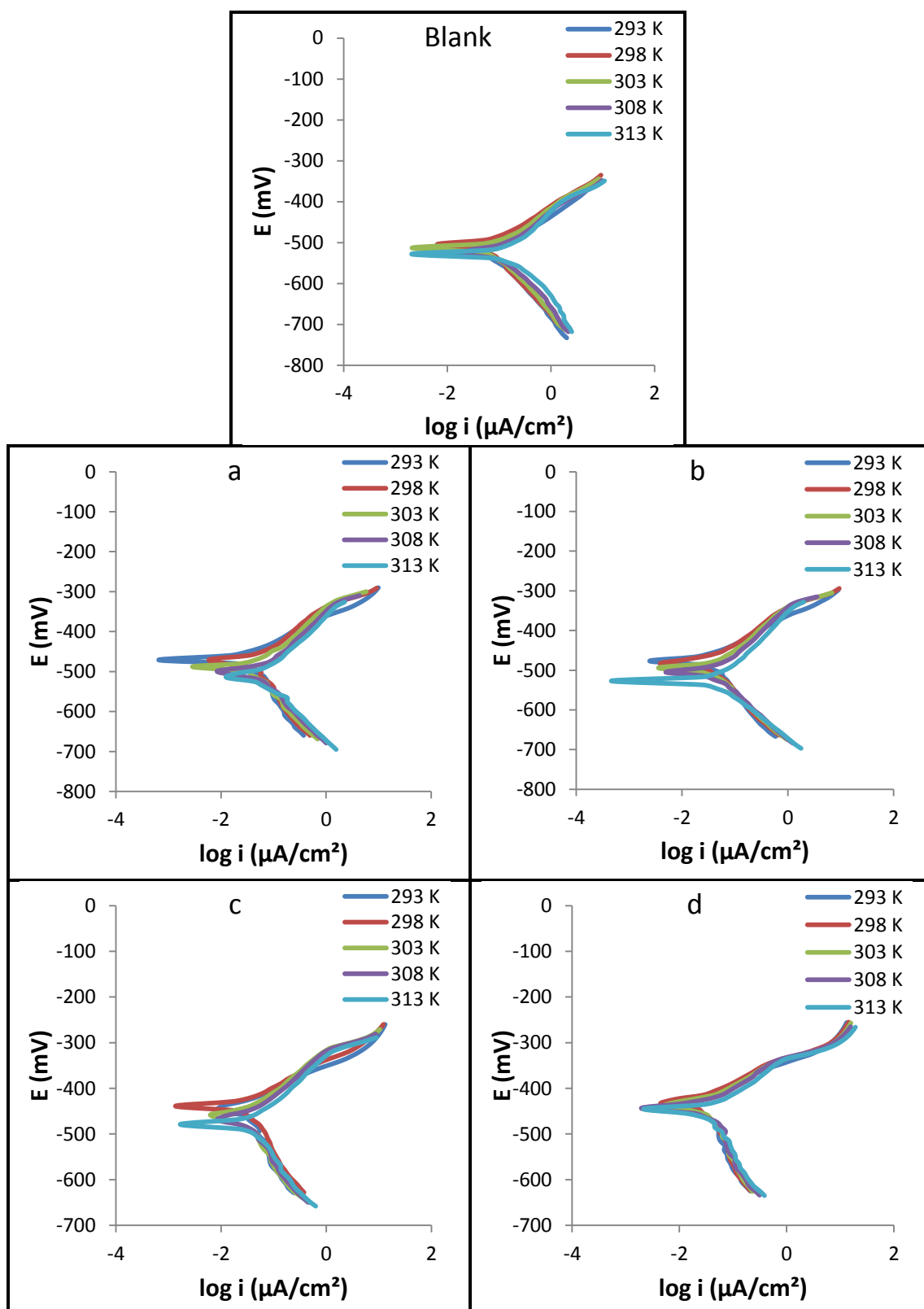


Figure (3-4): Polarization curves for carbon steel corrosion in the blank (saline solution) and in presence of Lys with different concentrations (a) 5×10^{-4} M, (b) 1×10^{-3} M, (c) 5×10^{-3} M and (d) 1×10^{-2} M at temperature range (293-313)K and pH 2.

Table (3-4): Corrosion parameters of carbon steel in the blank (saline solution) and in presence of Lys with different concentrations (5×10^{-4} , 1×10^{-3} , 5×10^{-3} and 1×10^{-2}) M at temperature range (293-313) K and pH 2.

Inh. [M]	T (K)	$-E_{\text{corr}}$ (mV)	i_{corr} ($\mu\text{A}/\text{cm}^2$)	Tafel slope (mV/dec)		CR ($\text{g}/\text{m}^2\text{d}$)	PR (mm/Y)
				$-b_c$	$+b_a$		
0	293	507.1	51.09	92.5	62.60	12.8	0.593
	298	513.9	55.67	136.7	73.20	13.9	0.646
	303	516.8	66.99	120.9	81.30	16.7	0.778
	308	525.8	87.14	107.0	95.10	21.8	1.010
	313	530.3	92.28	103.5	91.90	22.1	1.700
5×10^{-4}	293	469.7	27.16	127.6	72.40	6.79	0.315
	298	475.0	32.03	136.9	80.70	8.01	0.372
	303	487.6	38.63	164.8	91.40	9.66	0.448
	308	500.6	51.00	147.8	91.60	12.8	0.592
	313	515.4	57.01	126.9	82.60	14.3	0.662
1×10^{-3}	293	471.9	22.93	141.0	71.00	5.73	0.273
	298	482.4	27.76	122.5	71.50	6.94	0.322
	303	493.2	33.75	131.4	78.70	8.44	0.392
	308	507.5	44.38	129.2	81.60	11.1	0.515
	313	528.6	49.40	190.4	101.8	12.4	0.573
5×10^{-3}	293	433.2	19.76	106.5	57.30	4.94	0.229
	298	437.7	25.61	148.4	76.90	6.40	0.297
	303	458.7	30.90	208.2	99.90	7.73	0.359
	308	469.2	41.24	240.6	112.4	10.3	0.479
	313	477.1	45.25	203.7	102.6	11.3	0.525
1×10^{-2}	293	431.4	16.47	101.9	54.20	4.12	0.191
	298	434.1	21.89	153.7	73.10	5.47	0.254
	303	437.8	28.18	196.6	93.10	7.05	0.327
	308	440.8	37.47	125.5	77.70	9.37	0.435
	313	448.2	43.80	124.5	80.20	11.8	0.504

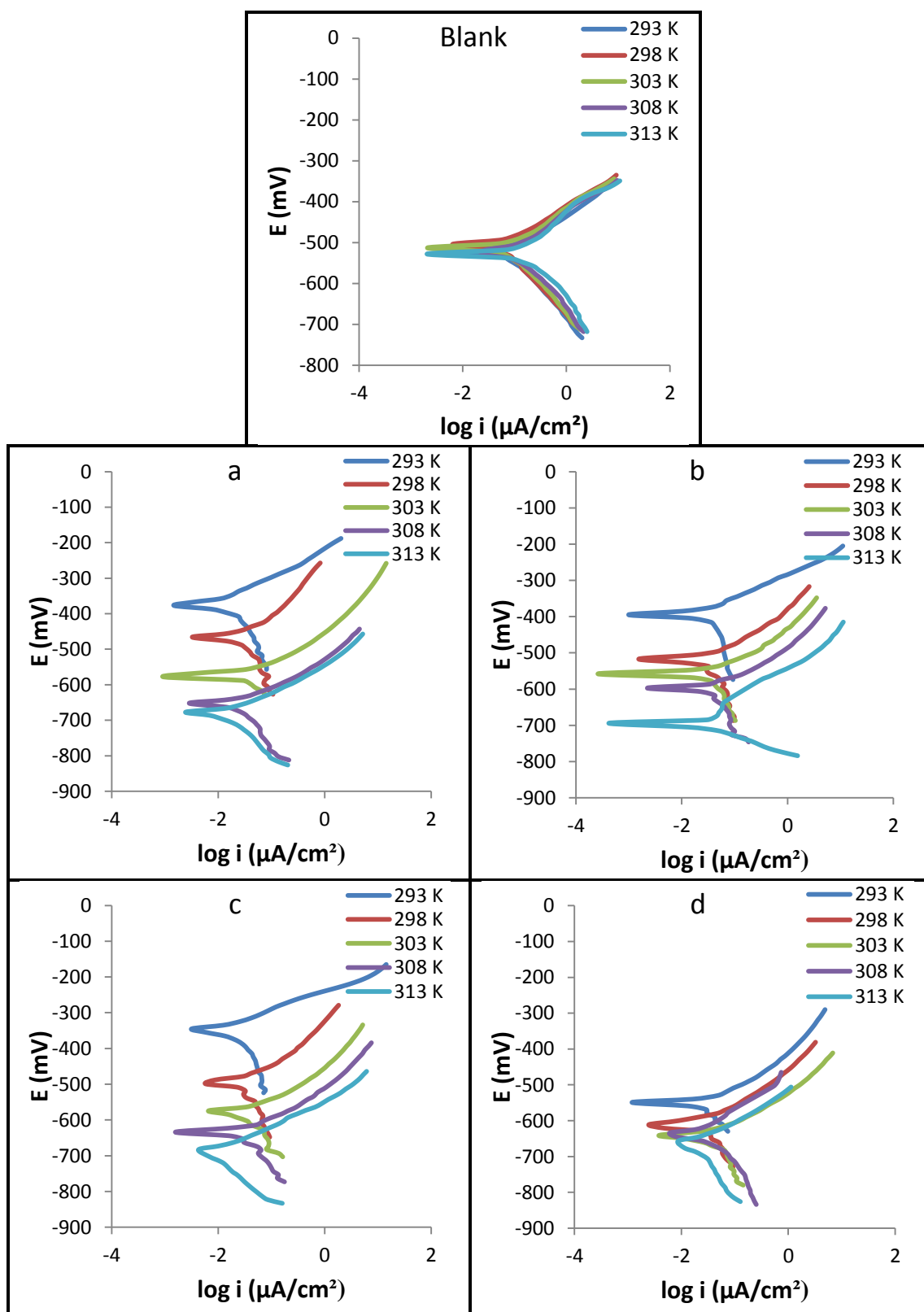


Figure (3-5): Polarization curves for carbon steel corrosion in the blank (saline solution) and in presence of Val with different concentrations (a) 5×10^{-4} M, (b) 1×10^{-3} M, (c) 5×10^{-3} M and (d) 1×10^{-2} M at temperature range (293-313)K and pH 11.

Table (3-5): Corrosion parameters of carbon steel in the blank (saline solution) and in presence of Val with different concentrations (5×10^{-4} , 1×10^{-3} , 5×10^{-3} and 1×10^{-2}) M at temperature range (293-313) K and pH 11.

Inh. [M]	T (K)	$-E_{\text{corr}}$ (mV)	i_{corr} ($\mu\text{A}/\text{cm}^2$)	Tafel slope (mV/dec)		CR ($\text{g}/\text{m}^2\text{d}$)	PR (mm/Y)
				$-b_c$	$+b_a$		
0	293	507.1	51.09	92.5	62.60	12.8	0.593
	298	513.9	55.67	136.7	73.20	13.9	0.646
	303	516.8	66.99	120.9	81.30	16.7	0.778
	308	525.8	87.14	107.0	95.10	21.8	1.010
	313	530.3	92.28	103.5	91.90	22.1	1.700
5×10^{-4}	293	376.2	19.55	249.6	89.60	4.89	0.227
	298	478.0	23.05	142.7	74.80	5.83	0.280
	303	589.2	29.12	189.4	60.10	7.33	0.335
	308	659.6	39.12	204.0	72.90	9.49	0.448
	313	698.5	44.63	185.6	61.20	10.5	0.514
1×10^{-3}	293	393.2	17.91	116.5	61.80	4.48	0.208
	298	581.6	21.52	140.1	72.00	5.38	0.250
	303	551.3	27.18	227.7	60.50	6.54	0.304
	308	595.4	36.13	151.6	62.90	9.10	0.428
	313	698.8	41.16	297.9	74.20	10.4	0.471
5×10^{-3}	293	443.1	15.53	166.5	68.30	3.88	0.180
	298	493.1	19.75	168.8	75.60	4.94	0.229
	303	581.6	24.84	141.0	70.70	6.16	0.287
	308	632.7	33.10	268.1	85.70	8.35	0.387
	313	693.1	37.45	363.6	96.80	9.15	0.429
1×10^{-2}	293	450.4	14.25	104.8	62.20	3.59	0.161
	298	483.9	18.23	159.8	89.50	5.40	0.252
	303	546.0	23.01	109.6	74.10	5.77	0.276
	308	651.7	31.12	199.4	119.4	7.81	0.361
	313	683.5	35.71	226.7	116.4	8.87	0.413

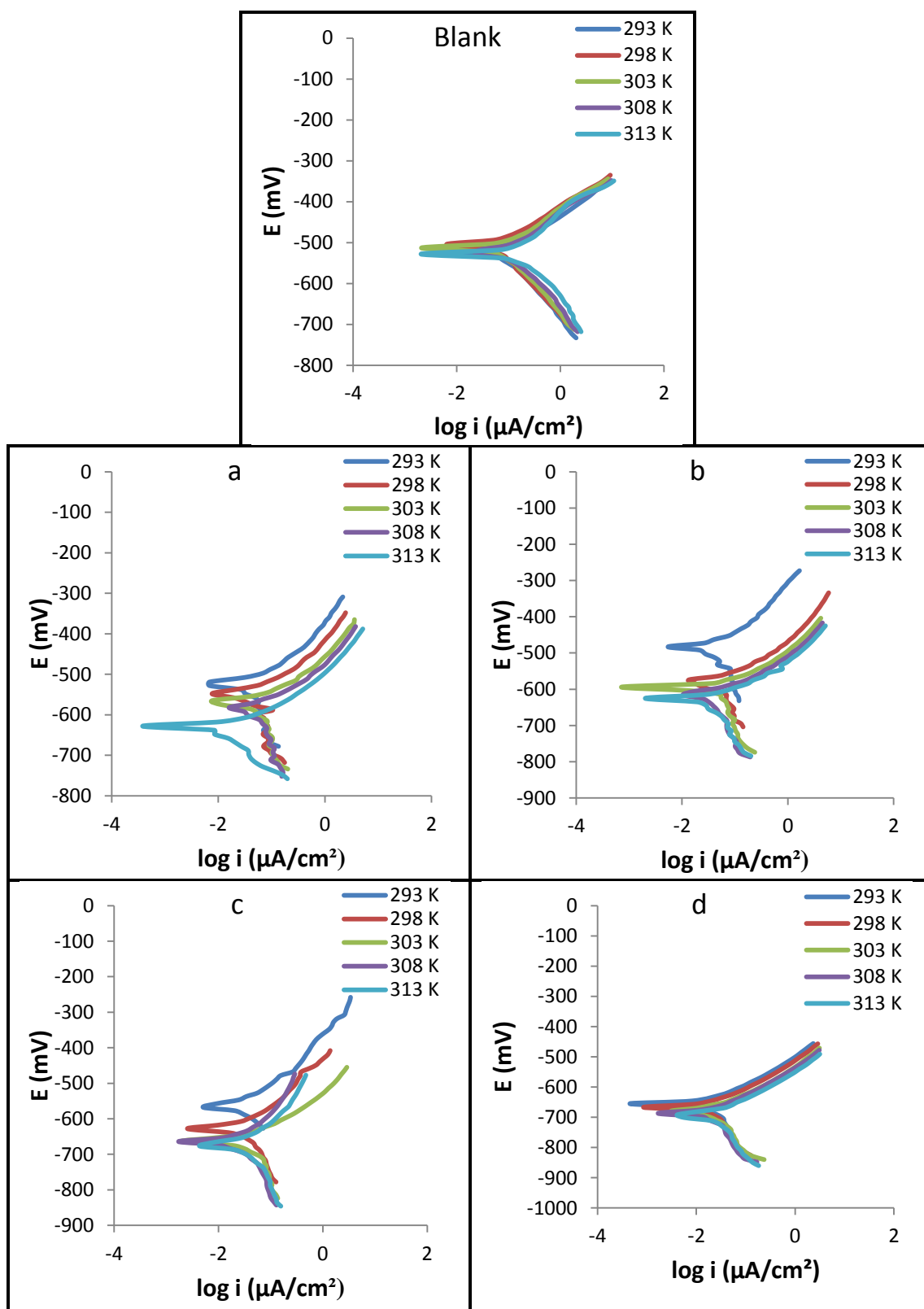


Figure (3-6): Polarization curves for carbon steel corrosion in the blank (saline solution) and in presence of Ser with different concentrations (a) 5×10^{-4} M, (b) 1×10^{-3} M, (c) 5×10^{-3} M and (d) 1×10^{-2} M at temperature range (293-313) K and pH 11.

Table (3-6): Corrosion parameters of carbon steel in the blank (saline solution) and in presence of Ser with different concentrations (5×10^{-4} , 1×10^{-3} , 5×10^{-3} and 1×10^{-2}) M at temperature range (293-313) K and pH 11.

Inh. [M]	T (K)	$-E_{\text{corr}}$ (mV)	i_{corr} ($\mu\text{A}/\text{cm}^2$)	Tafel slope (mV/dec)		CR ($\text{g}/\text{m}^2\text{d}$)	PR (mm/Y)
				$-b_c$	$+b_a$		
0	293	507.1	51.09	92.5	62.60	12.8	0.593
	298	513.9	55.67	136.7	73.20	13.9	0.646
	303	516.8	66.99	120.9	81.30	16.7	0.778
	308	525.8	87.14	107.0	95.10	21.8	1.01
	313	530.3	92.28	103.5	91.90	22.1	1.70
5×10^{-4}	293	504.3	17.44	120.3	63.20	5.28	0.196
	298	546.1	23.76	116.7	56.10	6.50	0.302
	303	569.3	28.83	123.7	57.00	8.18	0.370
	308	587.1	37.81	181.3	67.30	9.32	0.433
	313	635.0	43.57	214.1	72.50	11.2	0.502
1×10^{-3}	293	482.5	16.98	110.7	59.90	4.39	0.196
	298	531.4	20.26	90.50	50.70	5.08	0.236
	303	597.6	25.95	162.2	65.50	6.37	0.292
	308	619.6	34.52	271.8	77.50	8.15	0.407
	313	630.6	40.15	203.4	76.10	10.1	0.466
5×10^{-3}	293	562.9	15.17	94.8	56.10	3.96	0.185
	298	603.1	17.56	130.7	64.80	4.41	0.209
	303	632.3	24.02	143.8	69.10	5.98	0.274
	308	665.7	31.67	262.7	100.3	8.07	0.367
	313	677.3	36.55	178.1	77.80	9.31	0.433
1×10^{-2}	293	651.4	13.43	152.5	75.10	3.40	0.158
	298	662.2	16.78	183.9	74.70	4.19	0.195
	303	675.3	22.10	301.5	88.70	5.53	0.256
	308	688.0	29.59	294.8	100.4	7.36	0.341
	313	693.4	34.65	320.3	96.60	8.21	0.410

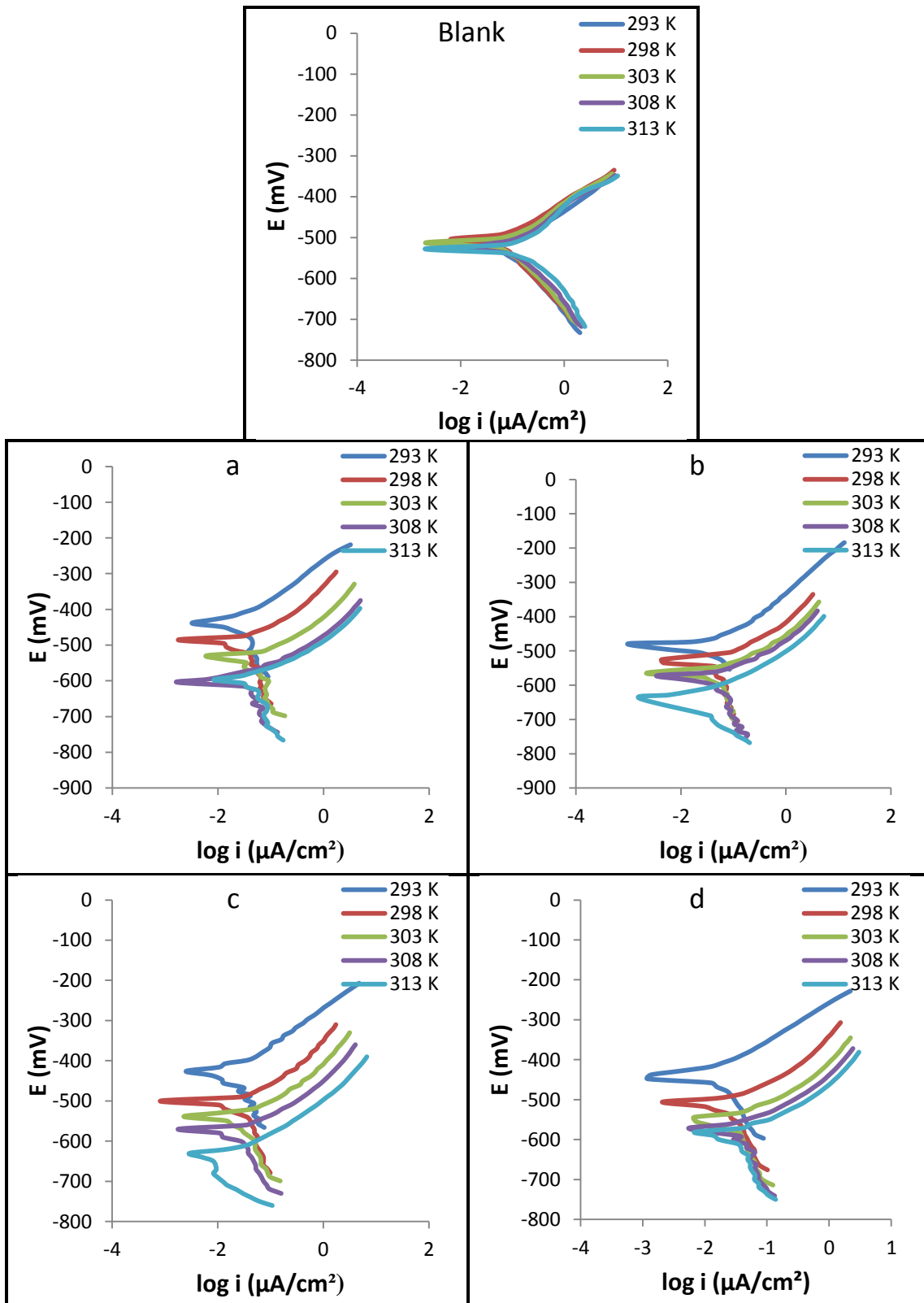


Figure (3-7): Polarization curves for carbon steel corrosion in the blank (saline solution) and in presence of Trp with different concentrations (a) 5×10^{-4} M, (b) 1×10^{-3} M, (c) 5×10^{-3} M and (d) 1×10^{-2} M at temperature range (293-313) K and pH 11.

Table (3-7): Corrosion parameters of carbon steel in the blank (saline solution) and in presence of Trp with different concentrations (5×10^{-4} , 1×10^{-3} , 5×10^{-3} and 1×10^{-2}) M at temperature range (293-313) K and pH 11.

Inh. [M]	T (K)	$-E_{\text{corr}}$ (mV)	i_{corr} ($\mu\text{A}/\text{cm}^2$)	Tafel slope (mV/dec)		CR ($\text{g}/\text{m}^2\text{d}$)	PR (mm/Y)
				$-b_c$	$+b_a$		
0	293	507.1	51.09	92.50	62.6	12.8	0.593
	298	513.9	55.67	136.7	73.2	13.9	0.646
	303	516.8	66.99	120.9	81.3	16.7	0.778
	308	525.8	87.14	107.0	95.1	21.8	1.010
	313	530.3	92.28	103.5	91.9	22.1	1.700
5×10^{-4}	293	437.5	22.78	269.6	102.1	5.70	0.264
	298	488.5	25.77	262.9	77.7	6.40	0.291
	303	537.0	32.91	179.3	68.1	8.25	0.385
	308	585.3	43.13	339.5	74.2	10.4	0.500
	313	598.6	48.07	277.6	77.6	11.8	0.547
1×10^{-3}	293	486.8	20.09	114.3	68.8	5.02	0.233
	298	533.7	24.30	139.3	68.8	6.07	0.282
	303	565.1	31.15	159.8	76.2	7.37	0.345
	308	579.5	41.95	167.2	69.8	10.9	0.431
	313	629.4	45.22	285.6	86.1	11.2	0.523
5×10^{-3}	293	433.3	19.40	191.5	96.1	4.87	0.225
	298	504.6	22.88	179.3	91.2	6.14	0.236
	303	538.8	28.76	193.9	89.6	7.27	0.303
	308	576.6	38.47	185.9	95.8	9.60	0.433
	313	624.2	42.84	135.5	80.4	9.97	0.489
1×10^{-2}	293	466.6	15.45	135.9	74.5	4.11	0.191
	298	510.4	18.85	155.9	79.2	4.72	0.222
	303	544.4	24.28	143.4	80.7	6.74	0.288
	308	572.9	33.05	134.8	84.9	8.32	0.386
	313	588.4	38.16	156.1	89.5	9.50	0.423

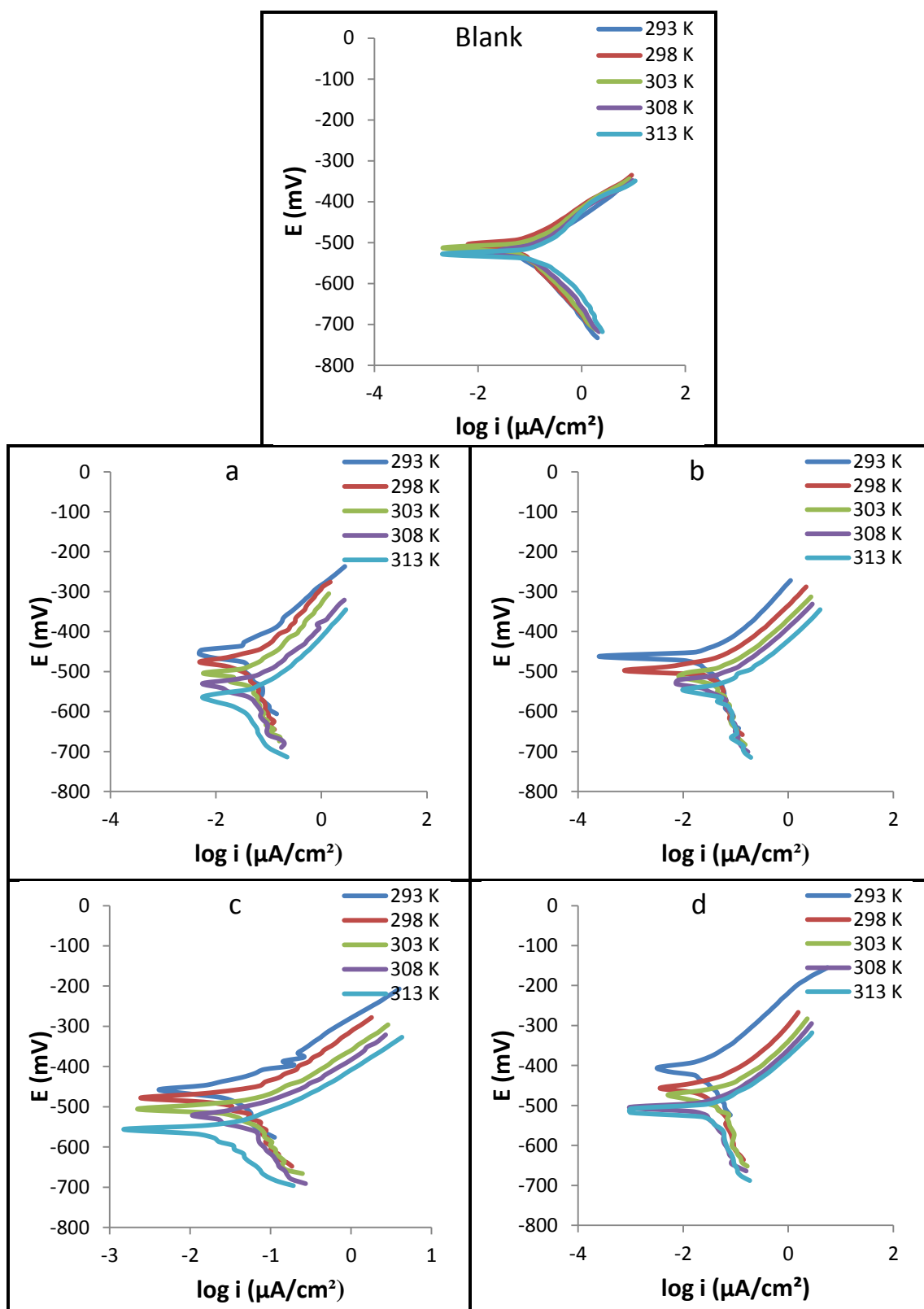


Figure (3-8): Polarization curves for carbon steel corrosion in the blank (saline solution) and in presence of Lys with different concentrations (a) 5×10^{-4} M, (b) 1×10^{-3} M, (c) 5×10^{-3} M and (d) 1×10^{-2} M at temperature range (293-313) K and pH 11.

Table (3-8): Corrosion parameters of carbon steel in the blank (saline solution) and in presence of Lys with different concentrations (5×10^{-4} , 1×10^{-3} , 5×10^{-3} and 1×10^{-2}) M at temperature range (293-313) K and pH 11.

Inh. [M]	T (K)	$-E_{\text{corr}}$ (mV)	i_{corr} ($\mu\text{A}/\text{cm}^2$)	Tafel slope (mV/dec)		CR ($\text{g}/\text{m}^2\text{d}$)	PR (mm/Y)
				$-b_c$	$+b_a$		
0	293	507.1	51.09	92.5	62.6	12.8	0.593
	298	513.9	55.67	136.7	73.2	13.9	0.646
	303	516.8	66.99	120.9	81.3	16.7	0.778
	308	525.8	87.14	107.0	95.1	21.8	1.010
	313	530.3	92.28	103.5	91.9	22.1	1.700
5×10^{-4}	293	441.4	24.12	151.0	79.3	6.10	0.267
	298	485.5	28.34	169.0	81.6	7.08	0.329
	303	508.6	35.15	311.9	112.1	8.43	0.428
	308	531.1	46.31	189.2	89.1	11.3	0.530
	313	581.2	49.92	276.3	105.6	12.6	0.577
1×10^{-3}	293	464.1	22.89	168.1	83.3	5.70	0.263
	298	488.9	26.11	183.7	82.3	6.53	0.303
	303	510.2	32.80	269.6	85.0	8.18	0.380
	308	530.7	44.15	219.5	93.5	10.4	0.469
	313	546.5	46.71	171.2	85.4	11.6	0.540
5×10^{-3}	293	453.0	21.37	149.9	88.9	5.27	0.224
	298	483.2	24.70	130.5	81.4	6.18	0.287
	303	514.8	31.12	120.2	68.1	7.50	0.346
	308	525.0	40.49	133.1	67.6	1.01	0.467
	313	555.9	45.97	189.3	80.2	11.6	0.542
1×10^{-2}	293	427.5	16.97	164.8	85.7	4.24	0.197
	298	461.9	21.01	142.3	81.1	5.12	0.230
	303	478.6	26.96	182.7	78.8	6.45	0.295
	308	507.4	36.10	269.8	85.8	9.02	0.420
	313	517.3	39.95	253.5	82.7	9.90	0.456

3.1.1 Corrosion Current Density and Corrosion Potential

The results showed that the values of the corrosion current densities (i_{corr}) for carbon steel in saline solution in the absence of inhibitors were increased with increasing temperature, due to the presence of chloride

ions that act as aggressive ions for carbon steel. In the presence of inhibitors at basic medium, i_{corr} values were less than in acidic medium due to the presence of hydroxide ions $[\text{OH}^-]$. These ions may be absorbed on the carbon steel surface and act as an anodic inhibitor which leads increase anodic polarization by forming a protective oxide film, while in acidic medium the corrosion current densities were increased due to the presence of SO_4^{2-} ions. These ions are aggressive corrosion species that degrades the carbon steel surface in saline solution below the neutral medium, so the corrosion product in this case should be iron sulphide. At different pH the i_{corr} values may be arranged in a sequence as follows:

$$\text{pH } 11 < \text{pH } 2$$

The corrosion potential (E_{corr}) is the potential at which the rate of oxidation reaction is equal to the rate of reduction reaction ⁽⁹⁾. After addition of the inhibitors to different media the values of corrosion potential (E_{corr}) were shifted to less negative (amino acid acts as anodic type inhibitor) or shifted to more negative (amino acid acts as cathodic type inhibitor) and in some cases the inhibitor acts as mixed type ⁽²⁹⁾. The inhibitors that used in this research (amino acids) have alpha carbon, which are bonded by four groups; hydrogen, an amino group, a carboxyl group, and a unique side chain known as R-group. They differ in their unique side chain, which can be used to classify the molecules into functional types. Many amino acids have been used to inhibit the corrosion of metals and alloys ⁽³⁷⁾. In this study, four of amino acids were used which have different properties basis on their structure and functional groups that effected by the pH of solution. The data presented in tables (3-1) to (3-8) show that the addition of the inhibitors to the saline solution at pH (2 and 11) caused a decrease in the values of the corrosion current densities of carbon steel. Similarly the corrosion current

densities decrease when the concentration of inhibitors increases in the rang (5×10^{-4} , 1×10^{-3} , 5×10^{-3} and 1×10^{-2}) M, while i_{corr} values were increased with increasing temperature.

The behavior of each amino acids that were used in this research are summarized as follows:

❖ L-valine

It was shown from the molecular structure of Val (figure (2-1)) that the nitrogen atom of amino group interacted by the lone pairs of electrons with the empty d-orbitals of carbon steel surface and forming Fe-Val complex, this complex serve as a stable passive layer on the steel and then decreasing corrosion rate. Corrosion potentials of carbon steel in presence of Val were shifted toward less negative and more negative values at acidic medium, that means Val acts as mixed type inhibitor⁽⁶⁴⁾, while in the basic medium the corrosion potentials were shifted toward more negative values, that means Val acts as cathodic type inhibitor⁽⁶⁵⁾.

❖ L-serine

The molecular structure of Ser (figure (2-1)) shows that it can be adsorbed on the metal surface through the bonded of lone pairs electrons of oxygen and nitrogen atoms with empty d-orbitals of metal to form protective layer on metal surface and decreasing corrosion current. The addition of Ser to the acidic medium, the corrosion potentials were shifted to less negative values with the increasing of the concentration untill reaching 1×10^{-2} M then a downfall in E_{corr} occured toward more negative values which indicates Ser acts as mixed type inhibitor. But in the basic medium the corrosion potentials were shifted to more negative values with the increasing of the concentration of Ser, that means Ser act as Cathodic type inhibitor⁽⁶⁶⁾.

❖ L-tryptophan

Trp is an indole derivative molecule. Depending on the analysis of molecular structure of Trp (figure (2-1)) it possess the potential to become an excellent corrosion inhibitor for metals and alloys ⁽⁶⁷⁾. The results confirmed that Trp adsorbs on Fe surface through the bonded between the empty orbitals of iron and the lone pairs electrons of nitrogen atom of the molecule and forming protective layer that isolated the surface of carbon steel from aggressive ions in solution ⁽⁶⁸⁾. The corrosion potentials of carbon steel in presence of Trp were shifted to less negative values in acidic medium, that means Trp acts as anodic inhibitor by lower the rate of the oxidation reactions, and in basic medium the corrosion potentials were shifted toward more negative values, that means Trp acts as cathodic inhibitor by lowering the rate of the reduction reactions (evolution of hydrogen) ^(69,67).

❖ L-lysine

Based on molecular structure of Lys (figure (2-1)), it is obvious that the lone pairs of electrons of nitrogen atom could be bonded with empty orbitals of iron and then forming protective layer on carbon steel surface to decrease the corrosion rate. In the presence of Lys in acidic medium the corrosion potentials were shifted toward less negative values with the increasing of inhibitor concentration, and in basic medium corrosion potentials were also shifted toward less negative values, that means Lys acts as anodic type inhibitor ⁽⁷⁰⁾.

The addition of the inhibitors (Val, Ser, Trp and Lys) to the saline solution at pH (2 and 11) leads to decrease the corrosion current densities (i_{corr}) values. The variation in i_{corr} values of amino acids can be interpreted to their possession of different properties at different media. On the other hand, increasing temperature causes to an increase in i_{corr}

values. The decreases in the i_{corr} values due to addition of different amino acids (Val, Ser, Trp and Lys) into the saline solution at different pH can be arranged as follows:

$$\text{pH 2} \quad \text{Trp} > \text{Val} > \text{Ser} > \text{Lys}$$

$$\text{pH 11} \quad \text{Lys} > \text{Trp} > \text{Val} > \text{Ser}$$

3.1.2 The Tafel Slopes

The cathodic (b_c) and anodic (b_a) Tafel slopes values, which were obtained from the slopes of the cathodic and anodic Tafel regions were given in tables (3-1) to (3-8). The results showed that the cathodic and anodic Tafel slopes (b_a and b_c) values are varied at all the amino acids concentrations and temperature. These results refer to the variation of the rate-determining step from charge transfer process to either chemical-deposition or to electrochemical desorption in the cathodic reactions and also to the variation of the rate determining step in the metal dissolution reaction ⁽⁷¹⁾.

3.2 Inhibition Efficiency and Surface Coverage

The inhibition efficiency (IE%) and surface coverage (θ) are calculated by using the following equations ^(72,73):

$$IE\% = \frac{I_{corr}^0 - I_{corr}}{I_{corr}^0} \dots\dots\dots (3-3)$$

$$\theta = \frac{IE\%}{100} \dots\dots\dots (3-4)$$

Where I_{corr}^0 and I_{corr} are the corrosion current densities in the absence and presence of inhibitor, respectively. The IE% and θ were obtained from these equations are given in tables (3-9) and (3-10).

Table (3-9): Inhibition efficiencies and surface coverages of (Val, Ser, Trp and Lys) at various concentration with temperature range (293-313)K in saline solution at PH 2.

Inh.	T (K)	5×10^{-4} M		1×10^{-3} M		5×10^{-3} M		1×10^{-2} M	
		IE%	θ	IE%	θ	IE%	θ	IE%	θ
Trp	293	13.31	0.133	24.25	0.243	32.37	0.324	37.97	0.380
	298	11.59	0.116	22.45	0.225	31.11	0.311	35.46	0.355
	303	10.94	0.109	20.33	0.203	27.14	0.271	32.41	0.324
	308	10.17	0.102	16.97	0.170	26.70	0.267	30.57	0.306
	313	6.190	0.062	16.43	0.164	24.46	0.245	29.15	0.292
Val	293	28.71	0.287	37.85	0.379	43.61	0.436	53.28	0.533
	298	26.15	0.262	35.64	0.357	42.36	0.424	51.52	0.515
	303	25.30	0.253	33.69	0.337	42.10	0.421	51.16	0.512
	308	23.90	0.239	32.96	0.330	39.92	0.399	49.58	0.496
	313	22.41	0.224	31.57	0.316	35.90	0.359	40.00	0.400
Ser	293	33.92	0.339	50.09	0.501	54.79	0.548	62.22	0.622
	298	32.26	0.323	45.25	0.453	51.19	0.512	54.36	0.544
	303	30.33	0.303	44.13	0.441	50.96	0.510	54.17	0.542
	308	30.66	0.307	43.03	0.430	50.56	0.506	53.26	0.533
	313	27.06	0.271	42.40	0.424	45.62	0.456	48.62	0.486
Lys	293	46.84	0.468	55.12	0.551	61.32	0.613	67.76	0.678
	298	42.46	0.425	50.13	0.501	54.00	0.540	60.68	0.607
	303	42.33	0.423	49.62	0.496	53.87	0.539	57.93	0.579
	308	41.47	0.415	49.07	0.491	52.67	0.527	57.00	0.570
	313	38.22	0.382	46.47	0.465	50.96	0.510	52.54	0.525

Table (3-10): inhibition efficiencies and surface coverages of (Val, Ser, Trp and Lys) at various concentration with temperature range (293-313)K in saline solution at PH 11.

Inh.	T (K)	5×10^{-4} M		1×10^{-3} M		5×10^{-3} M		1×10^{-2} M	
		IE%	θ	IE%	θ	IE%	θ	IE%	θ
Lys	293	52.79	0.528	55.20	0.552	58.17	0.582	66.78	0.668
	298	49.09	0.491	53.10	0.531	55.63	0.556	62.26	0.623
	303	47.53	0.475	51.04	0.510	53.55	0.535	59.76	0.598
	308	46.86	0.469	49.33	0.493	53.53	0.535	58.57	0.586
	313	45.90	0.459	49.38	0.494	50.18	0.502	56.71	0.567
Trp	293	55.41	0.554	60.68	0.607	62.03	0.620	69.76	0.698
	298	53.71	0.537	56.35	0.563	58.90	0.589	66.14	0.661
	303	50.87	0.509	53.50	0.535	57.07	0.571	63.76	0.638
	308	50.50	0.505	51.86	0.519	55.85	0.559	62.07	0.621
	313	47.91	0.479	51.00	0.510	53.58	0.536	58.65	0.587
Val	293	61.73	0.617	64.94	0.649	69.60	0.696	72.11	0.721
	298	58.60	0.586	61.34	0.613	64.52	0.645	67.25	0.673
	303	56.53	0.565	59.43	0.594	62.92	0.629	65.65	0.657
	308	55.11	0.551	58.54	0.585	62.02	0.620	64.29	0.643
	313	51.64	0.516	55.40	0.554	59.42	0.594	61.30	0.613
Ser	293	65.86	0.659	66.76	0.668	70.31	0.703	73.71	0.737
	298	57.32	0.573	63.61	0.636	68.46	0.685	69.86	0.697
	303	56.96	0.570	61.26	0.613	64.14	0.641	67.01	0.670
	308	56.61	0.566	60.39	0.604	63.66	0.637	66.04	0.660
	313	52.79	0.528	56.49	0.565	60.39	0.604	62.45	0.625

The results in tables (3-9) and (3-10) showed that the use of amino acids (Val, Ser, Trp and Lys) in this study are a good inhibitors for corrosion of carbon steel in acidic and basic saline solution, with maximum inhibition efficiency of 73.71% by Ser at 1×10^{-2} M in basic medium and with minimum inhibition efficiency of 6.19% by Trp at 5×10^{-4} M in acidic medium. It was noticed that the protection efficiency and surface coverage increase with increasing concentration of inhibitors and decrease with increasing temperature ⁽⁷⁴⁾. The inhibition efficiencies of amino acids have been arranged as follows:

Lys > Ser > Val > Trp at pH 2

Ser > Val > Trp > Lys at pH 11

The trend above shows that Lys have highest efficiency in acidic medium among amino acids due to presence more than one active site to receive proton discharge from the bulk. As for the basic medium Lys shows lowest efficiency despite having more than hetero atom in its structure that's attributed to complexity (Steric hindrance) of inhibitor molecule that prevents the two nitrogen atoms to adsorb instantly on metal surface.

The inhibition processes were summarized by adsorption molecules of the amino acids on the carbon steel surface. The atoms such as oxygen, nitrogen and sulfur present in these molecules act as active sites for the adsorption process. Existence of lone pairs in these atoms (O, N and S) accelerates electrons transfer from the amino acids to the metal. In this case, coordinate covalent bonds may be formed (chemisorption). The strength of these bonds depends on the electron density and polarizability of the donor atoms in amino acids. Figure (3-9) represents the mechanism of corrosion inhibition by amino acids in acidic media ⁽⁷⁵⁾.

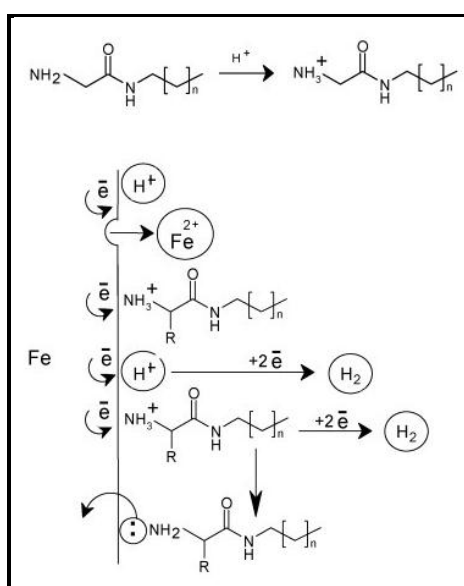


Figure (3-9): Mechanism of inhibition of amino acids in acidic media ⁽⁷⁵⁾.

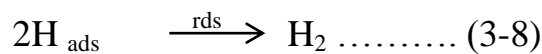
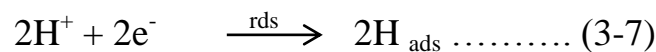
3.3 Transfer Coefficients

Values of the transfer coefficients for the cathodic (α_c) and anodic (α_a) processes were calculated from the corresponding cathodic (b_c) and anodic (b_a) Tafel slopes in the absences and presence of the inhibitors by using the relationships ⁽⁷⁶⁾:

$$b_c = \frac{2.3 RT}{\alpha_c nF} \dots\dots\dots (3-5)$$

$$b_a = \frac{2.3 RT}{\alpha_a nF} \dots\dots\dots (3-6)$$

The results obtained have been tabulated in tables (3-11) to (3-18). The transfer coefficient (α) is a quantity that used in the kinetic investigation of electrode processes. This definition applies only to an electrode reaction that consists of an elementary step involving the accept of n electrons from the electrode in the case of (α_c), or their release to the electrode in the case of (α_a). The value of transfer coefficient (α) is often close to 0.5 and n value is identified with the number of electrons involved in a hypothetical rate-determining step or with that involved in the overall electrode reaction. A mechanism of an electrode involving the the reductions twice for hydrogen evolution as ⁽⁷⁷⁾:



During charge transfer, the electrons are moved from anode-electrolyte interface towards the cathodic through the external circuit. The drive of electrons toward the region of lower potential required energy to be supplied, these energy depends on the potential difference between the anode and the electrolyte. The electric potential of the anode is always less than the electric potential of the electrolyte, so the forward reaction can be facilitated by increasing the anode potential ⁽⁷⁸⁾.

3.4 The Polarization Resistances

When electrode is polarized, its potential is forced away from its original value at open circuit or corrosion potential E_{corr} . Polarization of an electrode causes flow of current due to electrochemical reactions which induces at the electrode surface. Corrosion rates can be measured with a corrosion monitoring technique e.g. linear polarization resistance (1).

The polarization resistance (R_p) values were calculated by using the following rearranged Stern-Geary equation (79):

$$i_{\text{corr}} = \frac{b_a b_c}{2.3(b_a + b_c) R_p} \dots\dots\dots (3-9)$$

For a simple and symmetrical anodic and cathodic charge transfer controlled process, the small portion of the polarization curve approximately ≤ 20 mV either side of the corrosion potential, E_{corr} , the current versus potential response is expected to be linear (79).

At equilibrium potential E_{eq} , the absolute value of both of the anodic and cathodic component currents are equal to the exchange current and the net current is zero. For small overpotential the Tafel equation reduced to the linear equation as follows (80):

$$i = \frac{i_0 F \eta}{RT} \dots\dots\dots (3-10)$$

Where i_0 is the equilibrium exchange current density. The polarization resistance for the interface to the charge transfer reaction is represent the term η/i . i_0 can be calculated from the following equation:

$$i_0 = \frac{RT}{R_p F} \dots\dots\dots (3-11)$$

The results of R_p and i_0 have been tabulated in tables (3-11) to (3-18). These results were showed that the R_p values were decreased with

increasing temperature and increased with increasing inhibitors concentration at constant temperature. On the other hand, the greatest value of the polarization resistance ($4.784 \times 10^3 \Omega \cdot \text{cm}^2$) was observed in the presence of ($1 \times 10^{-2} \text{ M}$) of Ser in 3.5% NaCl at pH 11.

Table (3-11): Values of transfer coefficient (α_c , α_a), the polarization resistance (R_p) and equilibrium exchange current density (i_o) for corrosion of carbon steel in saline solution (blank) and in the presence of Val at pH 2 with various temperature range (293-313) K.

Conc. (M)	T (K)	α_c	α_a	$R_p \times 10^3$ ($\Omega \cdot \text{cm}^2$)	$i_o \times 10^{-5}$ (A/cm^2)
Blank	293	0.314	0.464	1.646	1.534
	298	0.216	0.404	1.229	2.089
	303	0.249	0.416	1.166	2.240
	308	0.208	0.339	1.160	2.288
	313	0.202	0.357	0.942	2.862
5×10^{-4}	293	0.321	0.442	2.866	0.881
	298	0.279	0.395	2.690	0.954
	303	0.319	0.454	1.937	1.348
	308	0.354	0.464	1.821	1.458
	313	0.337	0.441	1.806	1.494
1×10^{-3}	293	0.325	0.460	2.941	0.858
	298	0.323	0.454	2.734	0.939
	303	0.278	0.404	2.333	1.119
	308	0.335	0.449	1.987	1.336
	313	0.394	0.507	1.889	1.427
5×10^{-3}	293	0.404	0.546	3.071	0.822
	298	0.412	0.547	2.982	0.861
	303	0.385	0.502	2.877	0.907
	308	0.360	0.478	2.135	1.243
	313	0.320	0.438	1.934	1.394
1×10^{-2}	293	0.412	0.570	3.341	0.756
	298	0.284	0.437	3.109	0.826
	303	0.276	0.414	2.908	0.898
	308	0.305	0.410	2.870	0.925
	313	0.336	0.436	2.617	1.031

Table (3-12): Values of transfer coefficient (α_c , α_a), the polarization resistance (R_p) and equilibrium exchange current density (i_o) for corrosion of carbon steel in saline solution (blank) and in the presence of Ser at pH 2 with various temperature range (293-313) K.

Conc. (M)	T (K)	α_c	α_a	$R_p \times 10^3$ ($\Omega \cdot \text{cm}^2$)	$i_o \times 10^{-5}$ (A/cm^2)
Blank	293	0.314	0.464	1.646	1.534
	298	0.216	0.404	1.229	2.089
	303	0.249	0.416	1.166	2.240
	308	0.208	0.339	1.160	2.288
	313	0.202	0.357	0.942	2.862
5×10^{-4}	293	0.238	0.423	2.025	1.247
	298	0.318	0.493	1.943	1.321
	303	0.307	0.482	1.601	1.631
	308	0.345	0.485	1.567	1.694
	313	0.316	0.466	1.339	2.015
1×10^{-3}	293	0.347	0.561	2.305	1.095
	298	0.300	0.505	2.055	1.250
	303	0.285	0.495	1.658	1.575
	308	0.307	0.469	1.644	1.614
	313	0.285	0.457	1.471	1.833
5×10^{-3}	293	0.269	0.489	2.481	1.018
	298	0.229	0.420	2.474	1.038
	303	0.229	0.464	1.691	1.544
	308	0.198	0.390	1.606	1.652
	313	0.245	0.433	1.403	1.922
1×10^{-2}	293	0.292	0.500	3.146	0.802
	298	0.232	0.435	2.486	1.033
	303	0.254	0.502	1.715	1.523
	308	0.292	0.495	1.602	1.657
	313	0.223	0.423	1.420	1.900

Table (3-13): Values of transfer coefficient (α_c , α_a), the polarization resistance (R_p) and equilibrium exchange current density (i_o) for corrosion of carbon steel in saline solution (blank) and in the presence of Trp at pH 2 with various temperature range (293-313) K.

Conc. (M)	T (K)	α_c	α_a	$R_p \times 10^3$ ($\Omega \cdot \text{cm}^2$)	$i_o \times 10^{-5}$ (A/cm^2)
Blank	293	0.314	0.464	1.646	1.534
	298	0.216	0.404	1.229	2.089
	303	0.249	0.416	1.166	2.240
	308	0.208	0.339	1.160	2.288
	313	0.202	0.357	0.942	2.862
5×10^{-4}	293	0.193	0.294	2.814	0.897
	298	0.272	0.365	2.804	0.916
	303	0.352	0.434	2.305	1.133
	308	0.353	0.436	2.051	1.294
	313	0.343	0.506	0.956	0.837
1×10^{-3}	293	0.242	0.333	3.563	0.709
	298	0.251	0.335	3.522	0.729
	303	0.237	0.342	2.323	1.124
	308	0.268	0.357	2.068	1.284
	313	0.238	0.386	1.183	2.280
5×10^{-3}	293	0.325	0.426	3.614	0.699
	298	0.335	0.430	3.542	0.725
	303	0.314	0.429	2.331	1.120
	308	0.299	0.396	2.141	1.2398
	313	0.286	0.441	1.249	2.160
1×10^{-2}	293	0.258	0.364	3.698	0.683
	298	0.301	0.402	3.561	0.721
	303	0.357	0.480	2.348	1.112
	308	0.324	0.424	2.185	1.215
	313	0.290	0.424	1.539	1.752

Table (3-14): Values of transfer coefficient (α_c , α_a), the polarization resistance (R_p) and equilibrium exchange current density (i_o) for corrosion of carbon steel in saline solution (blank) and in the presence of Lys at pH 2 with various temperature range (293-313) K.

Conc. (M)	T (K)	α_c	α_a	$R_p \times 10^3$ ($\Omega \cdot \text{cm}^2$)	$i_o \times 10^{-5}$ (A/cm^2)
Blank	293	0.314	0.464	1.646	1.534
	298	0.216	0.404	1.229	2.089
	303	0.249	0.416	1.166	2.240
	308	0.208	0.339	1.160	2.288
	313	0.202	0.357	0.942	2.862
5×10^{-4}	293	0.228	0.402	2.676	0.944
	298	0.216	0.366	2.665	0.964
	303	0.182	0.329	2.307	1.132
	308	0.207	0.334	2.051	1.294
	313	0.244	0.376	1.802	1.497
1×10^{-3}	293	0.206	0.409	2.708	0.932
	298	0.241	0.414	2.686	0.956
	303	0.229	0.382	2.525	1.034
	308	0.237	0.375	2.167	1.225
	313	0.163	0.305	1.923	1.403
5×10^{-3}	293	0.273	0.507	2.726	0.926
	298	0.199	0.385	2.706	0.949
	303	0.144	0.301	2.699	0.967
	308	0.127	0.272	2.221	1.195
	313	0.152	0.303	1.984	1.360
1×10^{-2}	293	0.285	0.536	3.053	0.827
	298	0.192	0.404	2.765	0.929
	303	0.153	0.323	2.725	0.958
	308	0.244	0.393	2.364	1.123
	313	0.249	0.387	2.234	1.207

Table (3-15): Values of transfer coefficient (α_c , α_a), the polarization resistance (R_p) and equilibrium exchange current density (i_o) for corrosion of carbon steel in saline solution (blank) and in the presence of Val at pH 11 with various temperature range (293-313) K.

Conc. (M)	T (K)	α_c	α_a	$R_p \times 10^3$ ($\Omega \cdot \text{cm}^2$)	$i_o \times 10^{-5}$ (A/cm^2)
Blank	293	0.314	0.464	1.646	1.534
	298	0.216	0.404	1.229	2.089
	303	0.249	0.416	1.166	2.240
	308	0.208	0.339	1.160	2.288
	313	0.202	0.357	0.942	2.862
5×10^{-4}	293	0.116	0.324	3.105	0.813
	298	0.207	0.395	2.961	0.867
	303	0.159	0.500	1.313	1.989
	308	0.150	0.419	1.259	2.108
	313	0.167	0.507	0.888	3.036
1×10^{-3}	293	0.250	0.470	3.191	0.791
	298	0.211	0.411	2.989	0.859
	303	0.132	0.497	1.3161	1.984
	308	0.202	0.486	1.292	2.054
	313	0.104	0.419	1.042	2.587
5×10^{-3}	293	0.175	0.426	3.238	0.780
	298	0.175	0.391	3.010	0.853
	303	0.213	0.425	2.479	1.053
	308	0.114	0.357	1.652	1.606
	313	0.085	0.321	1.530	1.763
1×10^{-2}	293	0.277	0.467	4.663	0.541
	298	0.185	0.330	4.846	0.530
	303	0.274	0.406	4.317	0.605
	308	0.153	0.256	4.152	0.639
	313	0.137	0.267	2.909	0.927

Table (3-16): Values of transfer coefficient (α_c , α_a), the polarization resistance (R_p) and equilibrium exchange current density (i_o) for corrosion of carbon steel in saline solution (blank) and in the presence of Ser at pH 11 with various temperature range (293-313) K.

Conc. (M)	T (K)	α_c	α_a	$R_p \times 10^3$ ($\Omega \cdot \text{cm}^2$)	$i_o \times 10^{-5}$ (A/cm^2)
Blank	293	0.314	0.464	1.646	1.534
	298	0.216	0.404	1.229	2.089
	303	0.249	0.416	1.166	2.240
	308	0.208	0.339	1.160	2.288
	313	0.202	0.357	0.942	2.862
5×10^{-4}	293	0.242	0.460	3.315	0.762
	298	0.253	0.527	1.974	1.301
	303	0.243	0.527	1.592	1.640
	308	0.169	0.454	1.230	2.160
	313	0.145	0.428	1.092	2.469
1×10^{-3}	293	0.263	0.485	3.338	0.756
	298	0.327	0.583	2.471	1.039
	303	0.185	0.459	1.838	1.420
	308	0.112	0.394	1.364	1.946
	313	0.153	0.408	1.315	2.051
5×10^{-3}	293	0.307	0.518	3.934	0.642
	298	0.226	0.456	3.178	0.808
	303	0.209	0.435	2.405	1.086
	308	0.116	0.305	2.225	1.193
	313	0.174	0.399	1.641	1.643
1×10^{-2}	293	0.191	0.387	4.784	0.528
	298	0.161	0.396	3.255	0.789
	303	0.010	0.339	2.469	1.057
	308	0.104	0.304	2.234	1.188
	313	0.097	0.321	1.733	1.556

Table (3-17): Values of transfer coefficient (α_c , α_a), the polarization resistance (R_p) and equilibrium exchange current density (i_o) for corrosion of carbon steel in saline solution (blank) and in the presence of Trp at pH 11 with various temperature range (293-313) K.

Conc. (M)	T (K)	α_c	α_a	$R_p \times 10^3$ ($\Omega \cdot \text{cm}^2$)	$i_o \times 10^{-5}$ (A/cm^2)
Blank	293	0.314	0.464	1.646	1.534
	298	0.216	0.404	1.229	2.089
	303	0.249	0.416	1.166	2.240
	308	0.208	0.339	1.160	2.288
	313	0.202	0.357	0.942	2.862
5×10^{-4}	293	0.108	0.285	3.132	0.806
	298	0.112	0.381	1.858	1.382
	303	0.168	0.442	1.449	1.802
	308	0.090	0.412	0.956	2.776
	313	0.112	0.400	0.973	2.772
1×10^{-3}	293	0.254	0.308	3.736	0.676
	298	0.212	0.430	2.429	1.057
	303	0.188	0.395	2.030	1.286
	308	0.438	0.183	1.240	2.140
	313	0.361	0.109	1.184	2.279
5×10^{-3}	293	0.162	0.319	4.552	0.555
	298	0.165	0.415	3.522	0.729
	303	0.215	0.336	2.515	1.038
	308	0.164	0.319	2.231	1.190
	313	0.229	0.386	2.004	1.346
1×10^{-2}	293	0.347	0.390	4.634	0.545
	298	0.373	0.373	3.708	0.692
	303	0.210	0.373	3.301	0.791
	308	0.227	0.360	3.013	0.881
	313	0.199	0.347	2.387	1.130

Table (3-18): Values of transfer coefficient (α_c , α_a), the polarization resistance (R_p) and equilibrium exchange current density (i_o) for corrosion of carbon steel in saline solution (blank) and in the presence of Lys at pH 11 with various temperature range (293-313) K.

Conc. (M)	T (K)	α_c	α_a	$R_p \times 10^3$ ($\Omega \cdot \text{cm}^2$)	$i_o \times 10^{-5}$ (A/cm^2)
Blank	293	0.314	0.464	1.646	1.534
	298	0.216	0.404	1.229	2.089
	303	0.249	0.416	1.166	2.240
	308	0.208	0.339	1.160	2.288
	313	0.202	0.357	0.942	2.862
5×10^{-4}	293	0.193	0.367	3.006	0.840
	298	0.175	0.362	2.418	1.062
	303	0.096	0.268	2.162	1.208
	308	0.162	0.343	1.579	1.681
	313	0.112	0.2941	1.487	1.814
1×10^{-3}	293	0.173	0.349	3.132	0.806
	298	0.161	0.359	2.480	1.036
	303	0.112	0.354	1.643	1.589
	308	0.139	0.327	1.602	1.657
	313	0.181	0.364	1.584	1.703
5×10^{-3}	293	0.194	0.327	4.439	0.569
	298	0.227	0.363	3.803	0.675
	303	0.250	0.441	2.192	1.191
	308	0.230	0.452	1.473	1.802
	313	0.164	0.387	1.314	2.052
1×10^{-2}	293	0.176	0.339	4.569	0.553
	298	0.208	0.365	3.897	0.659
	303	0.165	0.382	2.232	1.170
	308	0.113	0.356	1.513	1.754
	313	0.123	0.376	1.334	2.022

3.5 Effect of Temperature on the Corrosion of Carbon Steel

Corrosion process for carbon steel specimen in saline solution (blank) and in the presence of amino acids (Val, Ser, Trp and Lys) over the range of temperature of (293-313) K at pH (2 and 11) were studied using Arrhenius equation ⁽⁸¹⁾:

$$i_{corr} = A \exp\left(\frac{-E_a}{RT}\right) \dots\dots\dots (3-12)$$

Equation (3-12) Can be converted into logarithmic form and became as:

$$\log i_{corr} = \frac{-E_a}{2.303 RT} + \log A \dots\dots\dots (3-13)$$

Where E_a is the activation energy, R is the gas constant, T is the absolute temperature, A is the pre-exponential factor and i_{corr} is the current density.

Figures (3-10) and (3-12) represent Arrhenius plots for both of the blank solution (saline solution in the absence of inhibitors) and saline solution in the presence of inhibitors at pH (2 and 11); values of E_a and A were derived from the slopes and intercept of the plots respectively. Tables (3-19) and (3-20) give the resulting values of E_a and A for the corrosion of carbon steel in saline solution (blank) and in the presence of inhibitors (Val, Ser, Trp and Lys) of various concentrations and over the temperature range (293-313) K at pH (2 and 11). The data presented in tables (3-19) and (3-20) indicate that the activation energy (E_a) values are higher in the presence of the inhibitor molecules as compared with the values of blank solution and they are increase with increasing concentration of inhibitor due to the adsorption of inhibitor molecules on the metal surface. The obtained values of A increases with increase in the concentrations of inhibitors ⁽⁸²⁾.

A replacement formula of Arrhenius equation is

$$i_{corr} = \left(\frac{RT}{Nh}\right) \exp\left(\frac{\Delta S^*}{R}\right) \exp\left(\frac{-\Delta H^*}{RT}\right) \dots\dots\dots (3-14)$$

Where h is planks constant, N is Avogadro's number, ΔS^* is the entropy of activation and ΔH^* is the enthalpy of activation. Equation (3-14) can be converted to:

$$\ln\left(\frac{i_{corr}}{T}\right) = \ln\left(\frac{R}{Nh}\right) + \left(\frac{\Delta S^*}{R}\right) - \left(\frac{\Delta H^*}{RT}\right) \dots\dots\dots (3-15)$$

Figures (3-11) and (3-13) show the plots of $\ln (i_{\text{corr}}/T)$ against $1/T$ through which the enthalpy change of activation (ΔH^*) and entropy change of activation (ΔS^*) were determined from the slopes and intercepts respectively. Values of (ΔH^*) and (ΔS^*) obtained are listed in tables (3-19) and (3-20). The positive sign of the activation enthalpies (ΔH^*) in the absence and presence of the inhibitor molecules means the endothermic nature of the carbon steel dissolution process which means that the dissolution of carbon steel is difficult in the presence of the inhibitor. Large and negative change in the values of activation entropy (ΔS^*) in the absence and presence of the inhibitor molecules means that the activated complex in the rate determining step represents association rather than the dissociation step, that means a decrease in disorder take place, going from reactant to the activate complex ^(83,84).

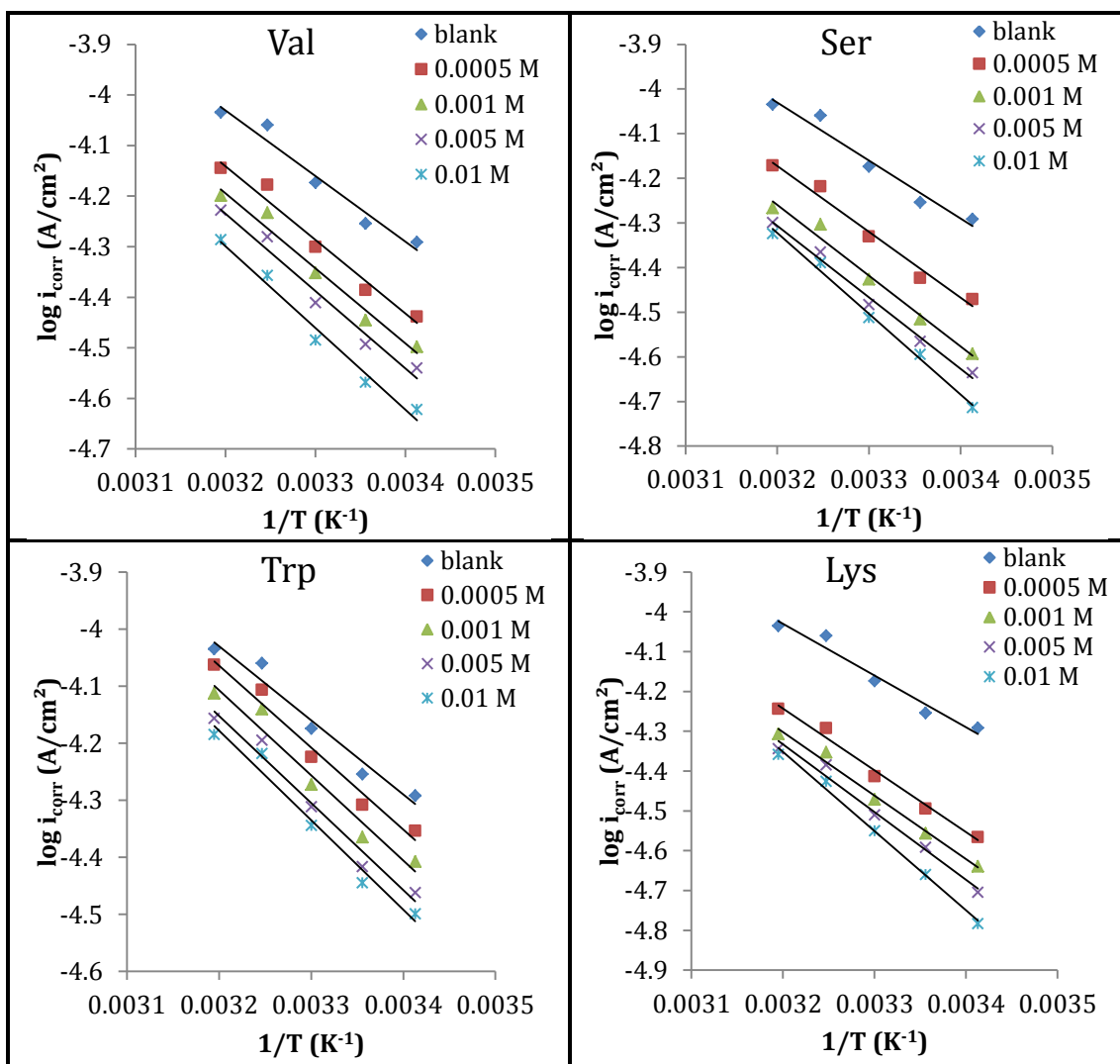


Figure (3-10): Arrhenius plots of $\log i_{\text{corr}}$ versus $1/T$ for the corrosion of carbon steel in saline solution (blank) and in the presence of inhibitors (Val, Ser, Trp and Lys) of various concentrations at pH 2.

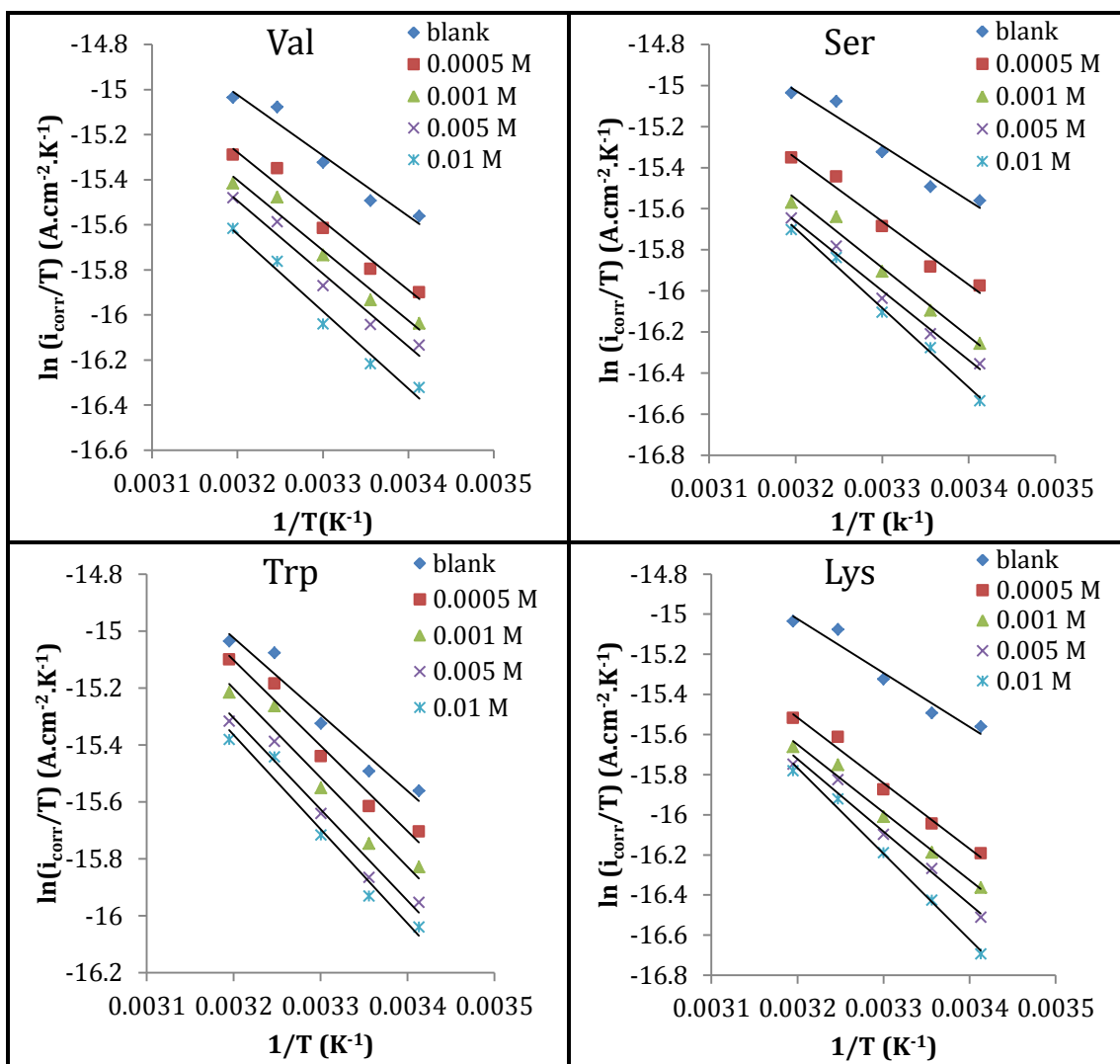


Figure (3-11): Arrhenius plots of $\ln(i_{\text{corr}}/T)$ versus $1/T$ for the corrosion of carbon steel in saline solution (blank) and in the presence of inhibitors (Val, Ser, Trp and Lys) of various concentrations at pH 2.

Table (3-19): Activation energy (E_a), activation enthalpy (ΔH^*), and the entropy of activation (ΔS^*) for the corrosion of carbon steel in saline solution (blank) and in the presence of inhibitors (Val, Ser, Trp and Lys) of various concentrations at pH 2.

Inh.	Con. (M)	E_a (kJ.mol ⁻¹)	$A \times 10^{24}$ (molecules.cm ⁻² .s ⁻¹)	ΔH^* (kJ.mol ⁻¹)	$-\Delta S^*$ (J.K ⁻¹ .mol ⁻¹)
Blank	-	24.86	0.80	22.34	250.97
Trp	5×10^{-4}	27.50	2.05	24.97	243.18
	1×10^{-3}	28.57	2.80	26.04	240.58
	5×10^{-3}	29.19	3.20	26.66	239.47
	1×10^{-2}	30.04	4.19	27.52	237.22
Val	5×10^{-4}	27.91	2.01	25.38	243.34
	1×10^{-3}	28.43	2.17	25.91	242.68
	5×10^{-3}	29.37	2.84	26.84	240.46
	1×10^{-2}	30.94	6.61	28.42	236.65
Ser	5×10^{-4}	28.22	2.11	25.70	242.93
	1×10^{-3}	30.39	3.97	27.86	237.67
	5×10^{-3}	30.67	3.98	28.15	237.65
	1×10^{-2}	34.64	17.7	32.12	225.26
Lys	5×10^{-4}	29.71	3.17	27.19	239.53
	1×10^{-3}	30.59	3.88	28.06	237.85
	5×10^{-3}	32.59	7.83	30.07	232.03
	1×10^{-2}	38.09	62.1	35.56	214.81

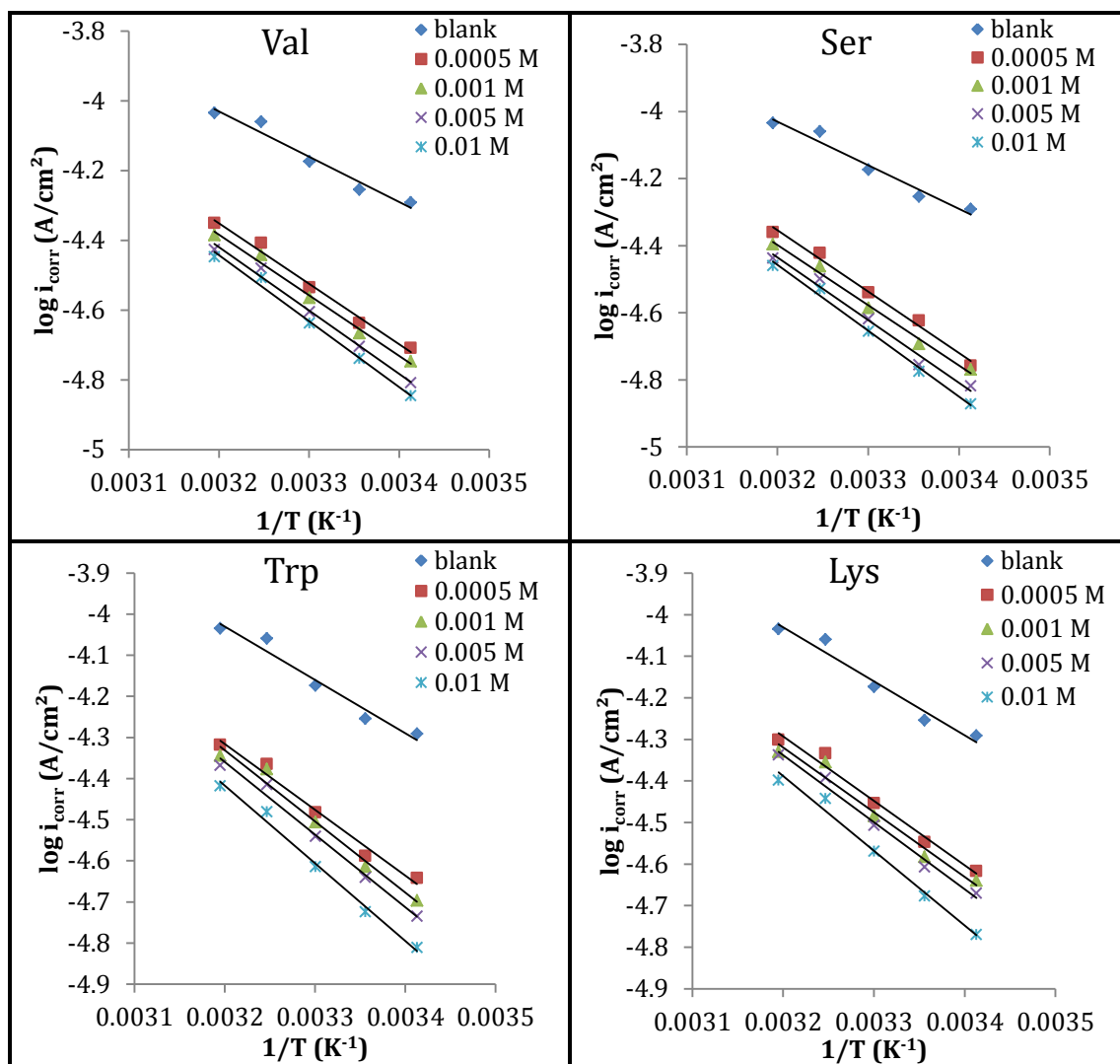


Figure (3-12): Arrhenius plots of $\log i_{\text{corr}}$ versus $1/T$ for the corrosion of carbon steel in saline solution (blank) and in the presence of inhibitors (Val, Ser, Trp and Lys) of various concentrations at pH 11.

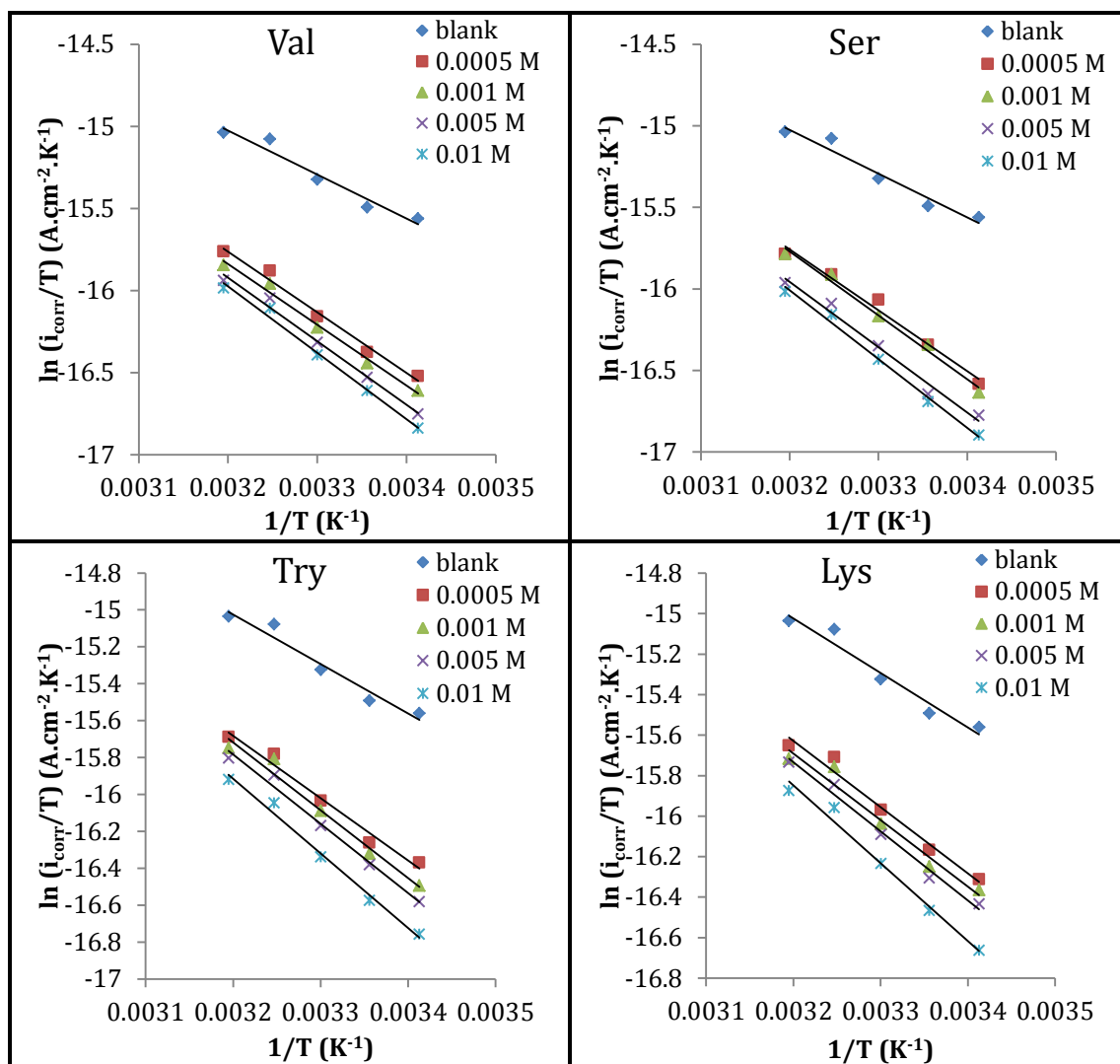


Figure (3-13): Arrhenius plots of $\ln(i_{\text{corr}}/T)$ versus $1/T$ for the corrosion of carbon steel in saline solution (blank) and in the presence of inhibitors (Val, Ser, Trp and Lys) of various concentrations at pH 11.

Table (3-20): Activation energy (E_a), activation enthalpy (ΔH^*), and the entropy of activation (ΔS^*) for the corrosion of carbon steel in saline solution (blank) and in the presence of inhibitors (Val, Ser, Trp and Lys) of various concentrations at pH 11.

Inh.	Con. (M)	E_a (kJ.mol ⁻¹)	$A \times 10^{24}$ (molecules.cm ⁻² .s ⁻¹)	ΔH^* (kJ.mol ⁻¹)	$-\Delta S^*$ (J.K ⁻¹ .mol ⁻¹)
Blank	-	24.86	0.80	22.34	250.97
Lys	5×10^{-4}	29.70	2.82	27.18	240.51
	1×10^{-3}	29.78	2.74	27.26	240.76
	5×10^{-3}	30.90	4.03	28.37	237.54
	1×10^{-2}	34.41	13.88	31.89	227.26
Trp	5×10^{-4}	30.63	3.82	28.10	237.98
	1×10^{-3}	33.11	9.60	30.59	230.32
	5×10^{-3}	33.74	11.4	31.21	228.88
	1×10^{-2}	36.15	25.4	33.63	222.25
Val	5×10^{-4}	33.24	9.64	30.72	230.28
	1×10^{-3}	33.29	9.11	30.77	230.75
	5×10^{-3}	34.75	14.8	32.32	226.72
	1×10^{-2}	36.21	24.5	33.69	222.53
Ser	5×10^{-4}	35.07	19.4	30.97	229.45
	1×10^{-3}	34.37	13.4	32.55	224.48
	5×10^{-3}	35.82	21.4	33.31	223.61
	1×10^{-2}	37.58	40.1	35.07	218.42

3.7 Thermodynamic Parameters of Corrosion

Thermodynamic laws can be explained as the tendency for any chemical reaction to go, including the reaction of a metal with components of its environment, is measured by the Gibbs free-energy change (ΔG). The more negative value of (ΔG) the greater the tendency for the reaction to occur. The electrochemical mechanisms of corrosion (the tendency for a metal to corrode) can also be explained in terms of the electromotive force (emf) of the corrosion cells that are an integral part of the corrosion process. Since electrical energy is explained as the product

of volts by coulombs (joule), the relation between (ΔG) in joule and emf in volts (E) is defined by the following equation ⁽²⁰⁾:

$$\Delta G = -nFE \dots\dots\dots (3-16)$$

Where n is the number of electron in corrosion reaction, F is the Faraday constant and E is equal to the reverse sign of the E_{corr} .

There are other thermodynamic quantities can be derived from electrochemical measurements. For instance, the entropy change (ΔS) in a cell reaction that given by the thermodynamic relations of the temperature (T) dependence on ΔG ⁽¹⁾:

$$\Delta S = -\left(\frac{\partial \Delta G}{\partial T}\right)_P \dots\dots\dots (3-17)$$

The enthalpy change values (ΔH) of the corrosion process were determined by using the well known relation:

$$\Delta G = \Delta H - T\Delta S \dots\dots\dots (3-18)$$

Figure (3-14) and (3-15), show the plots of (ΔG) values against the absolute temperature (T) for the corrosion of carbon steel in saline solution (blank) and in the presence of inhibitors (Val, Ser, Trp and Lys) at pH (2 and 11), values of (ΔS) were derived from the slopes of various plots in figure (3-14) and (3-15). Values of (ΔG), (ΔH) and (ΔS) were presented in tables (3-21) to (3-28). The results show that the values of Gibbs free-energy change (ΔG) for the corrosion of carbon steel at different conditions (pH, temperature and absence or presence of inhibitors) are negative indicating spontaneous nature for the reaction.

The positive sign of entropy change (ΔS) mean loss in the degrees of randomness and the resultant of the corrosion products. Values of ΔS were positive (tables (3-21) to (3-28)) indicating that the corrosion process is entropically favorable.

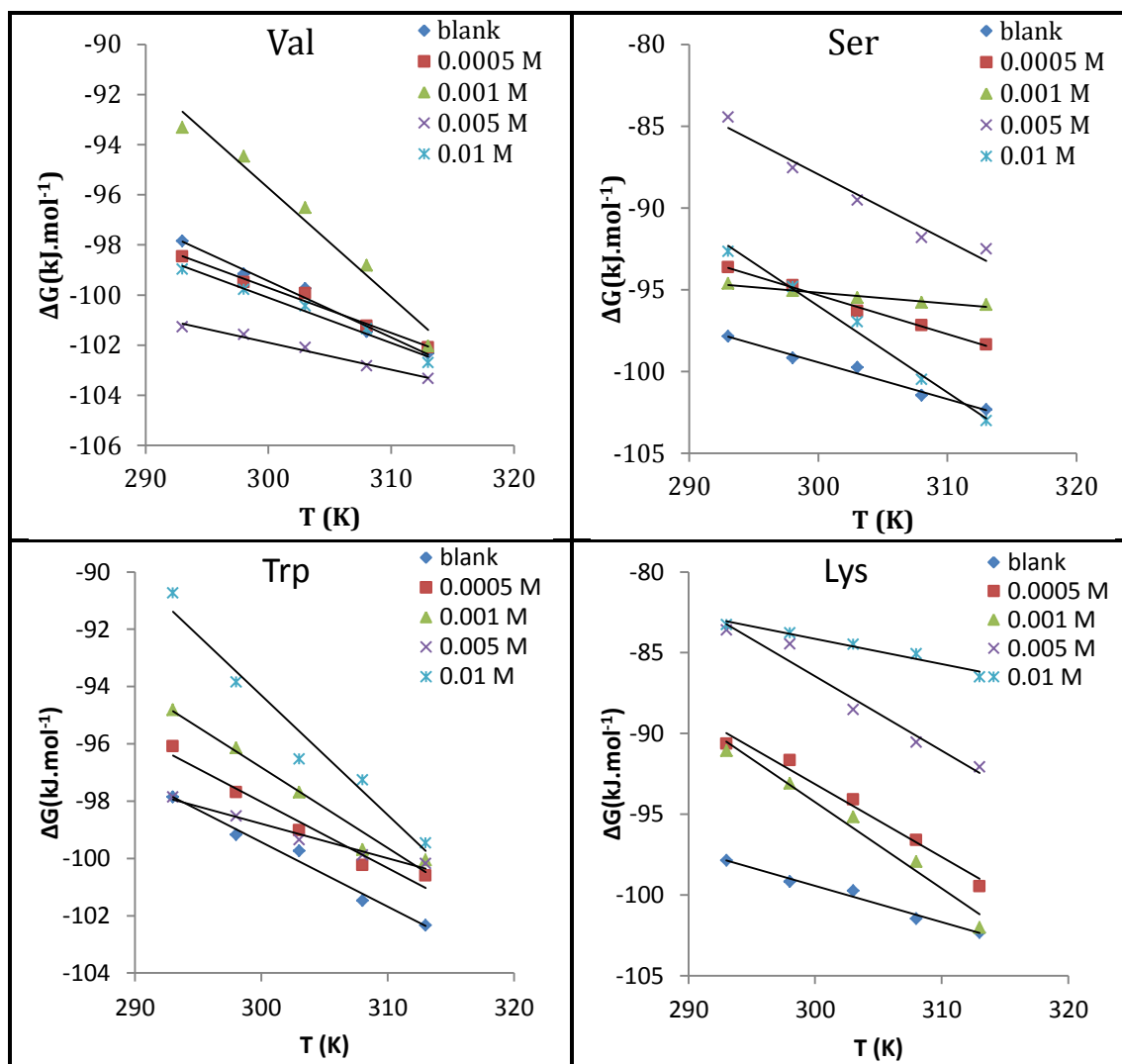


Figure (3-14): The variation of Gibbs free energies (ΔG) with temperature for the corrosion of carbon steel in saline solution (blank) and in the presence of inhibitors (Val, Ser, Trp and Lys) at pH 2.

Table (3-21): The thermodynamic parameters for the corrosion of carbon steel in saline solution (blank) and in the presence of Val over the temperature range (293-313) K at pH 2.

Conc. (M)	T (K)	$-\Delta G$ (kJ.mol)	ΔH (kJ.mol ⁻¹)	ΔS (J.K ⁻¹ .mol ⁻¹)
blank	293	97.860	-31.930	225
	298	99.170	-32.117	
	303	99.730	-31.571	
	308	101.46	-32.164	
	313	102.33	-31.907	
5×10^{-4}	293	98.470	-45.79	179.8
	298	99.500	-45.92	
	303	99.940	-45.46	
	308	101.23	-45.85	
	313	102.10	-45.82	
1×10^{-3}	293	93.320	34.34	435.7
	298	94.480	35.36	
	303	96.520	35.49	
	308	98.820	35.38	
	313	102.04	34.33	
5×10^{-3}	293	101.27	-69.72	107.7
	298	101.58	-69.49	
	303	102.10	-69.47	
	308	102.83	-69.66	
	313	103.34	-69.63	
1×10^{-2}	293	98.970	-46.18	180.2
	298	99.780	-46.09	
	303	100.44	-45.84	
	308	101.35	-45.85	
	313	102.70	-46.30	

Table (3-22): The thermodynamic parameters for the corrosion of carbon steel in saline solution (blank) and in the presence of Ser over the temperature range (293-313) K at pH 2.

Conc. (M)	T (K)	$-\Delta G$ (kJ.mol)	ΔH (kJ.mol ⁻¹)	ΔS (J.K ⁻¹ .mol ⁻¹)
blank	293	97.860	-31.930	225
	298	99.170	-32.117	
	303	99.730	-31.571	
	308	101.46	-32.164	
	313	102.33	-31.907	
5×10 ⁻⁴	293	93.630	-23.866	238.1
	298	94.730	-23.775	
	303	96.320	-24.167	
	308	97.180	-23.845	
	313	98.360	-23.831	
1×10 ⁻³	293	94.610	-75.041	66.8
	298	95.080	-75.170	
	303	95.500	-75.261	
	308	95.790	-75.216	
	313	95.930	-75.017	
5×10 ⁻³	293	84.460	34.847	407.2
	298	87.550	33.795	
	303	89.520	33.863	
	308	91.820	33.602	
	313	92.510	34.944	
1×10 ⁻²	293	92.660	61.923	527.6
	298	94.810	62.419	
	303	96.970	62.895	
	308	100.50	62.002	
	313	103.01	62.131	

Table (3-23): The thermodynamic parameters for the corrosion of carbon steel in saline solution (blank) and in the presence of Trp over the temperature range (293-313) K at pH 2.

Conc. (M)	T (K)	$-\Delta G$ (kJ.mol)	ΔH (kJ.mol ⁻¹)	ΔS (J.K ⁻¹ .mol ⁻¹)
blank	293	97.860	-31.930	225
	298	99.170	-32.117	
	303	99.730	-31.552	
	308	101.46	-32.164	
	313	102.33	-31.907	
5×10 ⁻⁴	293	96.080	-28.22	231.6
	298	97.680	-28.67	
	303	99.010	-28.84	
	308	100.23	-28.90	
	313	100.60	-28.11	
1×10 ⁻³	293	94.810	-12.47	281
	298	96.140	-12.40	
	303	97.680	-12.54	
	308	99.690	-13.14	
	313	100.06	-12.10	
5×10 ⁻³	293	97.860	-62.70	120
	298	98.510	-62.75	
	303	99.340	-62.98	
	308	99.880	-62.92	
	313	100.17	-62.61	
1×10 ⁻²	293	90.730	31.51	417.2
	298	93.840	30.48	
	303	96.520	29.89	
	308	97.260	31.24	
	313	99.460	31.13	

Table (3-24): The thermodynamic parameters for the corrosion of carbon steel in saline solution (blank) and in the presence of Lys over the temperature range (293-313) K at pH 2.

Conc. (M)	T (K)	$-\Delta G$ (kJ.mol)	ΔH (kJ.mol ⁻¹)	ΔS (J.K ⁻¹ .mol ⁻¹)
blank	293	97.860	-31.930	225
	298	99.170	-32.117	
	303	99.730	-31.571	
	308	101.46	-32.164	
	313	102.33	-31.907	
5×10 ⁻⁴	293	90.640	41.651	451.5
	298	91.660	42.886	
	303	94.090	42.712	
	308	96.600	42.461	
	313	99.460	41.863	
1×10 ⁻³	293	91.060	65.546	534.5
	298	93.090	66.192	
	303	95.170	66.781	
	308	97.930	66.694	
	313	102.01	65.295	
5×10 ⁻³	293	83.590	51.303	460.4
	298	84.460	52.736	
	303	88.520	50.986	
	308	90.540	51.262	
	313	92.070	52.039	
1×10 ⁻²	293	83.250	-37.686	155.5
	298	83.770	-37.429	
	303	84.480	-37.366	
	308	85.060	-37.167	
	313	86.490	-37.818	

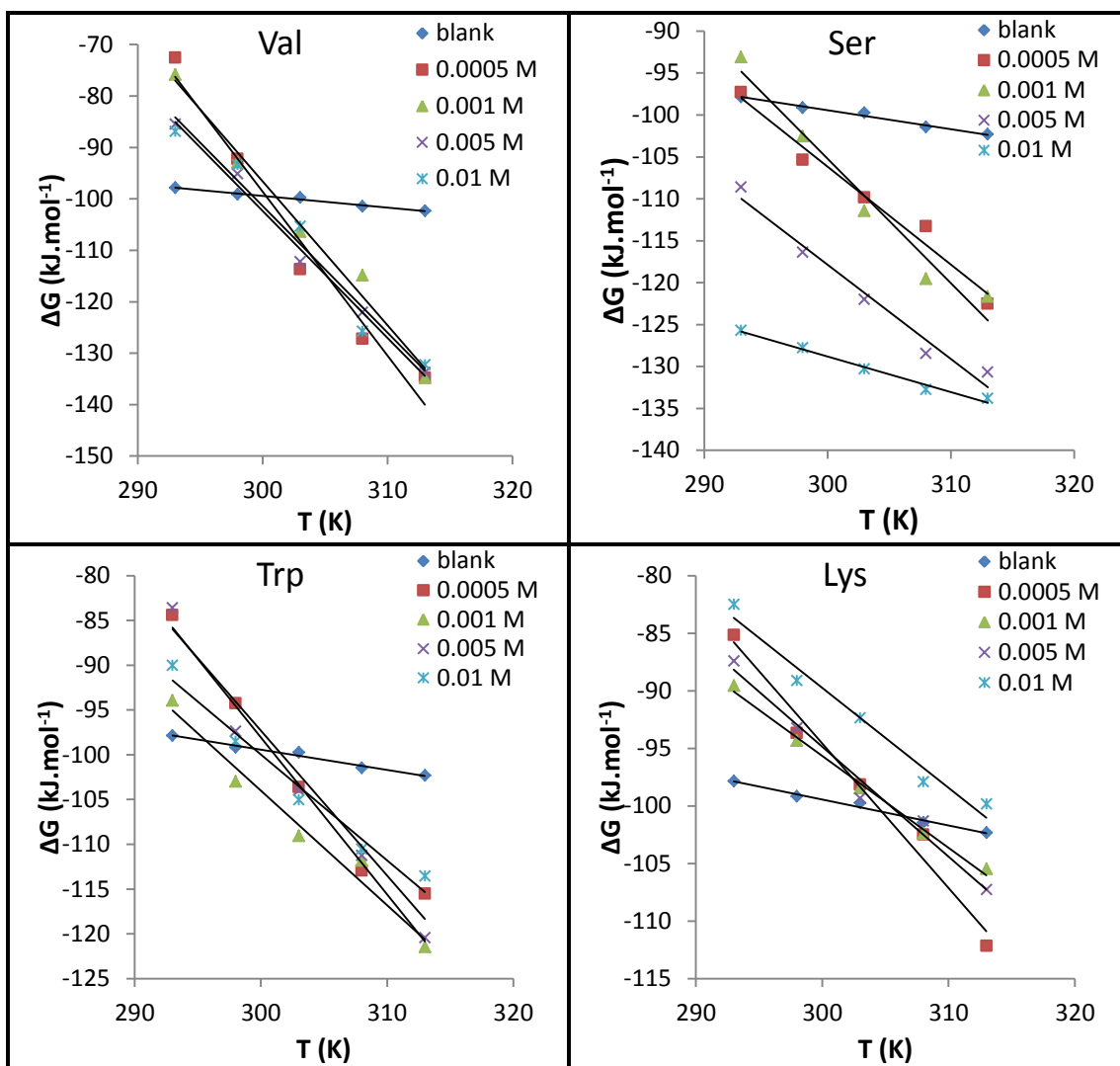


Figure (3-15): The variation of Gibbs free energies (ΔG) with temperature for the corrosion of carbon steel in saline solution (blank) and in the presence of inhibitors (Val, Ser, Trp and Lys) at pH 11.

Table (3-25): The thermodynamic parameters for the corrosion of carbon steel in saline solution (blank) and in the presence of Val over the temperature range (293-313) K at pH 11.

Conc. (M)	T (K)	$-\Delta G$ (kJ.mol)	ΔH (kJ.mol ⁻¹)	ΔS (J.K ⁻¹ .mol ⁻¹)
blank	293	97.860	-31.930	225
	298	99.170	-32.117	
	303	99.730	-31.552	
	308	101.46	-32.164	
	313	102.33	-31.907	
5×10 ⁻⁴	293	72.600	861.66	3188.6
	298	92.240	857.96	
	303	113.70	852.45	
	308	127.28	854.81	
	313	134.79	863.24	
1×10 ⁻³	293	75.880	743.97	2798.1
	298	92.930	740.90	
	303	106.38	741.44	
	308	114.89	746.92	
	313	134.85	740.96	
5×10 ⁻³	293	85.510	637.77	2468.5
	298	95.150	640.46	
	303	112.23	635.72	
	308	122.09	638.21	
	313	133.75	638.89	
1×10 ⁻²	293	86.910	634.54	2462.3
	298	93.380	640.39	
	303	105.36	640.72	
	308	125.76	632.63	
	313	132.28	638.42	

Table (3-26): The thermodynamic parameters for the corrosion of carbon steel in saline solution (blank) and in the presence of Ser over the temperature range (293-313) K at pH 11.

Conc. (M)	T (K)	$-\Delta G$ (kJ.mol)	ΔH (kJ.mol ⁻¹)	ΔS (J.K ⁻¹ .mol ⁻¹)
blank	293	97.860	-31.930	225
	298	99.170	-32.117	
	303	99.730	-31.552	
	308	101.46	-32.164	
	313	102.33	-31.907	
5×10 ⁻⁴	293	97.310	244.646	1167.1
	298	105.38	242.415	
	303	109.86	243.774	
	308	113.29	246.174	
	313	122.54	242.766	
1×10 ⁻³	293	93.110	341.587	1483.6
	298	102.54	339.569	
	303	111.46	338.071	
	308	119.56	337.385	
	313	121.69	342.680	
5×10 ⁻³	293	108.62	220.885	1124.6
	298	116.38	218.751	
	303	122.02	218.739	
	308	128.46	217.917	
	313	130.70	221.301	
1×10 ⁻²	293	125.70	-1.527	423.8
	298	127.79	-1.492	
	303	130.31	-1.901	
	308	132.76	-2.233	
	313	133.81	-1.156	

Table (3-27): The thermodynamic parameters for the corrosion of carbon steel in saline solution (blank) and in the presence of Trp over the temperature range (293-313) K at pH 11.

Conc. (M)	T (K)	$-\Delta G$ (kJ.mol)	ΔH (kJ.mol ⁻¹)	ΔS (J.K ⁻¹ .mol ⁻¹)
blank	293	97.860	-31.930	225
	298	99.170	-32.117	
	303	99.730	-31.552	
	308	101.46	-32.164	
	313	102.33	-31.907	
5×10^{-4}	293	84.420	389.39	1617.1
	298	94.270	387.63	
	303	103.62	386.36	
	308	112.95	385.12	
	313	115.51	390.64	
1×10^{-3}	293	93.940	303.43	1356.2
	298	102.99	301.16	
	303	109.05	301.88	
	308	111.83	305.88	
	313	121.46	303.04	
5×10^{-3}	293	83.610	429.55	1751.4
	298	97.370	424.54	
	303	103.97	426.70	
	308	111.27	428.16	
	313	120.45	427.74	
1×10^{-2}	293	90.040	256.11	1181.4
	298	98.490	253.57	
	303	105.05	252.91	
	308	110.55	253.32	
	313	113.54	256.23	

Table (3-28): The thermodynamic parameters for the corrosion of carbon steel in saline solution (blank) and in the presence of Lys over the temperature range (293-313) K at pH 11.

Conc. (M)	T (K)	$-\Delta G$ (kJ.mol)	ΔH (kJ.mol ⁻¹)	ΔS (J.K ⁻¹ .mol ⁻¹)
blank	293	97.860	-31.930	225
	298	99.170	-32.117	
	303	99.730	-31.552	
	308	101.46	-32.164	
	313	102.33	-31.907	
5×10 ⁻⁴	293	85.180	282.57	1255.1
	298	93.690	280.33	
	303	98.140	282.15	
	308	102.49	284.08	
	313	112.15	280.69	
1×10 ⁻³	293	89.560	144.08	797.4
	298	94.340	143.28	
	303	98.450	143.16	
	308	102.41	143.19	
	313	105.46	144.13	
5×10 ⁻³	293	87.420	192.58	955.6
	298	93.240	191.53	
	303	99.340	190.21	
	308	101.31	193.02	
	313	107.27	191.83	
1×10 ⁻²	293	82.490	172.06	868.8
	298	89.130	169.77	
	303	92.360	170.89	
	308	97.910	169.68	
	313	99.820	172.11	

3.7 Thermodynamic Parameters of the Adsorption Isotherm

The interaction between the surface of carbon steel and the inhibitor molecules is explained by adsorption isotherms. The adsorption of the inhibitor molecules (Val, Ser, Trp and Lys) on the carbon steel surface depends on the value of the surface coverage (θ). Values of

surface coverage (θ) were calculated from the equation (3-2). To determine the effect of concentrations of inhibitor molecules on the corrosion of carbon steel, Langmuir adsorption isotherms were used and which expressed by the following equation ⁽⁸⁵⁾:

$$\left(\frac{c_{inh}}{\theta}\right) = \frac{1}{K_{ads}} + c_{inh} \dots\dots\dots (3-19)$$

Where c_{inh} is the inhibitor concentration and K_{ads} is equilibrium constant of the adsorption process, values of K_{ads} were determined from the intercept of the straight line of plots of c_{inh}/θ versus c_{inh} as shown in figures (3-16) and (3-18).

By using the values of K_{ads} , ΔG°_{ads} values can calculated from the following relation:

$$\Delta G^{\circ}_{ads} = -RT \ln(55.5 K_{ads}) \dots\dots\dots (3-20)$$

where R is the gas constant and T is the absolute temperature. The value of 55.5 is the concentration of water in solution in mole/L. The values of K_{ads} and ΔG°_{ads} are tabulated in tables (3-29) and (3-30). The negative sign of ΔG°_{ads} values indicated that the adsorption of inhibitor molecules to form a stable adsorbed protective layer on surface of carbon steel is spontaneous. The values of ΔG°_{ads} ranging between the maximum value in minus (-32.53 kJ.mole⁻¹) for Ser at pH 11 and 313 K, to minimum value in minus (-24.52 kJ.mole⁻¹) of Trp at pH 2 and 293 K. The values of ΔG°_{ads} ranging between (-40 kJ.mol⁻¹) to (-20 kJ.mol⁻¹) meaning that the adsorption of these inhibitor molecules via chemisorptions and physisorption ^(86,87). In figures (3-17) and (3-19), the change of free energy were plotted versus temperature (K) in order to calculate the enthalpy change (ΔH_{ads}) and the entropy change (ΔS_{ads}) of adsorption process according to the following equation:

$$\Delta G_{ads} = \Delta H_{ads} - T\Delta S_{ads} \dots\dots\dots (3-21)$$

The intercept equals to ΔH_{ads} and slope equals to ΔS_{ads} the obtained values were listed in tables (3-29) and (3-30). The negative value of ΔH_{ads} means the exothermic nature of adsorption process of amino acids (Val, Ser, Trp and Lys) onto the carbon steel surface. The entropy change (ΔS_{ads}) is positive, that indicates an increase in freedom during the adsorption process ⁽⁸⁸⁾. The lone pairs of electron for nitrogen and oxygen atoms (hetero atoms) in the amino acids investigates that the amino acids adsorbed on carbon steel surface and fill the empty orbital depends upon electron density present around the hetero atoms, the number of adsorption active sides in the molecule of inhibitor and their charge density, molecular size, mode of adsorption, and formation of metallic complexes. According to these results, one can noted that the performance of amino acids depends on the nature and number of hetero atoms ^(68,71).

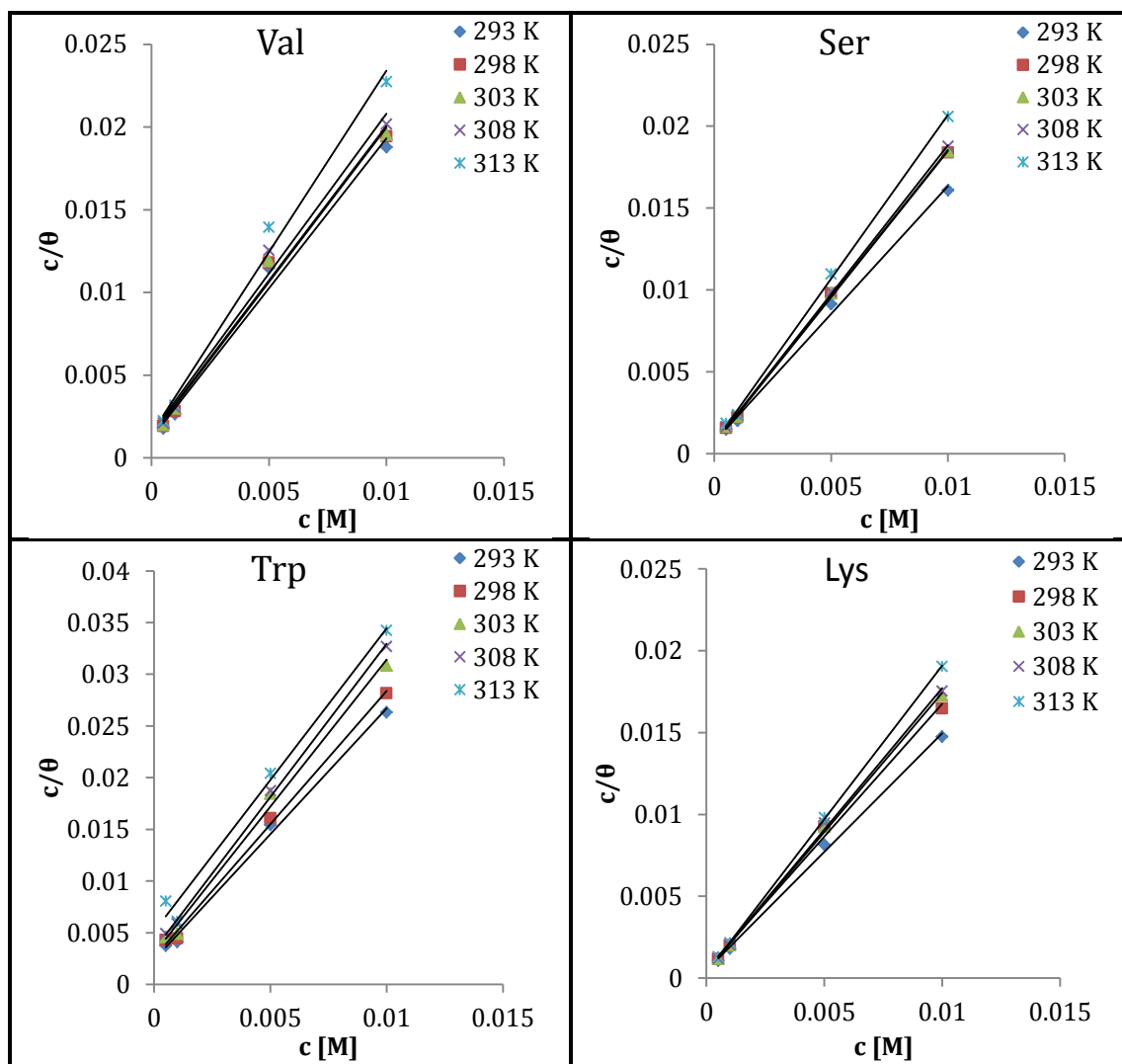


Figure (3-16): Langmuir isotherm plots for the adsorption of (Val, Ser, Trp and Lys) on carbon steel in saline solution at PH 2.

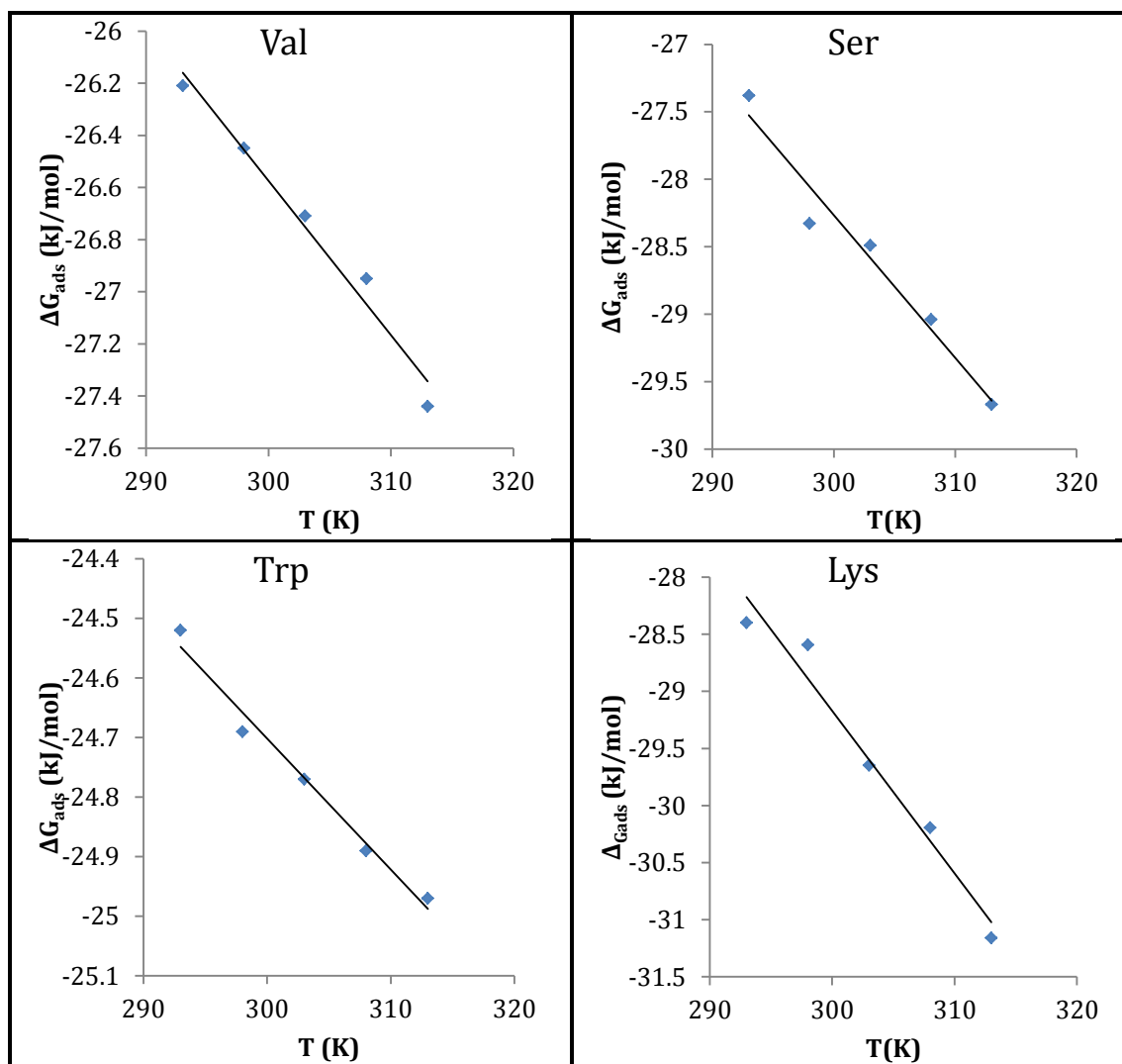


Figure (3-17): The variation of Gibbs free energies (ΔG_{ads}) with temperature for the adsorption of (Val, Ser, Trp and Lys) on carbon steel in saline solution at PH 2.

Table (3-29): Thermodynamic parameters for adsorption of the inhibitors on the surface of carbon steel in saline solution at PH 2.

Inh.	T (K)	K_{ads} (M^{-1})	$-\Delta G_{ads}$ ($kJ.mol^{-1}$)	$-\Delta H_{ads}$ ($kJ.mol^{-1}$)	ΔS_{ads} ($J.K^{-1}.mol^{-1}$)
Trp	293	423.730	24.52	18.102	22
	298	383.140	24.69		
	303	335.570	24.77		
	308	299.400	24.89		
	313	264.550	24.97		
Val	293	847.460	26.21	8.814	59.2
	298	781.250	26.45		
	303	724.640	26.71		
	308	671.140	26.95		
	313	684.930	27.44		
Ser	293	1369.86	27.38	3.475	105.8
	298	1666.67	28.33		
	303	1470.59	28.49		
	308	1515.15	29.04		
	313	1612.90	29.67		
Lys	293	2083.33	28.40	13.573	142.5
	298	1851.85	28.59		
	303	2325.58	29.65		
	308	2380.95	30.19		
	313	2857.14	31.16		

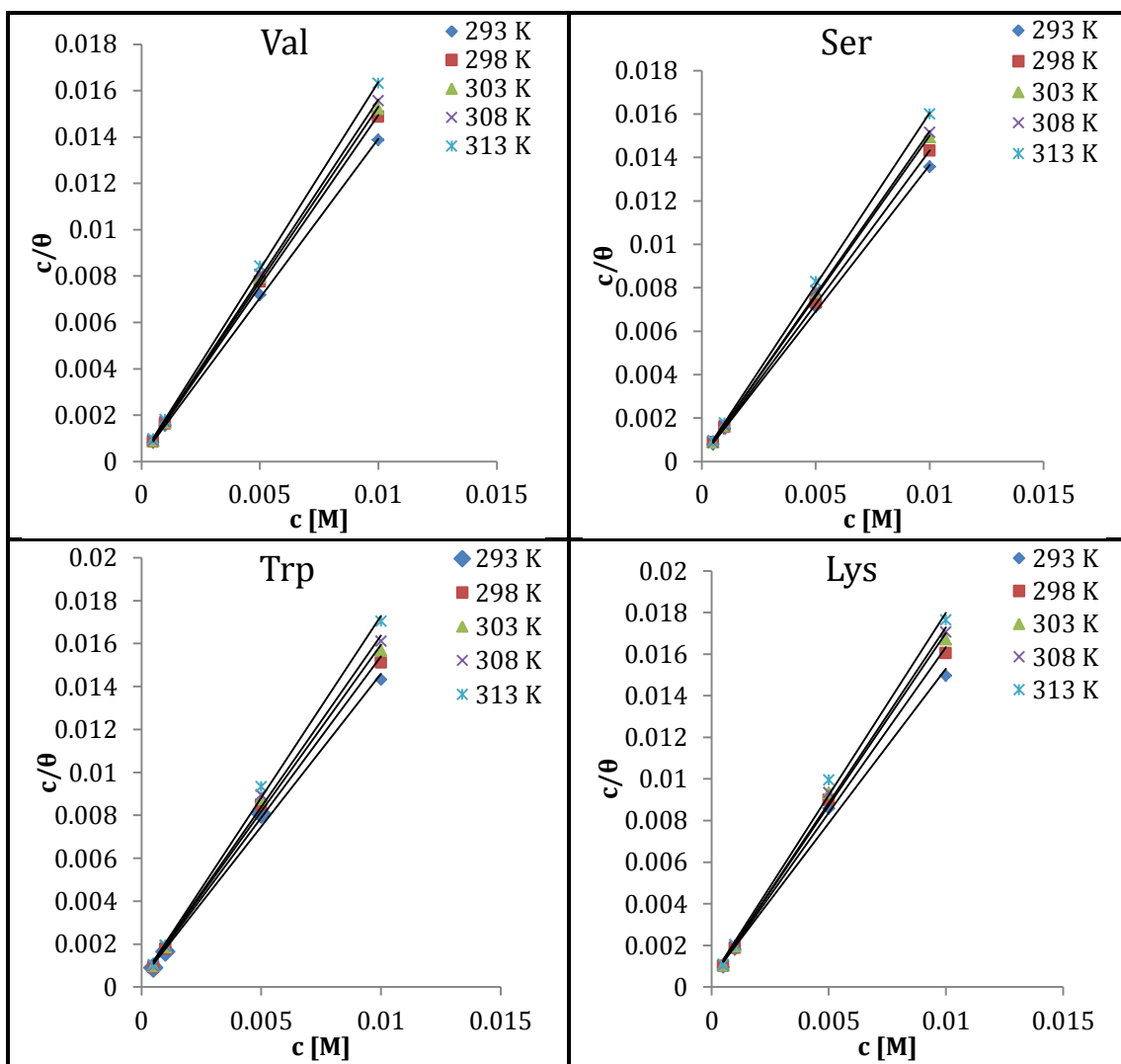


Figure (3-18): Langmuir isotherm plots for the adsorption of (Val, Ser, Trp and Lys) on carbon steel in saline solution at PH 11.

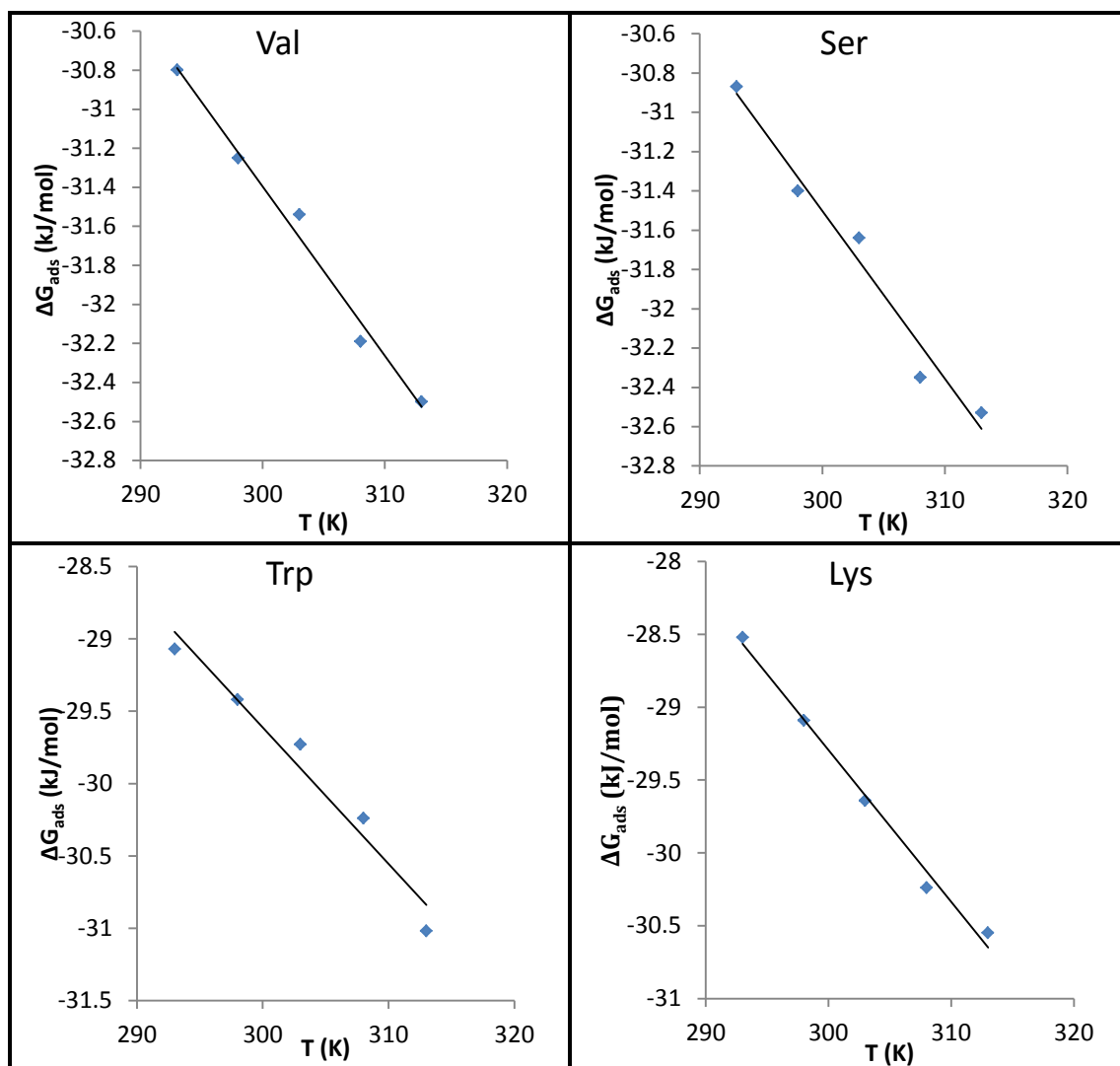


Figure (3-19): The variation of Gibbs free energies (ΔG_{ads}) with temperature for the adsorption of (Val, Ser, Trp and Lys) on carbon steel in saline solution at PH 2.

Table (3-30): Thermodynamic parameters for adsorption of the inhibitors on the surface of carbon steel in saline solution at PH 11.

Inh.	T (K)	K_{ads} (M^{-1})	$-\Delta G_{ads}$ ($kJ.mol^{-1}$)	$-\Delta H_{ads}$ ($kJ.mol^{-1}$)	ΔS_{ads} ($J.K^{-1}.mol^{-1}$)
Lys	293	2188.184	28.52	1.965	104.2
	298	2262.443	29.09		
	303	2320.186	29.64		
	308	2421.308	30.24		
	313	2257.336	30.55		
Trp	293	2739.73	29.07	1.293	94.4
	298	2583.98	29.42		
	303	2409.64	29.73		
	308	2427.18	30.24		
	313	2710.03	31.02		
Val	293	5586.592	30.80	5.356	86.6
	298	5405.405	31.25		
	303	4926.108	31.54		
	308	5181.347	32.19		
	313	4784.689	32.50		
Ser	293	5747.126	30.87	5.882	85.4
	298	5747.126	31.40		
	303	5128.205	31.64		
	308	5524.862	32.35		
	313	4830.918	32.53		

3.8 Theoretical Studies

Quantum chemical calculations have been investigated the effect of structural parameters on the protection efficiency of amino acids (Val, Ser, Trp and Lys) and study its adsorption mechanism on the carbon steel surface. Number of molecular parameters such as the energy of highest occupied molecular orbital (E_{HOMO}), energy of lowest unoccupied molecular orbital (E_{LUMO}) as shown in figure (3-20), the energy gap ΔE , dipole moment (μ), the total energy (E_{total}), the electronegativity (χ) and the hardness (η) were calculated from the optimized molecular structure as shown in figure (3-21).

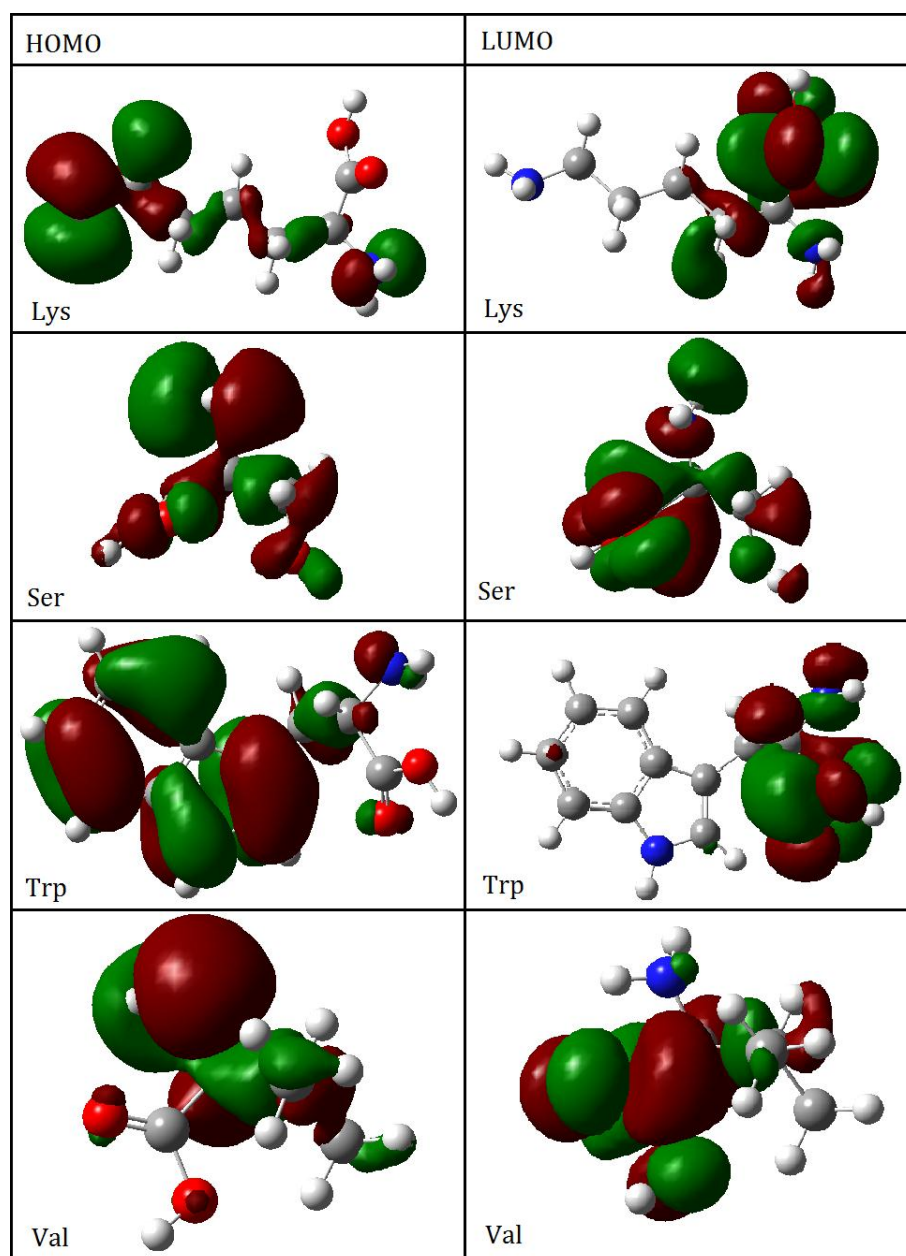


Figure (3-20): The energy of lowest unoccupied molecular orbital (E_{LUMO}) and the energy of highest occupied molecular orbital (E_{HOMO}) of amino acids.

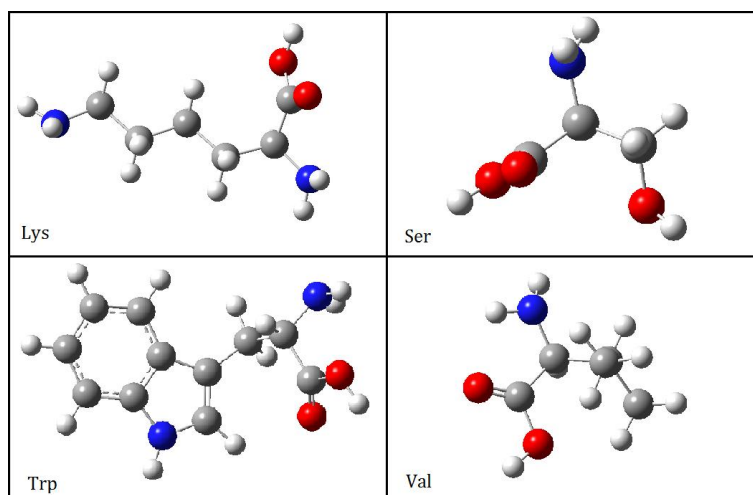


Figure (3-21): Optimized structure of amino acids.

Quantum chemical calculations were determined by using density functional theory (DFT) method according to the following equations ⁽⁸⁹⁾:

$$\chi = \frac{(I+A)}{2} \dots\dots\dots (3-22)$$

$$\eta = \frac{(I-A)}{2} \dots\dots\dots (3-23)$$

Depending on Koopman's theorem, the E_{HOMO} and E_{LUMO} of the inhibitor molecules means the ionization potential (I), and the electron affinity (A), respectively, by using the following relations ⁽⁸⁹⁾:

$$I = -E_{\text{HOMO}} \qquad A = -E_{\text{LUMO}}$$

The fraction of electrons transferred (ΔN) can be calculated from the relation ⁽⁹⁰⁾:

$$\Delta N = \frac{(\chi_{\text{Fe}} - \chi_{\text{inh}})}{2(\eta_{\text{Fe}} + \eta_{\text{inh}})} \dots\dots\dots (3-24)$$

Where $\chi_{\text{Fe}} \approx 7.0$ eV is a theoretical value of iron and $\eta_{\text{Fe}} = 0$ is taken assuming that $I = A$ for bulk metals. The calculated theoretical parameters were presented in table (3-31).

High value of E_{HOMO} for the molecule indicating its tendency to donate electrons to the acceptor molecules (at the metal surface) at low

energy empty molecular orbitals and enhance the inhibition efficiency. The negative values of E_{HOMO} increased in the following order:

$$\text{Trp} > \text{Val} > \text{Lys} > \text{Ser}$$

The lower of energy of the lowest unoccupied molecular orbital (E_{LUMO}) means its ability to accept electrons. When value of ΔE decreases, the reactivity of the inhibitor increases, So it is increase the inhibition efficiency of the molecule ⁽⁹¹⁾. The dipole moment (μ) is indicator of the electronic distribution in molecules of inhibitor. A high values of dipole moment indicates polar character for the molecule, while a low values of dipole moment indicates nonpolar character for the molecule. Although there is no convention in the literature about the relation between the dipole moment and the inhibition efficiency, it can be used as a descriptor to describe the charge movement across the molecule ⁽⁸⁹⁾. The values of χ and η were used to calculate the fraction of electrons transferred (ΔN). The higher value of ΔN indicates higher inhibition efficiency of the inhibitor molecules and the higher value of dipole moment suggest that the adsorption of inhibitor molecules on metal surface basis on the sharing electrons between the hetero atoms (N and O) of inhibitors and carbon steel iron atom ⁽⁹⁰⁾. The higher values of ΔN and the best compound as inhibitor, in the following order:

$$\text{Trp} > \text{Val} > \text{Lys} > \text{Ser}$$

Table (3-31): Quantum parameters of amino acids.

Terms	Ser		Lys		Val		Trp	
	gas phase	aqueous phase	gas phase	aqueous phase	gas phase	aqueous phase	gas phase	aqueous phase
$-E_{\text{HOMO}}$ (ev)	6.5263	6.1336	6.2307	6.0358	5.9251	5.6903	5.5523	5.2642
$-E_{\text{LUMO}}$ (ev)	0.3494	0.2033	0.6803	0.4963	0.0914	0.0906	0.2969	0.0174
ΔE (ev)	6.1769	5.9303	5.5504	5.5395	5.8337	5.5997	5.2555	5.2467
μ (Debye)	2.2437	2.9643	3.2929	2.0624	2.2280	1.5818	3.6237	3.0281
$-E_{\text{total}} \times 10^4$ (kJ.mol)	105.14	104.56	130.99	130.99	105.49	105.46	179.90	179.89
χ (ev)	3.4378	3.1684	3.4555	3.2660	3.0082	2.8905	2.9246	2.6408
η (ev)	3.0884	2.9652	2.7752	2.7698	2.9168	2.7999	2.6277	2.6234
ΔN (ev)	0.5767	0.6461	0.6386	0.6740	0.6842	0.7339	0.7755	0.8308

3.9 Scanning electron microscopy (SEM)

The effect of inhibitors on corrosion process was examined by the SEM images of corroded carbon steel surface in the absence and the presence of inhibitors.

The SEM images of polished carbon steel specimens show the smooth surface of the alloy without any corrosion products as compared with the uninhibited steel surface in saline solution as shown in figure (3-22) (a and b), respectively. Figure (3-22 b) shows the SEM image of carbon steel surface after 24 hour immersion in the free chloride solution (saline solution). This micrograph clearly reveals that the metal surface was getting cracked due to the presence of aggressive chloride ion that attack on the surface. On the other hand, figures (3-23) and (3-24) represented the morphology of carbon steel surface in the presence of (Val, Ser, Trp and Lys) with concentration of $1 \times 10^{-2} \text{M}$ of pH 2 and pH 11, respectively. Figure (3-23 e) and (3-24 e) shows that there was much less damage on the carbon steel surface in the presence of $1 \times 10^{-2} \text{M}$ of Lys and Ser respectively. This may be due to protective film formation by adsorption of these inhibitors on the carbon steel surface that the film is responsible for the inhibition of corrosion.

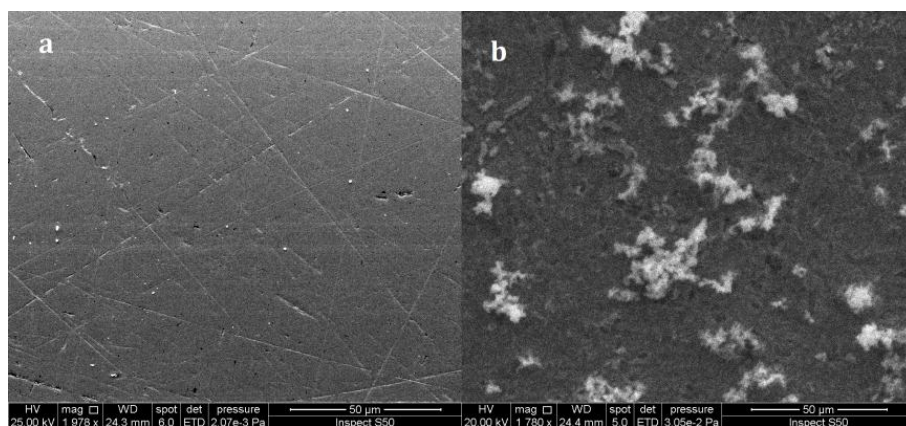


Figure (3-22): Scanning electron micrographs of (a) Polished carbon steel alloy, (b) carbon steel alloy immersed in saline solution.

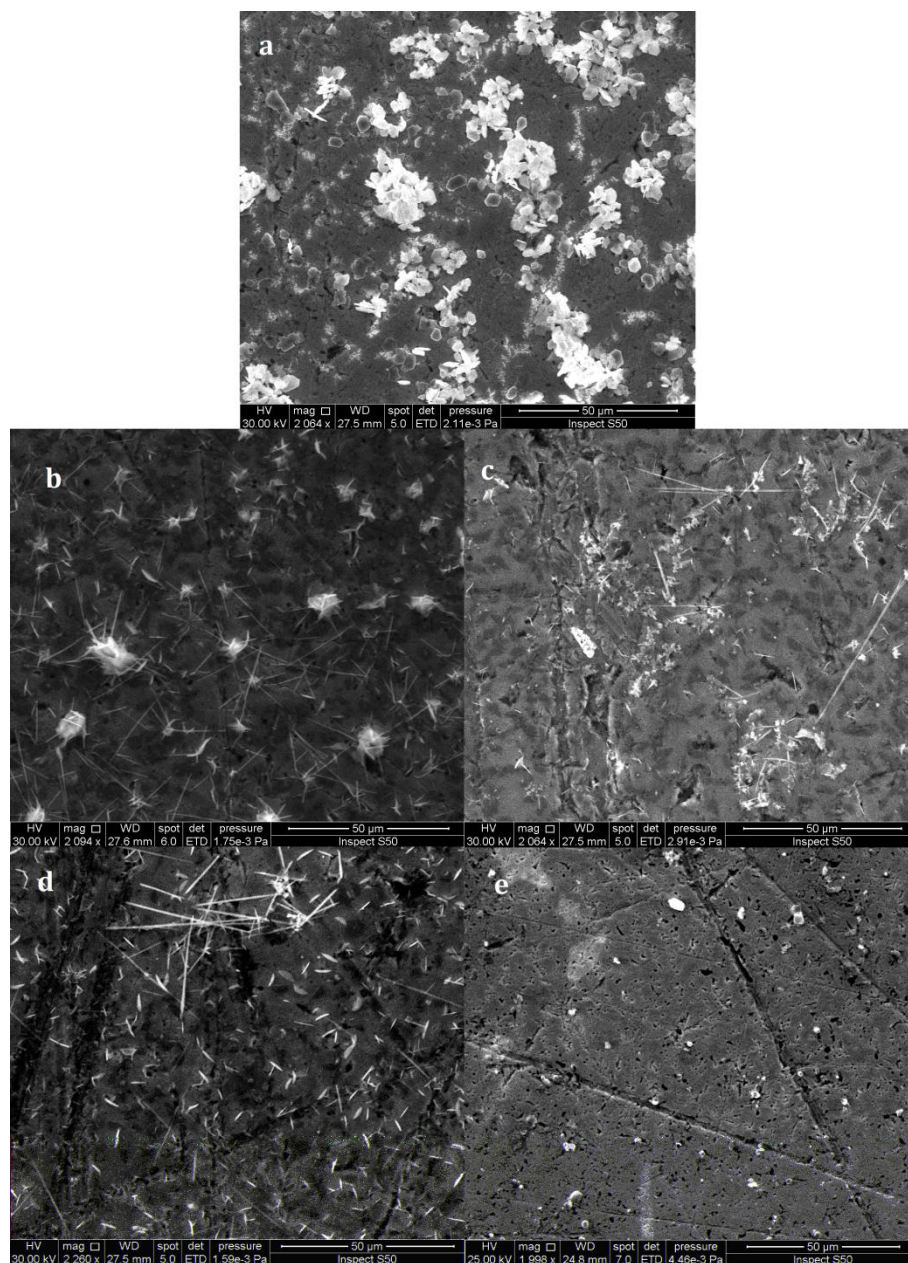


Figure (3-23): Scanning electron micrographs of carbon steel immersed in (a) saline solution at pH 2 (b) saline solution at pH 2 in presence of 1×10^{-2} M Trp (c) saline solution at pH 2 in presence of 1×10^{-2} M Val (d) saline solution at pH 2 in presence of 1×10^{-2} M Ser and (e) saline solution at pH 2 in presence of 1×10^{-2} M Lys respectively.

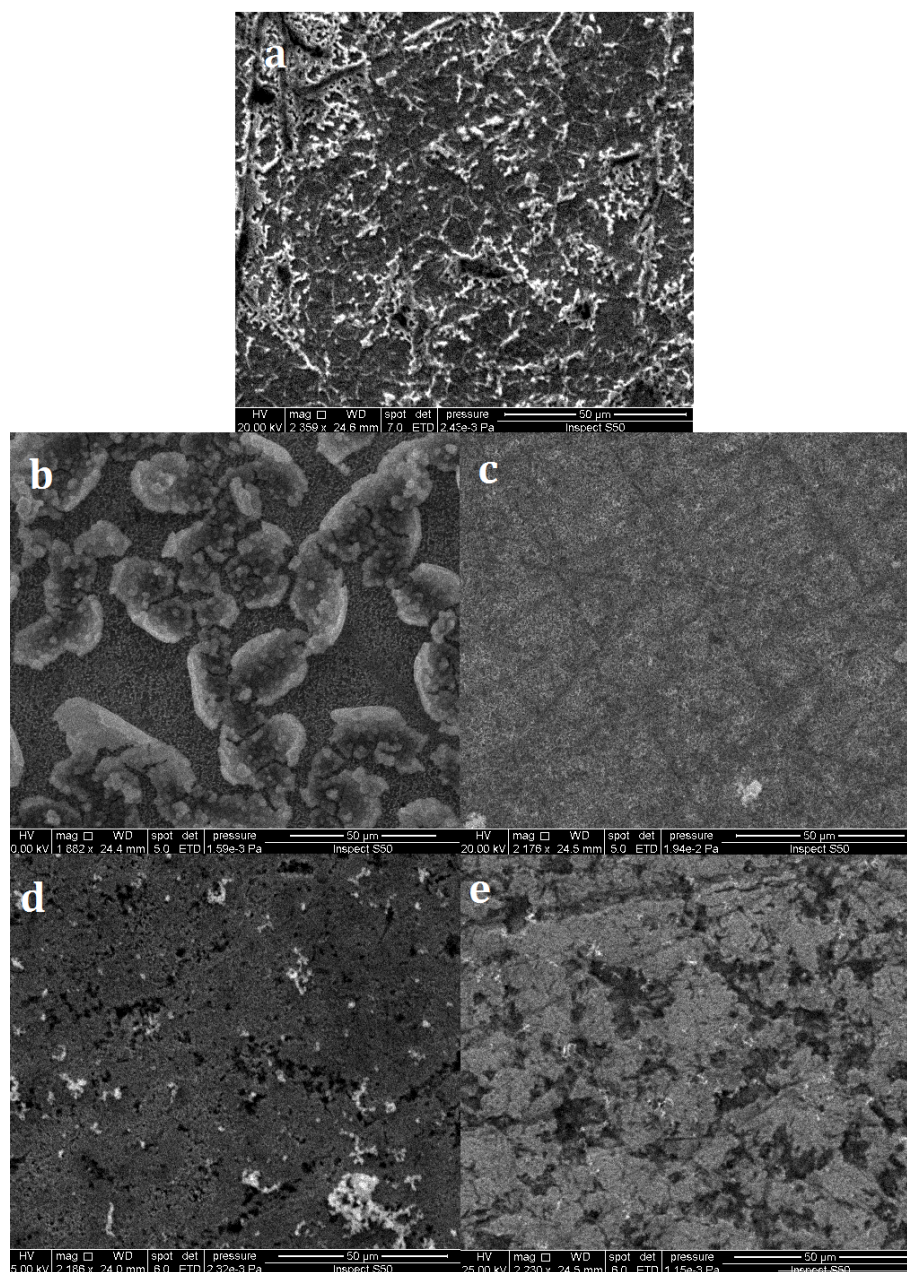


Figure (3-24): Scanning electron micrographs of carbon steel immersed in (a) saline solution at pH 11 (b) saline solution at pH 11 in presence of 1×10^{-2} M Lys (c) saline solution at pH 11 in presence of 1×10^{-2} M Trp (d) saline solution at pH 11 in presence of 1×10^{-2} M Val and (e) 3.5% NaCl solution at pH 11 in presence of 1×10^{-2} M Ser respectively.

Chapter Four

Conclusions and Recommendations

4.1 Conclusions

It provides research work on the corrosion of carbon steel in the saline solution (3.5% NaCl) at temperatures ranging between (293-313)K. The results and its discussion can be summarized in the following listed points:

1. The corrosion rate and penetration rate of carbon steel in saline solution (blank) and in the presence of inhibitors at pH (2 and 11) increase as increasing temperature.
2. At constant temperature the corrosion current density of carbon steel in the saline solution at pH (2 and 11) in the presences of inhibitors listed as increasing as the following sequence:

$$\text{pH } 11 < \text{pH } 2$$

3. The inhibition efficiency increase as increase concentration of inhibitor and decrease as temperature increase. The efficiency of inhibitors can be listed as increasing as follows:

$$\text{pH } 2 \quad (\text{Trp} < \text{Val} < \text{Ser} < \text{Lys})$$

$$\text{pH } 11 \quad (\text{Lys} < \text{Trp} < \text{Val} < \text{Ser})$$

4. In acidic medium Lys and Trp were acted as anodic type inhibitors, while Ser and Val were acted as mixed type inhibitors.
5. In basic medium Ser, Val and Trp were acted as cathodic type inhibitors, while Lys was acted as anodic type inhibitors.
6. The kinetic data indicated that the activation energies E_a for solution in the presence of inhibitors is higher than blank, which means the presence of inhibitors lower the corrosion rate of carbon steel because the molecules of inhibitor that adsorbed on the surface of alloy. The positive sign of the activation enthalpies (ΔH^*) means the endothermic nature of the activated complex formation which means that required more energy to form its with

increasing inhibitors concentrations. The activation entropy (ΔS^*) values are large and negative sign that means the activated complex in the rate determined step represents association rather than the dissociation step, that means a decrease in disorder take place, going from reactant to the activated complex.

7. The ΔG values are negative of thermodynamic corrosion data in the absence and presence of the inhibitors, which indicate that the process is feasible and spontaneous in nature.
8. The adsorption isotherm results showed that:
 - ❖ Negative sign of ΔG means that the adsorption of inhibitor to form a stable adsorbed protective layer on carbon steel is spontaneous.
 - ❖ Negative values of ΔH means the exothermic nature of adsorption process of inhibitor onto the carbon steel surface.
 - ❖ The ΔS is positive, that indicates an increase in randomness during the adsorption process.
9. Quantum chemical calculation confirmed that the adsorption of inhibitor molecules on surface due to presence the nitrogen and oxygen atoms as active sites.

4.2 Recommendations

Many suggestions for the further studies on corrosion inhibition of carbon steel in the future are:

1. Study the inhibitive effect of a new series of amino acids potentiostatically and theoretically on the corrosion of carbon steel in aqueous media.
2. The corrosion medium may be acid or base in the absence and presence of studied amino acids.
3. Study the protection of carbon steel from corrosion through using of plant extracts as another source of eco-friendly inhibitors.
4. Study another techniques for corrosion protection of carbon steel like coating or electroplating.
5. Study the inhibition effect by using conductive polymers on the corrosion of carbon steel in saline media.

| References

References

1. P. R. Roberge, Corrosion Engineering Principles and Practice, McGraw-Hill Companies, P. (1, 51, 81, 82, 86, 112), (2008).
2. V. Cicek, Cathodic Protection Industrial Solutions for Protecting Against Corrosion, Scrivener Publishing, P. (4), (2013).
3. A. Soliz and L. Cáceres, Corrosion Behavior of Carbon Steel in LiBr in Comparison to NaCl Solutions under Controlled Hydrodynamic Conditions, Int. J. Electrochem. Sci., 10 (5673-5693), (2015).
4. M. M. Kabanda, I. B. Obot and E. E. Ebenso, Computational Study of Some Amino Acid Derivatives as Potential Corrosion Inhibitors for Different Metal Surfaces and in Different Media, Int. J. Electrochem. Sci., 8 (10839-10850), (2013).
5. J. A. Thangakani, S. Rajendran, J. Sathiabama, A. Krishnaveni and J. Jeyasundari, Inhibition of Corrosion of Carbon Steel in Well Water by L-Valine – Zn²⁺ System, Int. J. Nano. Corr. Sci. Engg. 2 (18-25), (2015).
6. F. Mansfeld, Classic Paper in Corrosion Science and Engineering with a Perspective, NACE International, 62 (10) (843-855), (2006).
7. C. A. Sequeira, Some Considerations on the Background of Passivity, Corros. Prot. Mater., 4 (126-137), (2010).
8. Z. Ahmad, Principles of Corrosion Engineering and Corrosion Control, Elsevier Science and Technology Books, P. (75), (2006).
9. Princeton Applied Research, Basics of Corrosion Measurements, Application Note CORR-1, 801 S. Illinois Ave., Oak Ridge, TN 37830.
10. Obuka, N. Sylvester, O. N. Celestine, Ikwu, G. Reuben, Chukwumuanya, E. Okechukwu, Review of Corrosion Kinetics

- and Thermodynamics of CO₂ and H₂S Corrosion Effects and Associated Prediction/Evaluation on Oil and Gas Pipeline System, IJSTR, 1 (4) (156-162), (2012).
- 11.M. G. Fontana, Corrosion Engineering, McGraw-Hill Book Company, pp. (19,20), (1987).
- 12.A. E. Hughes et al. (eds.), Active Protective Coatings, Chapter Two, G. S. Frankel, Fundamentals of Corrosion Kinetics, Springer Science+Business Media Dordrecht, P. (21), (2016).
- 13.J. Zhang, PEM Fuel Cell Electrocatalysts and Catalyst Layers, Fundamentals and application, Springer, pp. (91,92), (2008).
- 14.Modern Steel Handbook, Akron Steel Treating Company, Metal Treating Specialists, AST, P. (19), (1943).
- 15.D. Gandy, Carbon Steel Handbook, EPRI, P. (1), (2007).
- 16.Engineering Hand Book Technical Information, Industrial Press, Inc. of New York, NY, P. (13), (2000).
- 17.A. S. Abdul Nabi and H. M. Ali, Corrosion Inhibition of Carbon Steel on Hydrochloric Acid Using Zizyphus Spina-Christisi Extract, Journal Basrah Researches, 35 (1) (67-76), (2009).
- 18.M. Prabakaran, M. Venkatesh, S. Ramesh and V. Periasamy, Corrosion Inhibition Behavior of Propyl Phosphonic Acid–Zn²⁺ System for Carbon Steel in Aqueous Solution, Applied Surface Science, 276 (592-603), (2013).
- 19.E. M. Sherif, Corrosion and Corrosion Inhibition of Pure Iron in Neutral Chloride Solutions by 1,1'-Thiocarbonyldiimidazole, Int. J. Electrochem. Sci., 6 (3077-3092), (2011).
- 20.R. W. Revie and H. H. Uhlig, Corrosion and Corrosion Control an Introduction to Corrosion Science and Engineering, 4th, A JOHN WILEY & SONS, INC., P. (15), (2008).

21. High-Performance Alloys for Resistance to Aqueous Corrosion, Special Metals Corporation, Publication number SMC-026, P. (1-2), (2000).
22. P. Maaß and P. Peißker, Handbook of Hot-dip Galvanization, Corrosion and Corrosion Protection, P. Maaß, WILEY-VCH Verlag GmbH & Co. KGaA, Weinheim, P. (3), (2011).
23. P. R. Roberge, Handbook of corrosion Engineering, McGraw-Hill Companies, P. (349,350), (2000).
24. Grosshandler, W. L. Grosshandler, R. G. Gann and W. M. Pitts, Evaluation of Alternative In-Flight Fire Suppressants for Full-Scale Testing in Simulated Aircraft Engine Nacelles and Dry Bays, Section 7, Corrosion of Metals, R. E. Ricker, M. R. Stoudt, J. F. Dante, J. L. Fink, C. R. Beauchamp and T. P. Moffat, Materials Science and Engineering Laboratory, NIST, P. (669-728), (1994).
25. M. Aliofkhazraei, Developments in Corrosion Protection, Chapter 19, Environmentally Friendly Corrosion Inhibitors, R. M. Palou, O. Olivares-Xomelt and N. V. Likhanova, Publisher: InTech, P. (438-439), (2014).
26. A. S. Raja, S. Rajendran, J. Sathiyabama and P. Angel, Corrosion Control by Aminoacetic acid (Glycine) an Overview, IJRSET, 3 (4) (11455-11466), (2014).
27. A. S. Raja, S. Rajendran, J. Sathiyabama, V. Prathipa, S. Anuradha, A. Krishnaveni and J. Jeyasundari, Synergism and Antagonism in Carbon Steel Corrosion Inhibition by Aminoacetic Acid (Glycine), Int. J. Nano. Corr. Sci. Engg., 2 (2) (52-60), (2015).
28. F. Kadirgana and S. Suzer, Electrochemical and XPS Studies of Corrosion Behaviour of a Low Carbon Steel in the Presence of

- FT2000 Inhibitor, *Journal of Electron Spectroscopy and Related Phenomena*, 114–116 (597–601), (2001).
- 29.M. Aliofkhazraei, *Developments in Corrosion Protection*, Chapter 16, *Corrosion Inhibitors-Principles, Mechanisms and Applications*, C. G. Dariva and A. F. Galio, Publisher: InTech, P. (367), (2014).
- 30.D. Kesavan, M. Gopiraman and N. Sulochana, *Green Inhibitors for Corrosion of Metals: A Review*, *Che Sci Rev Lett*, 1 (1) (1-8), (2012).
- 31.R. Baboian, *NACE Corrosion Engineer's Reference Book*, 3rd, NACE international, P. (12), (2002).
- 32.J. G. Veldkamp, T. V. Goldberg, P. M. M. C. Bressers, F. Wilschut, *Corrosion in Dutch Geothermal Systems*, TNO innovation for life, P. (49), (2016).
- 33.R. W. Revie, *Uhlig's Corrosion Handbook*, 2nd Edition, *Corrosion Inhibitors*, S. Papavinasam, Wiley, P. (1091), (2000).
- 34.I. O. Arukalam, I. O. Madu, N. T. Ijomah, C. M. Ewulonu, and G. N. Onyeagoro, *Acid Corrosion Inhibition and Adsorption Behaviour of Ethyl Hydroxyethyl Cellulose on Mild Steel Corrosion*, *Journal of Materials*, P. (1-11), Vol. 2014.
- 35.A. A. Khadom, A. S. Yaro, A. S. AlTaie and A. A. H. Kadum, *Electrochemical, Activations and Adsorption Studies for the Corrosion Inhibition of Low Carbon Steel in Acidic Media*, *Port. Electrochim. Acta*, 27 (699-712), (2009).
- 36.B. E. A. Rani and B. B. J. Basu, *Green Inhibitors for Corrosion Protection of Metals and Alloys: An Overview*, *International Journal of Corrosion*, P. (1-15), Vol. (2012).
- 37.A. S. Raja, N. Rajendran, V. Prathipa, S. Rajendran, *Nano Analyses of Protective Film Formed by L-Alanine - Zinc Ion System onto Carbon Steel*, *JACS*, 1 (2) (78–81), (2015).

- 38.V. Prathipa and A. S. Raja, Synergistic and Antagonistic Effects of L-Alanine as Green Corrosion Inhibitor for Carbon Steel in Aqueous Medium, JACS, 1 (2) (45–48), (2015).
- 39.D. L. Nelson and M. M. Cox, Lehninger Principles of Biochemistry, 6th, W.H. Freeman, P. (76), (2013).
- 40.A. S. Raja, S. Rajendran, and P. Satyabama, Inhibition of Corrosion of Carbon Steel in Well Water by DL-Phenylalanine-Zn²⁺ System, Journal of Chemistry, P. (1-8), Vol. (2013).
- 41.L. G. Wade, Jr, Organic Chemistry, 7th, pearson education Inc, P. (1158), (2010).
- 42.T. McKee and J. R. McKee, Biochemistry The Molecular Basis of Life, 5th, Oxford University Press, P. (137), (2011).
- 43.V. Prathipa, A. S. Raja and S. Rajendran, Electrochemical Study and Spectroscopic Methods Used for Analyzing Protective Film Formed By L-Alanine on Carbon Steel in Well Water: A Green Approach, JACS, 1 (2) (59-63), (2015).
- 44.M. Mobin, S. Zehra, M. Parveen, L-Cysteine as Corrosion Inhibitor for Mild Steel in 1M HCl and Synergistic Effect of Anionic, Cationic and non-ionic Surfactants, Journal of Molecular Liquids, 216 (598-607), (2016).
- 45.V. Prathipa, A. S. Raja, A Review on the Assessment of Amino Acids Used as Corrosion Inhibitor of Metals and Alloys, JCBPSC, 5 (2) (1585-1619), (2015).
- 46.J. A. Thangakani, S. Rajendran, J. Sathiabama, P. Shanthi, N. Vijaya and J. Jeyasundari, Corrosion Inhibition by Amino Acids- A Birds Eye View, Int. J. Nano. Corr. Sci. Engg., 2 (2) (7-17), (2015).
- 47.W. J. Hehre, A Guide to Molecular Mechanics and Quantum Chemical Calculations, Wavefunction, Inc, P. (22-23), (2003).

- 48.G. Raja, K. Saravanan and S. Sivakumar, Quantum Chemical and Corrosion Inhibition Studies of an Organic Compound: 2, 5 Dichloroaniline, RJC, 8 (1) (8-12), (2015).
- 49.Ameh PO, Koha PU and Eddy NO, Experimental and Quantum Chemical Studies on the Corrosion Inhibition Potential of Phthalic Acid for Mild Steel in 0.1 M H₂SO₄, Chem Sci J, 6 (3) (1-8), (2015).
- 50.H. R. Obayes, G. H. Alwan, A. M. J. Alobaidy, A. A. Al-Amiery, A. H. Kadhum and A. Mohamad, Quantum Chemical Assessment of Benzimidazole Derivatives as Corrosion Inhibitors, Chemistry Central Journal, 8:21 (1-8), (2014).
- 51.M. Yadav, T. K. Sarkar and T. Purkait, Amino Acid Compounds as Eco-Friendly Corrosion Inhibitor for N80 Steel in HCl Solution: Electrochemical and Theoretical Approaches, Journal of Molecular Liquids, 212 (731-738), (2015).
- 52.M. ElBelghiti, Y. Karzazi, A. Dafali, B. Hammouti, F. Bentiss, I. B. Obot, I. Bahadur, E. E. Ebenso, Experimental, Quantum Chemical and Monte Carlo Simulation Studies of 3,5-disubstituted-4-amino-1,2,4-triazoles as Corrosion Inhibitors on Mild steel in Acidic Medium, Journal of Molecular Liquids, 218 (281-293), (2016).
- 53.S. Gowri, J. Sathiyabama, and S. Rajendran, Corrosion Inhibition Effect of Carbon Steel in Sea Water by L-Arginine-Zn²⁺ System, International Journal of Chemical Engineering, P. (1-9), Vol. (2014).
- 54.H. M. Abd El-Lateef, M. Ismael and I. M. A. Mohamed, Novel Schiff Base Amino Acid as Corrosion Inhibitors for Carbon Steel in CO₂-Saturated 3.5% NaCl Solution: Experimental and Computational Study, Corros Rev, 33 (1-2) (77-97), (2015).

- 55.A. S. Raja, S. Rajendran, R. Nagalakshmi, J. A. Thangakani and M. Pandiarajan, Eco-Friendly Inhibitor Glycine-Zn²⁺ System Controlling Corrosion of Carbon Steel in Well Water, *Eur. Chem. Bull.*, 1 (3) (130-136), (2012).
- 56.A. S. Raja and S. Rajendran, Inhibition of Corrosion of Carbon Steel in Well Water by Arginine-Zn²⁺ system, *J. Electrochem. Sci. Eng.*, 2 (91-104), (2012).
- 57.A. S. Raja, S. Rajendran, J. Sathiyabama, V. Prathipa, I. N. Karthika and A Krishnaveni, Use of L-Alanine as Nature-Friendly Corrosion Inhibitor for Carbon Steel in Aqueous Medium, *Int. J. Nano. Corr. Sci. Engg.*, 2 (2) (26-40), (2015).
- 58.M. A. Migahed, E. M. S. Azzam and S. M. I. Morsy, Electrochemical Behaviour of Carbon Steel in Acid Chloride Solution in the Presence of Dodecyl Cysteine Hydrochloride Self-Assembled on Gold Nanoparticles, *Corrosion Science*, 51 (1636–1644) (2009).
- 59.K. F. Al-Sultani¹ and S. A. Abdulsada, Improvement Corrosion Resistance of Low Carbon Steel by Using Natural Corrosion Inhibitor, *ijar*, 1 (4) (239-243), (2013).
- 60.H. Zarrok, A. Zarrouk, R. Salghi, B. Hammouti, M. Elbakri, M. Ebn Touhami, F. Bentiss and H. Oudda, Study of a Cysteine Derivative as a Corrosion Inhibitor for Carbon Steel in Phosphoric Acid Solution, *Res Chem Intermed*, 40 (801–815), (2014).
- 61.A. M. Al-Bonayan, Corrosion Inhibition of Carbon Steel in Hydrochloric Acid Solution by Senna Italica Extract, *IJRRAS*, 22 (2) (49-64), (2015).
- 62.J. Fu, S. Li, Y. Wang, L. Cao and L. Lu, Computational and Electrochemical Studies of Some Amino Acid Compounds as

- Corrosion Inhibitors for Mild Steel in Hydrochloric Acid Solution, *J Mater Sci*, 45 (6255-6265), (2010).
63. A. Ganash, Effect of Current Density on the Corrosion Protection of Poly(o-toluidine)-Coated Stainless Steel, *Int. J. Electrochem. Sci.*, 9 (4000-4013), (2014).
64. N. A. Abdel Ghanyl, The Inhibitive Effect of Some Amino Acids on the Corrosion Behaviour of 316L Stainless Steel in Sulfuric Acid Solution, *Modern Applied Science*, 5 (4), (19-29), (2011).
65. J. W. Sahayaraj, A. J. Amalraj, S. Rajendran, Green Corrosion Inhibitors Control the Disaster of Carbon Steel Surface, *JCPS*, 9 (3) (1491-1494), (2016).
66. H. T. Abdel-Fatah, H. S. Abdel-Samad, A. A. Hassan and H. E. El-Sehiety, Effect of Variation of the Structure of Amino Acids on Inhibition of the Corrosion of Low-Alloy Steel in Ammoniated Citric Acid Solutions, *Res Chem Intermed*, 40 (1675–1690), (2014).
67. J. Fu, S. Li, L. Cao, Y. Wang, L. Yan, L. Lu, L-Tryptophan as Green Corrosion Inhibitor for Low Carbon Steel in Hydrochloric Acid Solution, *J Mater Sci*, 45 (979–986), (2010).
68. M. Mobin, M. Parveen and M. A. Khan, Inhibition of Mild Steel Corrosion in HCl Solution Using Amino Acid L-tryptophan, *RRST*, 3 (12) (40-45), (2011).
69. M. Mobin, M. Parveen and M. A. Khan, Inhibition of Mild Steel Corrosion Using L-tryptophan and Synergistic Surfactant Additives, *Port. Electrochim. Acta*, 29 (391-403), (2011).
70. A. Jano, A. Lame and E. Kokalari, Inhibition Effect of Lysine for Low Alloy Carbon Steel in Acidic Media, *ICRAE*, University of Shkodra “Luigj Gurakuqi”, Shkodra, Albania, (2013).

- 71.O. Kasso, M. Galai, R. A. Ballakhmima, N. Dkhireche, A. Rochdi M. Ebn Touhami, R. Tourir and A. Zarrouk, Comparative Study of Low Carbon Steel Corrosion Inhibition in 200 ppm NaCl by Amino Acid Compounds, *J. Mater. Environ. Sci.*, 6 (4), (2015).
- 72.S. A. Kumar, A. Sankar, S. R. Kumar, Vitamin B-12 Solution as Corrosion Inhibitor for Mild Steel in Acid Medium, *IJCES*, 3 (1) (57-61), (2013).
- 73.L. A. Al Juhaiman, A. Abu Mustafa, W. K. Mekhamer, Polyvinyl Pyrrolidone as a Green Corrosion Inhibitor of Carbon Steel in Neutral Solutions Containing NaCl: Electrochemical and Thermodynamic Study, *Int. J. Electrochem. Sci.*, 7 (8578 – 8596), (2012).
- 74.M. Abdallah, B. A. AL Jahdaly, O. A. Al-Malyo, Corrosion Inhibition of Carbon Steel in Hydrochloric Acid Solution using Non-Ionic Surfactants Derived from Phenol Compounds, *Int. J. Electrochem Sci.*, 10 (2740 – 2754), (2015).
- 75.Albana JANO, Alketa LAME (GALO) and Efrosini KOKALARI (TELI), Lysine as Corrosion Inhibitor for Low Alloy Carbon Steel in Acidic Media, *VERSITA*, 25 (1) (11-14), (2014).
- 76.R. wood and F. M. Doyle, *Electrochemistry in Mineral and Metal Processing V*, The Electrochemical Society, Inc., P. (39-40), (2000).
- 77.R. Guidelli, R. G. Compton, J. M. Feliu, E. Gileadi, J. Lipkowski, W. Schmickler and S. Trasatti, Defining the Transfer Coefficient in Electrochemistry: An assessment (IUPAC Technical Report), *Pure Appl. Chem.*, 86 (2) (245-258), (2014).
- 78.V. M. Janardhanan and O. DeutsChmann, Modeling of Solid-Oxide Fuel Cell, *Z. Phys. Chem.*, 221 (443-478), (2007).

- 79.G. Kear, I. Flatley and S. Jones, Application of Polarization Resistance Measurements for the Estimation of Corrosion Rates of Galvanised Steel Structures in Soils, BRANZ, 127 (1-15), (2006).
- 80.D. Tang, J. Lu, L. Zhuang and P. Liu, Calculations of the Exchange Current Density for Hydrogen Electrode Reactions: A short review and a new equation, Journal of Electroanalytical Chemistry, 644 (144-149), (2010).
- 81.A. O. Yüce, E. Telli, B. D. Mert, G. Kardaş and B. Yazıcı, Experimental and Quantum Chemical Studies on Corrosion Inhibition Effect of 5,5 diphenyl 2-thiohydantoin on Mild Steel in HCl Solution, Journal of Molecular Liquids, 218 (384–392), (2016).
82. A. A. Al-Amiery, A. H. Kadhum, A. Kadhum, A. Mohamad, C. K. How and S. Junaedi, Inhibition of Mild Steel Corrosion in Sulfuric Acid Solution by New Schiff Base, Materials, 7 (787-804), (2014).
- 83.B. Joseph, S. John, A. Joseph and B. Narayana, Imidazolidine-2-thione as Corrosion Inhibitor for Mild Steel in Hydrochloric Acid, Indian Journal of Chemical Technology, 17 (366-374), (2010).
- 84.M. Mobin, S. Zehra and M. Parveen, L-Cysteine as Corrosion Inhibitor for Mild Steel in 1M HCl and Synergistic Effect of Anionic, Cationic and Non-Ionic Surfactants, Journal of Molecular Liquids, 216 (598–607), (2016).
- 85.K. R. Ansari, M. A. Quraishi and A. Singh, Pyridine Derivatives as Corrosion Inhibitors for N80 Steel in 15% HCl: Electrochemical, Surface and Quantum Chemical Studies, Measurement, 76 (136-147), (2015).
- 86.M. Yadav, L. Gope, N. Kumari and P. Yadav, Corrosion Inhibition Performance of Pyranopyrazole Derivatives for Mild Steel in HCl

- Solution: Gravimetric, Electrochemical and DFT Studies, *Journal of Molecular Liquids*, 216 (78-86), (2016).
- 87.P. Singh and M. A. Quraishi, Corrosion Inhibition of Mild Steel Using Novel Bis Schiff's Bases as Corrosion Inhibitor: Electrochemical and Surface Measurement, *Measurement*, 86 (114-124), (2016).
- 88.Mohamed Gobara, Ahmad Baraka and Basem Zaghrou, Green Corrosion Inhibitor for Carbon Steel in Sulfuric Acid Medium from "Calotropis Gigantica" Latex, *Res Chem Intermed*, 41 (9885-9901), (2015).
- 89.M. A. Bedair, The Effect of Structure Parameters on the Corrosion Inhibition Effect of Some Heterocyclic Nitrogen Organic Compounds, *Journal of Molecular Liquids*, 219 (128-141), (2016).
- 90.M. Yadav, T. K. Sarkar and T. Purkait, Amino Acid Compounds as Eco-Friendly Corrosion Inhibitor for N80 Steel in HCl Solution: Electrochemical and Theoretical Approaches, *Journal of Molecular Liquids*, 212 (731-738), (2015).
- 91.M. E. Belghiti, Y. Karzazi, A. Dafali, I. B. Obot, E. E. Ebenso, K. M. Emran, I. Bahadur, B. Hammouti and F. Bentiss, Anti-Corrosive Properties of 4-amino-3,5-bis(disubstituted)-1,2,4-triazole Derivatives on Mild Steel Corrosion in 2M H₃PO₄ Solution: Experimental and Theoretical Studies, *Journal of Molecular Liquids*, 216 (874-886), (2016).

تركيز المثبط معنى ذلك احتياج طاقة اكبر لتكوين المعقد المنشط في حين كانت قيم ΔS سالبة دلالة على استقرارية المعقد النشط في الخطوة المحددة للتفاعل.

٦. تخضع عملية الامتزاز إلى ايزوثيرمات لانكماير، القيم السالبة لل ΔH_{ads} و ΔG_{ads} تشير إلى أن العملية كانت تلقائية وباعثة للحرارة، بينما كانت قيم ΔG_{ads} تتراوح بين (-٤٠ الى -٢٠) كيلوجول/مول دلالة على ان الامتزاز كان من نوع فيزيائي وكيميائي.

النتائج التي تم الحصول عليها من الحسابات النظرية للأحماض الامينية (فالين، سيرين، تربتوفان، لايسين) باستخدام نظرية دوال الكثافة (DFT) لعناصر قاعدة (B3LYP) مع 6-31G تشير إلى أن التربتوفان هو أفضل مثبط في الطور المائي والطور الغازي.

الصور التي تم الحصول عليها من المجهر الالكتروني الماسح (SEM) للفولاذ الكربوني في وجود (١ × ١٠^{-٢} مولاري) من الأحماض الأمينية اظهرت ان المعدن به أضرار أقل بكثير من عدم وجودها نظرا إلى تشكيل طبقة واقية خلال عملية الامتزاز.

الملخص:

يتضمن هذا البحث دراسة سلوك تآكل سبائك الفولاذ الكربوني في المياه المالحة (٣,٥٪ كلوريد الصوديوم) باستخدام تقنية (potentiostat). النمط العام والتقنيات التجريبية المستخدمة يمكن تصنيفها إلى ثلاثة جوانب مختلفة على النحو التالي:

١. سلوك التآكل لعينة الفولاذ الكربوني في المحلول الملحي (٣,٥٪ كلوريد الصوديوم) وأيضا بوجود المثبطات (فال، سيرين، تربتوفان، لايسين) عند درجات حموضة (٢ و ١١) في مختلف درجات الحرارة في حدود ٢٩٣ كلفن إلى ٣١٣ كلفن من منحنيات الاستقطاب ضمن مدى من الجهود (-٧٠٠ إلى -٣٠٠) فولت.
٢. التأثير التثبيطي للأحماض الأمينية (فالين، سيرين، تربتوفان، لايسين) باعتبارها مثبطات صديقة للبيئة على تآكل سبائك الفولاذ الكربوني في محلول ملحي في خمس درجات حرارة مختلفة عند درجات حموضة (٢ و ١١).
٣. دراسات حسابية للمثبطات (فال، سيرين، تربتوفان، لايسين) باستخدام نظرية دوال الكثافة (DFT) مع (6-31G) في الطور الغازي والطور المائي.

ويمكن عرض أهم النتائج التي تم الحصول عليها من الدراسات التجريبية على النحو التالي:

١. كثافات تيار التآكل ومعدلات التآكل للمحلول الملحي بوجود المثبط وعدم وجوده تزداد مع زيادة درجة الحرارة على نطاق (٢٩٣-٣١٣) كلفن.
٢. قيم كفاءة التثبيط تزداد مع زيادة تركيز المثبطات (فالين، سيرين، تربتوفان، لايسين) وذلك بسبب امتزاز هذه المركبات على سطح المعدن وتتناقص هذه الكفاءة مع زيادة درجة الحرارة في حدود (٢٩٣-٣١٣) كلفن. تسلسل قيم الكفاءة كان كما يلي:

(لايسين < سيرين < فالين < تربتوفان) في درجة الحموضة ٢

(سيرين < فالين < تربتوفان < لايسين) في الرقم الهيدروجيني ١١

أظهر اللايسين أكثر كفاءة لحماية الفولاذ الكربوني في المحلول الملحي (درجة الحموضة ٢)، اما في المحلول الملحي القاعدي أظهر السيرين أكثر كفاءة و بشكل خاص في تركيز (١×١٠^{-٢}) مول/لتر.

٣. الأحماض الأمينية التي تم دراستها (فالين، سيرين، تربتوفان، لايسين) كانت بمثابة مثبطات انودية أو كاثودية أو كلاهما (انودية وكثودية)، وفقا لقيم جهد التآكل.

٤. تشير قيم ΔG إلى أن عملية التآكل تلقائية.

٥. حركية التآكل معتمدة من قبل معادلة أرينوس، أظهرت النتائج بوجود الأحماض الأمينية تكون طاقة التنشيط اكبر في حالة عدم وجودها هذا يدل على نقصان سرعة التآكل بوجود الاحماض الامينية بينما قيم ΔH كانت موجبة وتزداد قيمها بالموجب مع زيادة



جمهورية العراق
وزارة التعليم العالي
والبحرث العلمي
جامعة النهرين
كلية العلوم
قسم الكيمياء

الأحماض الأمينية كمشبطات لتآكل الفولاذ الكربوني في المحلول الملحي

رسالة
مقدمه إلى كلية العلوم / جامعة النهرين
كجزء من متطلبات نيل درجة الماجستير في علوم الكيمياء

من قبل
الإء بدر محمد
بكالوريوس ٢٠١٤

إشراف
الأستاذ المساعد الدكتور
تغريد علي سلمان